Proteomic analysis of endomyocardial biopsies and plasma of dilated cardiomyopathy patients treated by immunoadsorption therapy

Inauguraldissertation

zur Erlangung des akademischen Grades

Doktor rerum naturalium (Dr. rer. nat.)

an der Mathematisch-Naturwissenschaftliche Fakultät
der
Ernst-Moritz-Arndt-Universität Greifswald

Vorgelegt von
Gourav Bhardwaj
born on the 01.01.1983
at Moradabad – India

Greifswald, June 2016

Dekan: Prof. Dr. rer. nat. Werner Weitschies

1. Gutachter : Prof. Dr. rer. nat. Uwe Völker

2. Gutachter: Prof. Dr. Med. Anje Volgt

Tag der Promotion: 17/11/2016

Table of contents

Abstrakt

Die dilatative Kardiomyopathie (DCM) ist eine Myokarderkrankung, die durch eine ventrikuläre Erweiterung bei gleichzeitig verringerter linksventrikulärer Auswurffraktion (LVEF) charakterisiert ist. Eine Immunadsorptionstherapie mit nachfolgender Substitution der Immunglobuline (IA/IgG), führt zu einer Verbesserung der hämodynamischen Funktion, einem verringertem linksventrikulärem diastolischen Durchmesser (LVIDd), sowie einem geringerem Inflammationsgrad in DCM Patienten. Die der verbesserten Hämodynamik nach IA/IgG Therapie zugrunde liegenden molekularen Mechanismen sind jedoch weitestgehend unbekannt. Zudem profitieren nur etwa 60% der IA/IgG behandelten DCM Patienten, wobei die Ursache der unterschiedlichen Effekte noch unklar ist.

Ein Schwerpunkt dieser Studie bildete daher die globale Proteinanalyse der durch IA/IgG Therapie vermittelten Änderungen in Respondern (relative Änderung der LVEF $\leq$ 20%, LVEF $<$ 5% absolute) und Nonrespondern. Darüber hinaus wurden Proteinanalysen sowohl von endomyokardialen Biopsien als auch von Blutplasma erstellt, um potentielle Proteinbiomarker zu definieren, welche eine Unterscheidung von DCM Patienten bereits vor Therapiebeginn hinsichtlich ihres Therapieerfolges ermöglichen und somit eine optimierte, individuelle Behandlung unterstützen.

Zur Analyse Therapie-induzierter Änderungen myokardialer Proteine wurden humane Biopsien vor und nach Therapie verglichen. Die klinischen Parameter der Responder zeigten nach Therapie einen Anstieg der LVEF (32 ± 8 to 45 ± 7, $p<0.002$) und eine Verringerung des LVIDd (66 ± 6 to 60 ± 6, $p<0.040$), während die Gruppe der Nonresponder keine signifikanten Änderungen dieser Parameter zeigte. Um die Änderungen myokardialer Proteine nach Therapie zu adressieren, wurde ein Label-freier Proteomansatz angewandt. Es wurden signifikante Unterschiede zwischen den

Subgruppen für Proteine des Zytoskeletts, der extrazellulären Matrix, als auch für Fibrose-assoziierte Proteine erfasst.

Darüber hinaus wurden globale Proteomanalysen von endomyokardialen Biopsien und Plasma durchgeführt, um Unterschiede in der Proteinabundanz zwischen Respondern und Nonrespondern vor IA/IgG Therapie zu adressieren. Responder und Nonresponder zeigten keine signifikanten Unterschiede hinsichtlich klinischer Parameter (LVEF, LVIDd, Alter, Inflammations, etc.) vor Therapiebeginn. Jedoch zeigte die Gruppe der Nonresponder einen tendenziell längeren Krankheitszeitraum. Das Proteinprofil endomyokardialer Biopsien ergab 54 Proteine, die eine unterschiedliche Abundanz in Respondern und Nonrespondern zeigten. Unter diesen Proteinen wurden S100-A8 und Kininogen-1 in erhöhter Menge, und Perilipin 4 in geringerer Menge in Respondern detektiert. Die Plasmaproteinanalyse der Patientengruppen ergab fünf Proteine (S100-A8, S100-A9, C-Reactive Protein, Lipopolysacharid-Bindeprotein und Cystein-rich secretory Protein) die stark diskriminierend für die Unterscheidung von Respondern und Nonrespondern vor IA/IgG Therapie waren. Die höhere Abundanz des Protein S100-A8 in Respondern konnte, sowohl im Myokard, als auch im Plasma, nachgewiesen werden. Das Protein S100-A8 ist somit ein potentieller Kandidat für die Unterscheidung von Respondern und Nonrespondern vor IA/IgG Therapie, wobei die Relevanz im klinischen Bereich evaluiert werden muss.

Das letzte Ziel der Arbeit war es, einen Arbeitsablauf für die relative Quantifizierung von Phosphopeptiden aus Proben mit geringer Proteinmenge, wie es für Myokardbiopsien zutrifft, zu etablieren. Um diese Aufgabe zu lösen, wurde die Optimierung mit HL-1 Kardiomyozyten unter Verwendung des PolyMAC-Phosphopeptidanreicherungskits durchgeführt. Hierbei wurde in einer Vorstudie die Wirkung von TGF-β1 auf das Phosphoproteom untersucht. Mit nur 200 μg Proteinen jeder Probe konnten bis zu 2000 Phosphopeptide mit einem Wirkungsgrad von über 90 Prozent abgedeckt werden. Insgesamt wurden bei TGF-β1-Inkubationen nach 1, 6 und 24 Stunden die Veränderungen von 214, 92 und 53 Phosphopeptiden beobachtet. Differenziell veränderte

Phosphopeptide gehörten zu vielen Signalwegen, wie dem Ubiquitin-Proteasom-Weg, der Zytoskelett Regulation durch Rho-GTPasen, dem Calcium-Signalweg und dem TGF-β-Signalweg. Somit wurde in dieser Arbeit ein Arbeitsablauf zur relativen Quantifizierung von Phosphopeptiden etabliert, welcher später auf kostbare Biopsie Proben angewendet werden kann. Zusätzlich dazu konnte die TGF-β1 induzierte Veränderung des Phosphoproteoms in HL-1-Kardiomyozyten analysiert werden.

Summary

Dilated cardiomyopathy is a myocardial disorder characterized by ventricular dilation with reduced left ventricular ejection fraction. It is the most common indicator of heart failure and heart transplantation worldwide. Immunoadsorption (IA) followed by immunoglobulin (IgG) substitution (IA/IgG) has been shown to be a promising therapeutic intervention to recover myocardial functions in dilated cardiomyopathy patients. The beneficial effects of immunoadsorption therapy are associated with increased ventricular ejection fraction, decreased left ventricular inner diameter at diastole and reduced myocardial inflammation. Also, therapy linked cardiac benefits are accompanied by reduced levels of plasma heart failure markers (nt-BNP and nt-ANP), and oxidative stress markers (lipid peroxidase, anti-oxidized low-density lipoprotein, and thiobarbituric acid-reactive substances). Moreover, the therapy not only improves the hemodynamic parameters but also reduces the morbidity in DCM patients.

Despite knowing the cardiac benefits of IA/IgG, the precise molecular mechanism induced by therapy is still elusive. Additionally, only ≈60 % DCM patients treated with IA/IgG demonstrated improved heart function. Moreover, the reasons for this differential outcome among DCM patients after treatment have not been clearly understood. In the study presented here, efforts were made to uncover the therapy induced molecular changes in the heart of responder and non-responder DCM patients using a global proteomic approach. Apart from it, proteomic profiling of endomyocardial biopsies and plasma was performed to find protein biomarker candidates which might be useful to distinguish responder and non-responder DCM patients before immunoadsorption therapy and support a selective and personalized treatment.

Responder and non-responder DCM patients did not show any significant differences in the clinical parameters (LVEF, LVIDd, age, inflammation, etc.) before immunoadsorption therapy except disease duration that was in tendency higher among non-responders. To elucidate the myocardial proteomic differences between responder and non-responder DCM patients before

immunoadsorption therapy, a label-free mass spectrometric approach was applied in the discovery phase. Furthermore, a subset of differentially abundant proteins discovered in the label-free analysis were confirmed using multiple reaction monitoring (MRM). Initially, an endomyocardial proteomic study was performed on 16 DCM (seven responders, and nine non-responders) patients that revealed 1444 non-redundant proteins with high confidence (1%FDR). Among these, only 54 ($\approx$5%) proteins were found differentially abundant (p $\leq$ 0.05, and FC $\lfloor$1.3$\rfloor$) between responders and non-responders. Functional enrichment analysis of these proteins revealed differences in responders and non-responders prominently in energy and lipid metabolism, immune response as well as proteins involved in cardioprotection. Many proteins related to energy production were found as lower abundant in responder DCM patients. Three proteins of the glycolytic pathway were found lower in responders of which two, 6-phosphofructokinase and pyruvate kinase, are regulatory enzymes. The assumption of a lower energy state in responders was further supported by lower levels of mitochondrial proteins pertaining to each of the mitochondrial complexes (complex I-complexV) except complex IV. Along with this, several proteins related to cytoskeleton, apoptosis, and extracellular matrix categories were found as differentially regulated between responders and non-responders. Some of the proteins like perilipin-4, which plays a vital role in lipid droplet biogenesis, were found in lower abundance in the responder DCM patients. In addition, protein S100-A8, an immune regulatory protein was found as higher abundant in responders. Also, a cardioprotective protein, kininogen-1 was found at lower levels in responders. Seventeen proteins of various functional categories discovered in the label-free analysis were selected for the validation using MRM. Out of 17, MRM results of 13 proteins supported the discovery phase findings. Among those proteins, protein S100-A8, kininogen-1, and perilipin-4 were revealed as the most significant (p $\leq$ 0.05) candidates differentiating responders and non-responders. In addition, the validation phase was further extended in a larger sample set (n=33). Here, MRM result of 11 proteins displayed a similar trend as in the discovery phase, but the results were most robust for kininogen-

1 and protein S100-A8. To increase the utility of these proteins as a biomarker, their blood plasma levels must be screened to develop a clinically relevant diagnostic tool.

To reveal therapy induced myocardial proteomic changes, 23 patients with dilated cardiomyopathy treated with IA/IgG were included in the studies of the second part of the thesis. IA/IgG was well tolerated by all DCM patients and no adverse clinical, or physiological abnormalities were observed in any of the individuals after treatment. Left ventricular ejection fraction increased (32 ± 8 to 45 ± 7, $p<0.002$) and left ventricular inner diameter at diastole decreased (66 ± 6 to 60 ± 6, $p<0.040$) after therapy in responders, whereas non-responders did not show any significant changes in these clinical parameters. In addition, therapy reduced the levels of NT-proBNP (1081 ± 1205 to 532 ± 1211 pg/ml, $p<0.007$) in responders which is a heart failure marker generally increasing with the severity of heart failure. To address the changes in the myocardium induced by immunoadsorption therapy, a label-free proteomic approach was applied. Therapy related protein alterations were studied in responders and non-responders separately, but differences in the subgroups were also addressed by comparing the ratios (follow up / baseline) of responders versus non-responders. Out of 669 identified proteins, only 16 and 43 were altered by therapy in responders in non-responders, respectively. 57 proteins were found to be differentially affected in the subgroups. Functional enrichment analysis of these differentially abundant proteins revealed distinct classes of proteins among responders and non-responders, displaying a different molecular effect of immunoadsorption therapy in the subgroups. The most prominent proteomic differences between both the subgroups were observed in cytoskeletal, fibrosis, and extracellular matrix proteins. In general, the level of cytoskeletal proteins increases in dilated cardiomyopathy and heart failure, and in this study therapy-associated proteome alterations were observed on the expression of seven cytoskeleton proteins. Among these, six (myosin regulatory light polypeptide 9, fibronectin, myosin-11, actin cytoplasmic 2, myosin light chain kinase 3 and alpha-actinin-1) were present in lower abundance, while one protein (myosin regulatory light chain-2) was found at

higher levels in the responders after follow-up. In addition, therapy associated proteome changes were linked to fibrosis, which is one of the crucial molecular remodelings in the myocardium during the progression of heart diseases including DCM and heart failure. Fibrosis generally increases in heart failure patients, and the current study disclosed an immunoadsorption therapy associated reduction of fibrotic proteins (myosin regulatory light polypeptide 9, fibronectin, collagen alpha-1(I) chain, myosin 11 and collagen alpha-2 (I) chain) in responders, but not in non-responders. Hence, in the responder group a reduced fibrotic activity in comparison to non-responders can be assumed. This speculation was further strengthened, by the decrease of several proteins of extracellular matrix proteins (lumican, biglycan, mimecan, prolargin, and dermatopontin) upon therapy in responders. Based on the fibrotic and extracellular matrix proteins, lower activity of TGF-β was predicted by Ingenuity Pathway Analysis in responders. TGF-β signaling is reported to be increased in heart failure, and it stimulates fibrotic events and extracellular matrix deposition that further deteriorates the progression of heart disease. Thus, in the current study beneficial effects of therapy in responders were in line with the predicted lower activity of TGF-β signaling. In general, therapy linked benefit in responders seems to be highly associated with the lower abundance of fibrotic and extracellular matrix proteins which seems to reflect a lower activity of transforming growth factor-β signaling.

To discover plasma biomarkers that distinguish responders and non-responders at baseline, plasma proteome profiling was performed. To dig deeper into the plasma proteome, iTRAQ labeled peptides were fractionated using strong cation exchange (SCX) chromatography prior to mass spectrometric analysis. Discovery phase experiments included both iTRAQ-based and label-free quantification, and a set of differentially abundant plasma proteins was further confirmed by multiple reaction monitoring and ELISA. The iTRAQ approach included 20 samples (R++ 5, R-- 5, NR++ 5, controls 5), whereas label-free quantification was performed for samples from 34 DCM patients (responders 23, and non-responders 11). The combination of both approaches revealed 467

non-redundant plasma proteins, of which 154 were found to be present at different levels (p ≤ 0.05/or peptide tag variability ≤30 and │FC│1.3) in responders and non-responders at baseline. Functional categorization of differentially abundant plasma proteins revealed differences between responders and non-responders in many aspects including LXR activation, immune response, hematopoiesis, and coagulation system. The liver X receptors (LXR) are transcriptional factors that regulate glucose and lipid homeostasis, and several proteins linked to this receptor family like serum paraoxonase/arylesterase 1, pigment epithelium-derived factor, haptoglobin-related protein, and phospholipid transfer protein were found at different levels in the two subgroups. Along with this, the coagulation system is described to be commonly activated in dilated cardiomyopathy and heart failure patients. In this study coagulation factors VII, IX, XI, and XII were differentially regulated in the subgroups. Most interestingly, many proteins related to inflammation, acute phase response, and immune system were found to display different levels in the plasma of responders and non-responders. Thus, the acute phase proteins C-reactive protein, mannose-binding lectin protein, lipopolysaccharide-binding protein, and serum amyloid A-1 were found at higher levels in the responder DCM patients. Also, many immune regulatory proteins like protein S100-A8, S100-A9, S100-A7, and galectin-3-binding protein were found at higher levels in responder DCM patients. Thus, in general, responders seem to have a stronger activation of the immune system and the acute phase response than non-responders. Twenty proteins from various functional categories were selected and confirmed using MRM in a larger number of samples (total n=69; R n=38, NR n=31, and controls with preserved LVEF n=17). Among those, MRM results of ten proteins in trend confirmed the findings of the discovery phase. The most significant results were displayed for protein S100-A8, S100-A9, C-reactive protein-CRP, cysteine-rich secretory protein-CRISP3 and lipopolysaccharide-binding protein-LBP. The higher level of protein S100-A8 in plasma of responders was in line with the higher protein abundance and transcript levels in endomyocardial biopsies of this patient subgroup. Therefore, the levels of protein S100-A8 in plasma were further analyzed using a traditional immunoassay method (ELISA, R n=44, and NR n=38).

To evaluate the potential of the proteins S100-A8, S100-A9, CRP, LBP, and CRISP3 in differentiating responders and non-responders at baseline, receiver operating characteristic curves were plotted using the ratio data (light/heavy) of MRM. The calculated area under the receiver operating characteristic curve (AUC) was found highest for protein S100-A8 (AUC=0.70, and p=0.003), but sensitivity and specificity did not improve when all five signatures were analyzed together. Thus, protein S100-A8 might be a potential candidate to distinguish responders and non-responders at baseline, and its potential utility at clinical levels must be evaluated.

The last objective of the thesis was to establish a workflow for the relative quantitation of phosphopeptides for samples generally obtained in small amounts like myocardial biopsies. To address this question, optimization was performed with HL-1 cardiomyocytes using a PolyMAC phosphopeptide enrichment kit and the effect of TGF-β1 on the phosphoproteome was evaluated as a proof-of-principle study. Using only 200μg protein of each sample up to 2000 phosphopeptides with an efficiency of >90 percent could be covered. In total, upon TGF-β1 incubation alterations of 214, 92, and 53 phosphopeptides were observed after 1, 6 and 24 hours, respectively. Differentially altered phosphopeptides belonged to many signaling pathways including the ubiquitin-proteasome pathway, cytoskeletal regulation by Rho GTPase, calcium signaling, and TGF-β signaling. Thus, in this study a workflow for relative quantitation of phosphopeptides was established that may be later applied to precious biopsy samples. Along with this, TGF- β1 induced phosphoproteome was analysed in HL-1 cardiomyocytes.

1. Introduction

The term cardiomyopathy means "Disease of heart muscles" and was first used in 1957. The European Society of Cardiology (ESC) has initially defined cardiomyopathy as a myocardial disorder with structural and functional impairment of heart muscles, in the absence of coronary heart disease, hypertension, valvular disease, and congenital heart disease [1]. The World health organization (WHO) launched a task force "International Society and Federation of Cardiology" in 1980 to establish a consensus on the definition and nomenclature of cardiomyopathy [2]. Since then, as the understanding of this disease was growing rapidly, the nomenclature and classification of cardiomyopathy have likewise changed in steps with advancements in the field. The American Heart Association (AHA) had divided cardiomyopathies into two major groups; primary and secondary, based on prominent organ involvement [3]. Primary cardiomyopathies (genetic, mixed, or acquired) were predominantly confined only to heart muscles, whereas secondary cardiomyopathies show pathophysiological alterations of the myocardium along with a variety of multi-organ disorders. However, to differentiate primary and secondary cardiomyopathy becomes very tedious considering the fact that many primary cardiomyopathies are associated with extracardiac manifestations too, and many secondary cardiomyopathies are predominantly displayed by a dysfunctional heart alone. To simplify the issue, the European Society of Cardiology proposed a new classification system, wherein cardiomyopathies are grouped based on their morphology and functional phenotypes [1]. The new method of nomenclature is described in Fig. 1.
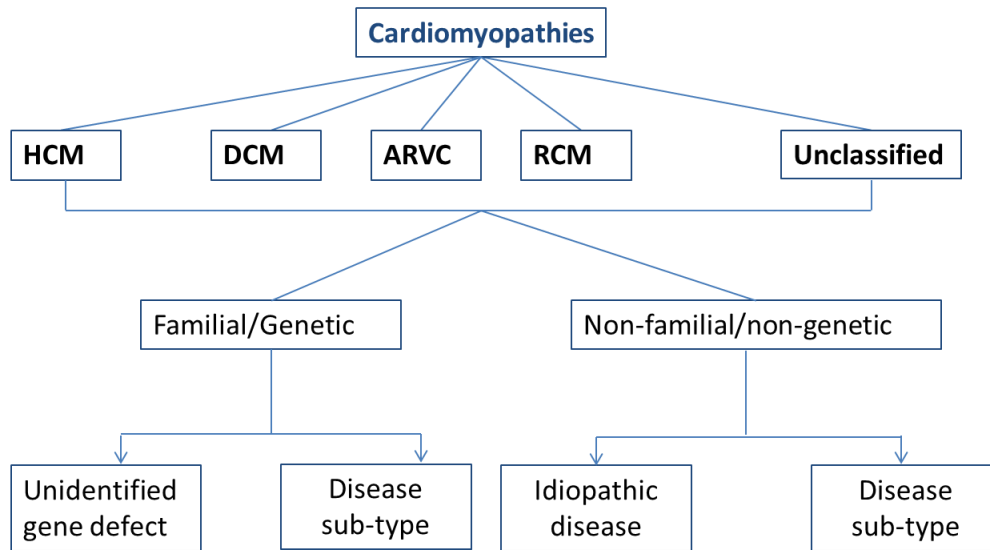
Fig. 1. Classification of cardiomyopathies proposed by the European Society of Cardiology: Cardiomyopathies are classified according to their morphology and phenotypes and grouped as HCM, DCM, ARVC, RCM, and unclassified. Further, based on their etiology these groups were subdivided into familial and non-familial subcategories. HCM- Hypertrophic cardiomyopathy; DCM- Dilated cardiomyopathy; ARVC- arrhythmogenic right ventricular cardiomyopathy; RCM- restrictive cardiomyopathy [1].

Hypertrophic cardiomyopathy is characterized by the presence of increased ventricular wall thickness in the absence of systemic disease (e.g., systemic hypertension, aortic valve stenosis), which is the most common cause of sudden cardiac death in younger individuals and athletes [1]. RCM is a heart disease of impaired ventricular filling with normal or reduced systolic volume of either one or both ventricles. It is known as restrictive because of restrictive filling of ventricles in which the increased stiffness of the myocardium causes high ventricular pressure by rising small volume in ventricles [1]. ARVC is characterized by the presence of progressive replacement of left ventricular myocardium with adipose or fibrous tissues [1].

Among all aforementioned different types, dilated cardiomyopathy is the most common and most studied cardiomyopathy. DCM is a chronic heart disease phenotypically recognized by dilation of either the left or both ventricles, systolic dysfunction and deterioration of the myocardium. It is a condition in which the heart muscles become thin, weakened, and cannot pump blood efficiently to the entire body [1, 3] (Fig.2).

Healthy Heart   **DCM Heart**
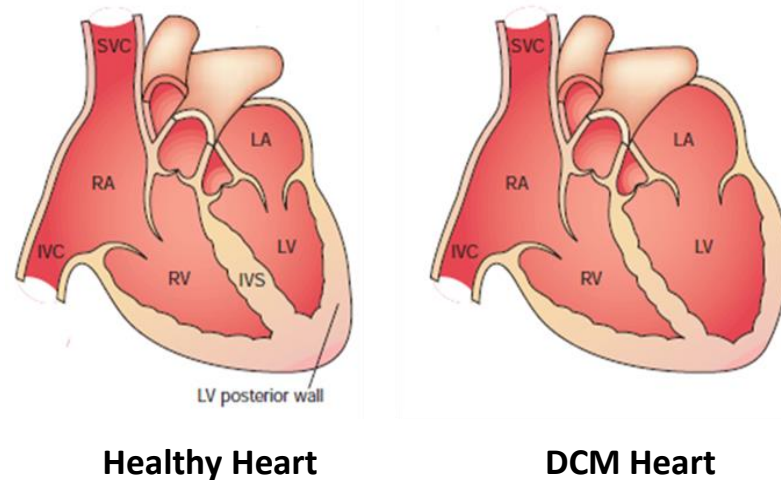
Fig. 2. Illustration of healthy and dilated cardiomyopathy heart: The healthy heart shows the proper size of ventricles, whereas the DCM heart displayed an enlarged left ventricle, thin ventricular wall and bulged interventricular septum. (LV-left ventricle, LA-left atrium, RV-right ventricle, RA-right atrium, IVS-interventricular septum, IVC-inferior vena cava, SVC-supra ventricular septum) [4].

DCM is a serious public health problem. It is the leading cause of heart failure and the primary indicator for heart transplantation with an associated cost of about $250 million per year in the United States [5]. The global number of deaths attributed to DCM and myocarditis increased to 40.8% from 286,800 to 403,900 between 1990-2010 [6]. The incidence of DCM is more prevalent between 18-50 year of age, but children and elder individuals are also affected. The disease frequency is higher in men than in women (2.5:1) and is higher in African Americans than in Caucasians.

About thirty to forty % of the DCM cases are attributed to familial background and caused by heterogeneous genetic mutations whereas a greater proportion (≈40%) of DCM patients are idiopathic (unknown origin) [4]. Besides these, a variety of factors causes DCM including; parasites (*Trypanosome cruzi*), bacteria (*Borrelia burgdorferi*), viruses, chemotherapeutic agents (anthracycline, doxorubicin, and daunorubicin), chronic alcohol consumption, and toxins.

More than 20 mutant gene loci in genes encoding contractile sarcomeric, cytoskeletal, nuclear envelope, and transcriptional coactivator proteins have been associated with DCM [3, 4, 7]. Among

them, ten genetic loci were mapped for pure DCM (Table 1). Mutations in cardiac actin (sarcomeric protein), alpha-tropomyosin, desmin, β-sarcoglycan, δ-sarcoglycan, and β-myosin heavy chain have been associated with DCM [8–12]. Additionally, a mutation in the nuclear envelope protein Lamin A/C has also been shown to be involved in the progression of dilated cardiomyopathy [13]. Cardiac actin protein interacts with tropomyosin, troponin and dystrophin proteins for the contraction of the sarcomere [14]. Desmin, a cytoskeletal protein forms intermediate filaments and helps in the stabilization of the sarcomere [9]. In general, several genes and proteins have a significant structural and functional role in a tightly coordinated fashion to maintain the proper functioning of the heart.

Table 1. Genes and proteins involved in dilated cardiomyopathy.

Ten genetic loci involved in pure DCM have been listed with their inheritance pattern, chromosomal positions, and associated gene with protein [3].

Inheritance pattern	Chromosomal locus	Gene and Protein
X-linked	Xp21	Dystrophin
X-linked	Xq28	G4.5
Autosomal dominant	15q14	Actin
	2q35	Desmin
	5q33	δ-Sarcoglycan
	1q32	Troponin T
	14q11	ß-Myosin heavy chain
	15q2	α- Tropomyosin
	MtDNA	Mitochondrial respiratory chain
	1q21	Lamin A/C

Genetic heterogeneity leads to cardiac remodeling which changes heart structure and function by alteration of multiple cellular and metabolic pathways. Delineation of these molecular events triggered by gene mutations in cardiomyocyte provided new fundamental knowledge about heart physiology and defined mechanistic pathways that lead to DCM and heart failure [15]. Hence, understanding the modulation of these networks in the DCM heart can be useful for therapeutic

interventions. Additionally, these genetic discoveries might be helpful to clinicians for the early diagnosis and prognosis of DCM patients from their family history [16].

Besides genetic roots, many viruses have been suggested as a causative agent of DCM [17–19]. Virus infection may lead to inflammation of the myocardium- a pathological condition known as viral myocarditis and often progresses to DCM [20]. The most common viruses involved in myocarditis includes adenoviruses and enteroviruses such as coxsackieviruses [21]. The variety of viruses that causes DCM has been listed in Table 2 along with their localization sites.

Table 2. List of viruses found in endomyocardial biopsies (EMBs) of DCM patients with their target locations [21].

Common viruses in EMBs	Major localization in the heart
Adenovirus	Cardiomyocytes, fibroblasts, endothelial cells
Enterovirus/Coxsackievirus	Cardiomyocytes
Parvovirus B19	Endothelial cells, cardiomyocytes
Human herpes virus 6	Endothelial cells
Cytomegalovirus	Cardiomyocytes
Epstein-Barr virus	Lymphocytes
Influenza virus	Macrophages, lymphocytes
Hepatitis C virus	Cardiomyocytes
HIV	Cardiomyocytes, Macrophages

Many clinical studies have documented virus persistence in endomyocardial biopsies, and it was assumed to initiate autoimmune mechanisms that may aggravate the pathological development of DCM [18, 19]. Impairment of both cellular (cell-mediated) and humoral immunity has been extensively discussed in DCM patients [22, 23].

Effector cells of cell-mediated immunity are T-lymphocytes that express T-cell receptors (TCR) on their cell surface. TCRs recognize peptide sequences presented to them by antigen-presenting cells (B-lymphocytes and dendritic cells) with the help of major histocompatibility complex (MHC) surface molecules [24]. Higher percentage of helper T-cells and higher T-cell helper/ suppressor

ratios have been observed in idiopathic dilated cardiomyopathy (IDCM) patients signifying an excessive immune reaction as part of the pathogenesis of IDCM [25]. The immunohistological analysis of endomyocardial biopsies has demonstrated increased lymphocytic infiltrates, and a higher number of major histocompatibility complex antigens and adhesion molecules in DCM patients [26]. The accumulation of lymphocytes in myocardial tissues induces cell-mediated cytotoxicity, leading to fibrotic events [23]. The naive helper T-cells (Th) stimulated by antigen presenting cells differentiate into two subcategories Th1 and Th2

Th1 (CD4$^+$ T cells) secrete interleukin-2, interferon-γ, and tumor necrosis factor that mainly promotes cellular immunity whereas Th-2 cells produce inteleukin-10, interleukin-5, and interleukin-4 that primarily induce humoral immunity. The regulation of Th1/Th2 has been shown pivotal in DCM patients, and its imbalance might aggravate DCM [27]. Additionally, animal studies also confirmed that either injury or infectious agents can trigger an immune response consequently resulting in dilated cardiomyopathy and myocarditis [28].

The humoral immunity is mediated by macromolecules such as secreted antibodies, complement proteins, and antimicrobial peptides found in extracellular fluids. The main effector molecules of humoral immunity are antibodies that recognize foreign antigens and differentiate into effector B cells to produce and secrete antigen-specific antibodies. In autoimmune conditions, the immune system is unable to discriminate between self and foreign antigens, and heart subcellular structures and cellular organelles also can be targeted by cardiac autoantibodies [29]. A high titer of circulating cardiac autoantibodies has been reported in the plasma of DCM patients [29, 30]. These antibodies initiate the activation of humoral and cellular immunity [31]. The cardio depressive role of autoantibodies in DCM has been reported in various human and animal studies [32–36]. These autoantibodies are produced against many cardiac structural proteins, mitochondrial proteins, and membrane proteins (Table 3).

Table 3. Overview of autoantibodies associated with DCM and other cardiomyopathies.

Autoantibodies related to cardiac disease and their antigenic locations with the possible pathomechanism according to Kaya el. al. [29].

Antibody	Cardiomyopathy	Antigenic Location	Pathomechanism
Anti-β1-receptor	DCM	Cell surface	Negative Ionotropic
Anti-M2-receptor	IDCM	Second extracellular loop M2	Positive ionotropic
Anti-mitochondrial M7	DCM, Myocarditis	mitochondrial membrane	Unknown
Adenine-nucleotide transporter	IDCM, DCM	Mitochondrial matrix	Alteration in energy metabolism
Myosin heavy chain α, β	DCM	Atrial cardiomyocytes	Negative ionotropic
Antitropin 1	DCM (Mouse)	Cell surface	Negative Ionotropic
Anti-Na-K-ATPase	IDCM (Human)	Alpha3-subunit	Anti arrhythmogenic effect
Anti-hsp60	DCM (Rabbit)	Sarcolemma transmembrane	Cardiac hypertrophy
	DCM (Human)	-	-
Antiserotoninergic 5-HT4 Receptor	Congenital heart block (Human)	Cell surface	Unknown
Anti-laminin	DCM	Extracellular	Unknown
Antiactin	DCM	-	Unknown
Anti-myosin light chain-1	DCM	-	Unknown

Autoantibodies against β1-adrenoreceptor (G-protein coupled receptor) were first discovered in serum of DCM patients [35], and their pathogenic role in the progressive development of DCM was experimentally proven in animal studies [37, 38]. Also, antibodies against β1-adrenoreceptor displayed a positive chronotropic effect when human sera of DCM patients were incubated with isolated rat cardiomyocytes [39]. In another study, circulating antibodies to muscarinic M2-receptor were discovered which reduced ventricular contractility and promoted dilated cardiomyopathy [37]. Many studies have shown antibodies against mitochondrial proteins including M7 and ATP/ADP translocase in DCM patients [40, 41].

Anti-myosin antibodies that alter the Ca^{+2} sensitivity of myofilaments and reduce the contractility of cardiomyocytes were also reported in sera of DCM patients [42]. Anti-cardiac myosin antibodies can cross-react with β1-adrenoreceptor and thereby induce cAMP-dependent PKA activity in heart cells, which may contribute to myocardial dysfunction and apoptosis of cardiomyocytes [43]. Studies using mouse models have also shown anti-cardiac myosin antibodies that might lead to myocarditis [44]. Cardiac troponin-I is an important component of the regulatory network of the thin filament of muscle fibers, which play a vital role in cardiomyocytes contraction [45]. Anti troponin-I antibodies were discovered in programmed cell death-1 (PD-1) deficient DCM mice and induced heart dysfunctions and dilation by stimulation of Ca^{+2} influx into cardiomyocytes [46]. Anti-Na-K-ATPase autoantibodies that led to electrical instability and sudden death of DCM patients were detected in 26% of DCM patients. Autoantibodies against stress proteins like hsp-60, hsp-70, and heat shock cognate protein (hsc) 70 were also detected in sera of DCM patients [47].

In general, the adverse effect of cardiac autoantibodies has been studied extensively; therefore, removal of these autoantibodies is expected to lead to clinical benefits in DCM patients. Hence, their elimination from plasma of DCM patients using immunoadsorption (IA) with IgG substitution (IA/IgG) was observed to be associated with long-term benefits in cardiac performance such as increased left ventricular ejection fraction (LVEF), cardiac index and endothelial function [48–51]. After IA cycles, 0.5 g/Kg polyclonal IgG was substituted intravenously to restore the IgG plasma levels and to reduce the risk of infection. The working mechanism of IA is shown in Fig. 3.
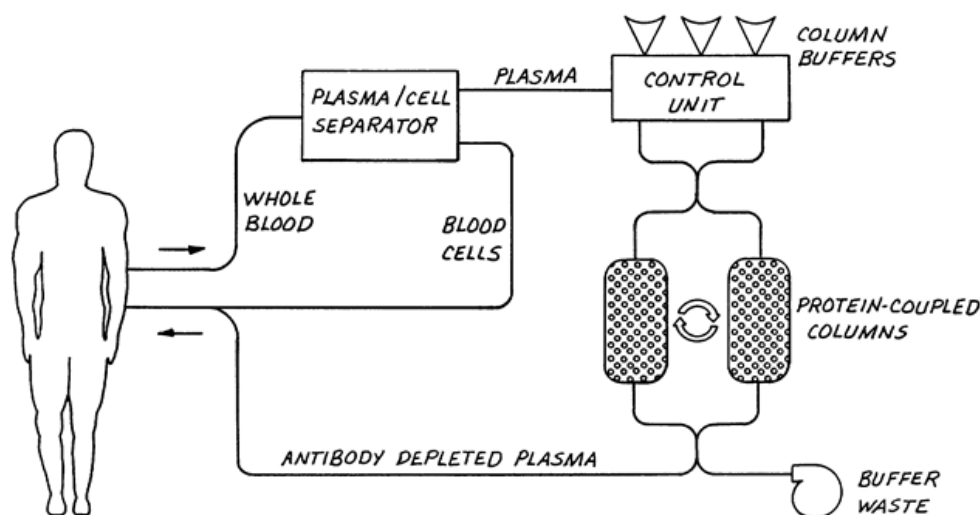
Fig. 3. Action mechanism of immunoadsorption therapy (IA/IgG)

The immunoadsorption (IA) treatment comprises passing the human plasma over a column coupled to a particular ligand to deplete human immunoglobulins, and re-infusion of plasma into the patient [52]. After IA, immunoglobulins were substituted intravenously to restore immune function.

The removal of circulating IgG antibodies using immunoadsorption therapy improved the heart function with a shift to a lower NYHA (New York Heart Association) class in DCM patients [53]. The beneficial effect of IA/IgG was also associated with a decrease in oxidative stress markers like lipid peroxidase, anti-oxidized low-density lipoprotein, and thiobarbituric acid-reactive substances (TBARS) in plasma of DCM patients [54]. Additionally, levels of the prominent heart failure plasma markers nt-BNP and nt-ANP were also decreased by IA/IgG after three months follow-up [55]. Immunoadsorption therapy also improved the cell-mediated immunity by decreasing circulatory activated T cells (CD4+/CD69+ and CD8+/CD69+) and a higher level of regulatory T cells and reduced myocardial inflammation [56]. It has also been shown that removal of autoantibodies was associated with a decreased gene expression of desmin in endomyocardial biopsies of DCM patients [57]. Moreover, IA/IgG not only improved the hemodynamic parameters but also reduced the morbidity in DCM patients [58].

Although the benefit of IA/IgG to DCM patients is given, the underlying mechanism of immunoadsorption therapy in DCM patients is still elusive. Also, therapy-induced molecular changes in the myocard have not been studied extensively so far. The comprehensive knowledge of mRNA and protein alterations upon IA/IgG in the heart might help to delineate pathways, networks and molecular processes affected by therapy.

The response rate of IA/IgG is variable among DCM patients [59], and the reason for this variability is barely understood. Only about 60-70% DCM patients profit from immunoadsorption therapy. Due to the invasive character and the high costs of the treatment [60], it would be desirable to know the individual response before the therapy is applied. However, no symptomatic prognostic biosignatures are known so far that could be clinically useful in guiding patient's treatment regimen. Felix et al. suggested that a Fcγ -receptor polymorphism in patients might lead to different binding efficiencies of autoantibodies to the receptor on the surface of cardiomyocytes thereby influencing the clinical manifestation of the disease and the opportunity to benefit from autoantibody removal [59]. Disease duration and titer of autoantibodies have also been shown as an independent predictors of therapy outcome. DCM patients with shorter disease duration tend to profit more from IA/IgG [59]. Additionally, negative inotropic and chronotropic activity of autoantibodies on rat cardiomyocytes could also be an independent predictor of therapy [61]. Recently, Ameling et al. have identified a myocardial gene signatures to predict improvement of LVEF after IA/IgG [62]. Protein based biosignatures might also be important in this aspect as proteins are the key functional player in cells.

The branch of science to study the proteome (entire proteins of the genome of a particular cell type or tissue at a particular stage of differentiation) is known as proteomics. The term "proteomics" was first coined in the year 1997 [63]. Proteomic-based technologies have gained momentum over the last decades with the evolution of several innovative approaches. The study of the proteome is challenging, and the wide spectrum of technologies used usually involves protein separation,

protein identification, relative as well as absolute quantification, and characterization of the nature and position of post-translational modifications (PTMs). Since 1975, two-dimensional gel electrophoresis (2-DE) along with mass spectrometry has been extensively used to decipher the proteome of cells, organs and biofluids [64]. In this technology, a mixture of proteins is separated in two dimensions based on their isoelectric points (pI) and molecular masses (Mw) on polyacrylamide gels. Further, coomassie brilliant blue or silver stained protein spots are identified using mass spectrometry. Later, a pre-electrophoretic fluorescent staining method called differential in-gel electrophoresis (DIGE) has become the preferred choice among gel-based methods to explore the differential abundance of proteins [65]. 2-DE has been extensively implemented to characterize the heart proteome for cardiac disease-specific changes in humans, animals, and in cultured cardiomyocytes [66–68]. Based on the 2D-gel identifications of cardiac proteins, heart 2-DE protein databases (HSC-2DPAGE, HP-2DPAGE, HEART-2DPAGE, RAT HEART-2DPAGE) were created by different working groups that may facilitate the proteomic research to heart disease [69–73]. 2-DE has also been implemented to decipher the heart disease associated phosphoproteomic changes in different studies [74, 75].

Although two-dimensional gel electrophoresis in combination with mass spectrometry provides robust identification and relative quantification of proteins, nonetheless it remains constrained in comparison to non-gel based proteomic approaches in several aspects. Gel based technologies fail to detect low abundance (cytokines, and chemokines), extremely acidic and basic, membrane, hydrophobic, and extreme high or low molecular weight proteins. These above-mentioned limitations can be at least partially overcome by the implementation of gel-free or LC-MS/MS approaches. The gel-free method includes two major strategies, named; top-down, and more commonly implemented bottom-up proteomics (shotgun proteomics). In the bottom-up strategy, proteins are digested using proteolytic enzymes (trypsin, chymotrypsin, Lys-C) and the resultant mixture of peptides is resolved by using different fractionation methods prior to mass spectrometry.

Bottom up proteomics offers high-throughput proteome data with wide proteome coverage [76–78]. Top-down MS methods focus on the analysis of intact proteins, rather than peptides.

Top-down proteomic preserves all information related to the intact proteins including PTMs and alternative splicing events [78, 79] but is limited in large scale due to a lack of intact protein fractionation methods prior to mass spectrometry.

Besides identification, relative quantification of proteins also plays a pivotal role in understanding the pathophysiology of diseases including DCM. Since a number of years, various label-free and label-based quantitative proteomic methods have been developed. The labeling methods for relative quantification can be classified into two major groups; chemical and metabolic labeling. Metabolic labeling includes Stable Isotopic Labelling with Amino Acids in Cell Culture (SILAC) [80]. In SILAC heavy arginine and lysine amino acid labels are introduced to the whole cell organism through the growth medium. Thus, it is restricted only to cell culture-based and animal studies. The chemical labeling methods include Isotope-Coded Affinity Tags (ICAT) [81], ^{18}O stable isotope labeling [82], Isotope-Coded Protein Labelling (ICPL) [83], Isobaric Tags for Relative and Absolute Quantification (iTRAQ) [84], and Tandem Mass Tag (TMT) [85]. In chemical labeling, peptides or proteins are tagged by a chemical reaction and chemical labeling methods have been extensively used for human, animal and cell culture-based studies [86]. All labeling approaches are based on the fact that the differentially labeled peptides exhibit the same chromatographic and ionization properties, and can be distinguished from each other by a mass shift signature. Unlike ICAT and IPCL, iTRAQ tags are isobaric (constant molecular mass, 4plex-145 Da, and 8plex-304 Da), and peptides are labeled at the N-terminus and lysine residues. The structure of iTRAQ reagents consists of a reporter group, a mass balance group and a peptide reactive group (NHS ester). The relative quantification of peptides in iTRAQ is based on the relative intensity of reporter ions (m/z range, 114-121), which are produced by the fragmentation of precursor ions during MS/MS fragmentation. The major advantage of the iTRAQ technology over label-free approaches

is multiplexing of up to eight different biological or technical replicates into a single LC-MS/MS run that reduces the technical variation and yields highly reproducible quantitative data. The iTRAQ technology has been implemented in many studies related to heart disease including human and animal studies [87–89].

Using iTRAQ in combination with nano-LS-MS/MS twelve proteins of HDL were discovered in plasma distinguishing patients with coronary heart disease (CHD) and healthy subjects [90]. Also, sixty-five differential mitochondrial proteins were found between diabetic heart failure and healthy rats using a iTRAQ LC-MS/MS workflow [91].

The iTRAQ technique has also been preferred to label-free quantitative methods to screen for protein biomarkers in plasma or serum because of its multiplexing option, which reduces the time of measurements in mass spectrometry in larger sample sets, or helps in covering low abundance plasma proteins by implementing cation or anion exchange fractionation after labeling.

Plasma is an important biofluid to screen for biomarkers because it is easily and minimally-invasively obtained. Proteome analysis of plasma is challenging due to the huge dynamic range of proteins ($\approx 10^{12}$) and the presence of highly abundant proteins that mask the identification of proteins of lower abundance [92]. Therefore, to increase the coverage of low abundance proteins, it is essential to remove (deplete) highly abundant proteins from plasma before LC-MS/MS analysis. Many commercial kits are available for the removal of highly abundant proteins such as albumin, IgG, IgA, transferrin, antitrypsin, haptoglobin, and fibrinogen from plasma. Thus, plasma depletion followed by iTRAQ labeling and strong cation or anion exchange fractionation prior to LC/MS-MS analysis has become a robust choice in protein biomarker discoveries. MS analysis of plasma, depletion of highly abundant proteins followed by digestion and iTRAQ labeling revealed seventeen plasma proteins associated with recovered heart function in heart transplant patients [87].

Quantitative proteomics based on labeling strategies often requires costly labeling reagents, high initial protein amounts, and tedious sample processing. Label-free LC-MS/MS is cost efficient and

rather simple in sample processing in comparison with labeling approaches, and could be therefore an alternative for relative quantification of peptides and corresponding proteins [93], specifically in biopsies analysis that is always restricted by small amount of materials. The relative quantification using label-free methods is either based on the precursor ion intensity or spectral ion counts. Intensity-based quantification relies on the relative area of precursor ions obtained in MS, and is highly dependent on the reproducibility of liquid chromatography and ionization levels.

In contrast, spectral count quantification is based on the number of spectral counts obtained in the MS/MS. The peptide abundance in both methods is directly correlated either to the intensity/area of precursor ion obtained in MS1 or number of spectra obtained in MS/MS [93]. A label-free strategy has also been implemented to decipher cardiac proteins of relevance in dilated cardiomyopathy. Recently, a using label-free approach, Hammer et al. discovered 174 proteins of endomyocardial biopsies that differed in intensity in inflammatory dilated cardiomyopathy patients in comparison to healthy controls [94].

Besides protein identification and quantification, the study of the phosphoproteome is equally pivotal as many signaling events are heavily perturbed in heart tissues in diseased states and altered signaling events might deteriorate the disease status. However, global phosphoproteome approaches to decipher signaling events in human specimen (endomyocardial biopsies) are challenging because in general these studies require a high amount of material (≈1-10 mg), which is a real challenge for the analysis of heart biopsies samples. However, a recently developed, polymer-based phosphopeptide enrichment strategy requires only microgram amounts of initial material, and it is suitable for relative quantitation of phosphopeptides in large-scale phosphoproteomic studies [95] but has not been optimized in heart tissue samples. For the optimization purpose, instead of using real biopsies samples, HL-1 cardiomyocytes can be used that mimic human cardiac physiology and have therefore already been extensively used to understand cardiac physiology [96, 97]. HL-1 cardiomyocytes divide continuously, contract

spontaneously, and maintain an adult cardiac phenotype [98]. Thus, it is a suitable model to decipher cardiac cellular and molecular events at proteome and phosphoproteome levels.

The results obtained in shotgun proteomics are usually further confirmed using another method like Western blot analysis or ELISA-based immunoassay methods. These traditional methods are often restricted by the availability of the antibody or appropriate amounts of tissue material (biopsy samples). Also, they are costly and time-consuming [99]. The advancement of innovative proteomic technology has led to the development of Multiple Reaction Monitoring (MRM), which can overcome aforesaid limitations and can be successfully applied to all kind of samples to validate dozens of proteins in a single LC-MS run with high precision and accuracy [100, 101].

MRM experiments are usually performed by triple quadrupole mass spectrometry. In the first quadrupole (Q1), ions of interest (precursor ions) are selected and fragmented in a second quadrupole (Q2) with collision-induced dissociation (CID) energy. Further specific fragment ions (transition ions) are detected in the third quadrupole (Q3). MRM has been extensively used for relative and absolute quantification of peptides, phosphopeptides, and their corresponding proteins in several heart diseases studies [87, 102, 103].

In general, proteomics has been tremendously applied in several heart diseases including dilated cardiomyopathy to understand the mechanistic changes in the heart and has the potential to explore disease-related biomarker discoveries. Careful experimental design and implementation of multiple advanced technologies definitely would provide us deeper insights into cardiac biology and in discoveries of drugs and treatment strategies.

Objectives of Study

Dilated cardiomyopathy is a myocardial disorder characterized by reduced left ventricular systolic function with diminished cardiac function. Immunoadsorption (IA) followed by immunoglobulin (IgG) substitution has been reported a promising therapeutic intervention to treat dilated

cardiomyopathy patients. However, the basic molecular alterations initiated by IA/IgG in the heart leading to improvement of cardiac performance remain elusive, and the reasons for the variable therapy outcome among DCM patients has been poorly understood. Thus, in the current study the following objectives have been addressed:

Objective 1. To understand the immunoadsorption (IA/IgG) therapy induced molecular changes in the heart, a label-free LC/MS-MS based proteome profiling of human endomyocardial biopsies from responder and non-responder DCM patients before and after six months of therapeutic intervention was performed, and therapy-induced protein alterations were compared. The differentially abundant proteins obtained by label-free quantification were further mapped for functional pathway categorization using PANTHER and Ingenuity Pathway Analysis (IPA) to understand the IA/IgG induced molecular alterations in the myocardium.

Objective 2. In this aim, efforts were made to discover a panel of protein biomarker candidates in endomyocardial biopsies and plasma of responder and non-responder DCM patients before immunoadsorption therapy that might be useful for clinicians for the selective treatment of a subgroup of patients, who tend to gain benefit from IA/IgG. To elucidate the proteome differences between responders and non-responders at baseline, a label-free method was used for endomyocardial biopsies analysis whereas an iTRAQ approach was implemented for plasma proteome profiling. The differentially abundant proteins that discriminate responder and non-responder DCM patients at baseline discovered in shotgun proteomics were further confirmed using multiple reaction monitoring mass spectrometry and ELISAs. Moreover, differentially abundant proteins were mapped for pathway enrichment and network analysis using PANTHER and Ingenuity Pathway Analysis (IPA). Also, biomarker potential of protein panels was assessed by plotting and interpretation of Receiver Operating Characteristic (ROC) curves.

Objective 3. The last aim of the thesis was to establish a workflow for phosphoproteome analyses for the relative quantitation of phosphopeptides that can be later applicable to minute amounts of

material (≈micrograms) as it is available from heart biopsies. The prerequisite for phosphoproteome profiling is to enrich the phosphopeptides prior to mass spectrometric analysis. Phosphopeptides enrichment was established using polyMAC Ti kit. Simultaneously, transforming growth factor beta-1 (TGFβ1) induced phosphoproteome in HL-1 cardiomyocytes were evaluated. This study might provide the TGFβ induced phosphoproteome changes in cardiomyocytes and would strengthen the understanding of TGFβ associated signaling in the heart.

2. Materials and Methods

2.1 Materials

2.1.1 Chemicals

Chemicals Name	Source
Acetic acid	Roth
Acetonitrile	J.T Baker
Ammonium bicarbonate	Sigma
Bradford reagent	BioRad
Dithiothreitol (DTT)	PlusOne
Ethanol	Roth
Formaldehyde	Roth
Formic acid	Merck
Hydrochloric acid	Roth
Iodoacetamide	Sigma
Isopropanol	Merck
Methanol	Roth
Phosphoric acid 85%	Roth
polyMAC-Ti phosphopeptides enrichment kit	Tymora Analytical
Protein S100-A8 ELISA kit	Circulex
Protein S100-A9 ELISA kit	Circulex
Sep-Pak C18 column	Sigma
Thiourea	Sigma
Trypsin	Sigma
Urea	Merck

2.1.2 Instruments

Name	Source
Heraeus Fresco 17 centrifuge	Thermo Scientific
LTQ Orbitrap Velos	Thermo Electron
LTQ Orbitrap XL	Thermo Electron
Sonicator	Bandelin Sonoplus
TSQ vantage	Thermo Electron
Ultrospec 2100 pro spectrophotometer	Amersham Biosciences
VarioskanFlash spectrophotometer	Thermo Scientific

2.1.3 Software's

Name	Source
Elucidator	Rosetta Ceiba Solutions
Gene Data Expressionist Analyst	Gene Data
Ingenuity Pathway Analyst	Ingenuity Systems
Proteome Discover	Thermo Scientific
Skyline	University of Washington, Seattle, WA, USA

2.2 Methods

2.2.1. Biological samples

2.2.2.1 Human endomyocardial biopsies and plasma samples

The study includes a subset of DCM patients who presented to University Hospital Greifswald, Germany and were treated with immunoadsorption therapy (IA/IgG). All patients exhibited severe heart failure symptoms (LVEF ≤ 45%) according to New York Heart Association (NYHA) class II and III. Patients with angiographically proven coronary heart disease or acute myocarditis as per Dallas classification were not considered. Patients had not suffered from cancer, hypertension, postpartum cardiomyopathy, infectious diseases, ischemic heart disease and alcoholic cardiomyopathy. Patients were on stable medical regimen 3 months before therapy start and along the whole study period of six months, including beta-blockers, angiotensin-converting enzyme (ACE) inhibitors, angiotensin 1 antagonists, diuretics, and digitalis. The endomyocardial biopsies (EMBs) (before and after six months of immunoadsorption therapy) were taken for histological and virological examination. Endomyocardial biopsies taken by clinicians were immediately frozen at -80^0 C and used for clinical examination; the remaining samples were employed in the following proteome studies. Also, EDTA-plasma was collected from DCM patients at baseline and six months after immunoadsorption therapy and stored in a freezer (-80^0C) for further use. Plasma was also sampled from healthy individuals.

Written informed consent was obtained from all DCM patients and probands, and the study was approved by the hospital ethics committee of University Medicine Greifswald, Germany. All medical and basic research was performed in accordance with the ethical standards given in 1964, Declaration of Helsinki.

2.2.1.2 HL-1 cardiomyocyte cultivation

HL-1 cardiomyocytes were a gift from Dr. Claycomb (Louisiana State University, LA, USA) and cultured as instructed to retain their morphology and physiology. Briefly, HL-1 cardiomyocytes were taken from the frozen stocks and transferred into culture dishes pre-coated with fibronectin and gelatin (0.02% each) with Claycomb medium supplemented with 10% fetal bovine serum, 10U/ml penicillin/streptomycin, 0.1mM norepinephrine, and 2mM L-glutamine. The cultures were maintained at 37^0C in a humidified atmosphere of 5% CO_2 until cells were fully confluent. Furthermore, confluent cells were passaged in eighteen T-24 flasks pre-coated with fibronectin/gelatin. Again, cells were cultured until full confluence in a CO_2 incubator and medium was changed every 24 hours. Consequently, cells were incubated in the presence of TGF-β1 (10ng/ml) for 1, 6 and 24 hours (three replicates each). Cells incubated without TGF-ß1 served as controls. After treatment for the appropriate time, controls and TGF-β1 treated cells were dislodged from the surface of flask by incubation with trypsin EDTA (2-3 min at 37^0C). Flasks were checked by microscopy and once all cells had been removed from the surface, trypsin inhibitor was added to inactivate the trypsin. Cells were collected into tubes and centrifuged at 500g for 5 minutes. The obtained cell pellets were re-suspended in 8 M urea/2 M thiourea solution (UT) and protein extraction was performed using multiple freeze-thaw cycles.

2.3 Clinical data

2.3.1 Immunoadsorption therapy in DCM patients

Immunoadsorption (IA) was carried out on DCM patients with one session daily for five consecutive days using Protein-A columns (Immunosorb®, Fresenius Medical Care AG, Bad Homburg, Germany) to deplete IgG3. After the last IA cycle, 0.5 g/Kg polyclonal IgG (Venimmun N® , Sandoglobulin® , CSL Behring, Germany) was administered intravenously to restore the IgG plasma levels and to reduce the risk of infection. All patients were under scrutiny at least for six months after IA/IgG. According to the IA/IgG effect on the cardiovascular potential patients were grouped as responders (R) if LVEF increased $\geq$ 20% relative to the BL value in addition to an increase in LVEF $\geq$ 5% absolute value whereas the rest were non-responders (NR) (relative change in LVEF < 20% or LVEF < 5% absolute value).

2.3.2 Histology and clinical findings

Left ventricular ejection fraction (LVEF), according to simpson rule and left ventricular inner diameter in diastole (LVIDd) were measured using 2-dimensional echocardiography. Two independent clinicians, who were unaware the clinical variables of patients, examined the echocardiographic images. Immunohistochemical analysis of endomyocardial biopsies was performed at the Department of Molecular Pathology, University Hospital Tübingen, to assess the inflammatory status of the myocardium and determined by quantification of mononuclear infiltrates of CD3+ T lymphocytes and/or CD68+ macrophages in the myocardium [104, 105]. The presence of viral genomes was evaluated using nested real-time polymerase chain reaction (qRT-PCR) [104].

2.4 Sample preparation

2.4.1 Protein extraction from endomyocardial biopsies (EMBs)

Three to four endomyocardial biopsies (EMBs) per patient were pooled and crushed with a pestle in liquid nitrogen to make a fine powder. 60% of this powder was homogenized using a bead mill (Micro dismembrator S, Sartorius, Gottingen, Germany) at 2600 rpm for two minutes, and reconstituted into 50 µl rehydration buffer (8M urea, 2M thiourea). The extract was further sonicated on ice three times each for five seconds with eight cycles. The extract was then centrifuged at 16,000 g for 1 hour at 4^0 C to remove cell debris. Supernatant was collected, and protein concentrations were measured using a Bradford assay kit (Pierce, Thermo Scientific, Bonn, Germany). Protein aliquots were stored at -80^0 C until further used.

2.4.2 Plasma isolation from human blood

The blood drawn from DCM patients before and after IA/IgG was collected in vacutainers (EDTA tubes, Beckton Dickinson, Heidelberg, Germany) and immediately stored at 4^0 C for 30 minutes. Subsequently, blood was centrifuged at 2,000 g at 4^0 C for 15 min and supernatant (plasma) was collected in reaction tubes. Furthermore, plasma was aliquoted immediately and stored at -80^0C until further use.

2.4.3 MARS depletion

To remove top six high abundant plasma proteins (albumin, IgG, IgA, transferrin, haptoglobin, and antitrypsin), multiple affinity removal column Human 6 (MARS6, Agilent Technologies, Waldbronn, Germany) coupled with a HPLC (Chromaster, VWR, Darmstadt, Germany) was used. The plasma samples were diluted with Agilent Buffer A (1:4) and filtered using 0.22-µm spin filters (Ultra free-MC 0.22 µm, Millipore) to remove particulates. Filtered plasma was injected through an autosampler onto a MARS6 column, run at 100% buffer A at a flow rate of 0.25 ml/min for 9 min. Flow-through fractions (depleted plasma) were collected between minutes 2 and 4. Bound

proteins were eluted with 100% buffer B at a flow rate of 1.0ml/min for 5 minutes. The column was regenerated by equilibration in 100% buffer A for 8 min, yielding a total run cycle of 22 min.

Flow-through fractions were concentrated and desalted by trichloroacetic acid (TCA) precipitation. 170 µl TCA (100%) was added to 1ml of depleted fraction and incubated for one hour at 4^0C. Furthermore, solution was centrifuged at 13,000 rpm for 45 min at 4^0C. The supernatant was discarded, and protein pellets were twice washed with chilled acetone. Afterwards, pellets were dried to remove all organic residuals by placing tubes in speed vacuum concentrator for 1 min. Dried protein pellets were dissolved in 100 µl UT by shaking on a heat block at 1400 rpm for 20 min at 20^0C. Furthermore, protein concentrations of depleted plasma were measured using a Bradford assay.

2.4.4 Protein estimation using Bradford assay

To quantitate the concentration of protein samples, a series of known concentrations of bovine serum albumin (BSA) was used to prepare a standard curve as described in Table 4.

Table 4. BSA concentrations used for standard curve

BSA amount (µg)	0	1	2	4	6	8	10	12
0.1 µg/µl BSA (µl)	0	10	20	40	60	80	100	120
water (µl)	800	790	780	760	740	720	700	680

To each of the mixtures of BSA and water (Table 4), 200µl of Bradford reagent was added and after 5-minute incubation absorbance was measured in a UV spectrophotometer at 595nm and a standard curve was made. Protein samples were diluted ten times in UT and 10 µl diluted sample was used for estimation of protein concentration. Three replicates of each sample were measured, and mean absorbance was used to calculate the final concentration of the protein extract using a standard curve.

2.4.5 Trypsin digestion

An appropriate amount of protein (4-10 µg) was taken and reduced with dithiothreitol (DTT) to break disulfide bonds. 25mM DTT was prepared in 20mM ammonium bicarbonate (ABC) and incubated with the samples (final concentration of 2.5mM) for 1 hour at 60^0C. Further, alkylation was performed with iodoacetamide (IAA) prepared in 20mM ABC and incubated (final concentration 10mM) for 30 minutes at 37^0C in the dark. Proteolysis was performed using trypsin with an enzyme to protein ratio 1:10 w/w at 37^0 C for 18 hours. Subsequently, trypsin digestion was stopped by addition of 1% v/v acetic acid, and the resulting peptides were purified using $_\mu$C18-ZipTip columns (Merck Millipore, Darmstadt, Germany) for mass spectrometric analysis.

2.4.6 Purification of peptides using µC18-ZipTip columns

Tryptic peptides were purified/ desalted using C-18 resin tips with a capacity of 2µg/5µg (Millipore Corporation, Billerica MA). Firstly, µC-18 Zip Tips (2µg/5µg) were activated three times with 10 µl of 100% acetonitrile (ACN), and equilibrated stepwise with 80%, 50%, and 30% ACN in 1% acetic acid (each solution aspirated and dispensed five times). Further, final equilibration was obtained by two times washing with 10 µl of 1% acetic acid. Tryptic peptides were bound to the C18 matrix by aspiring samples 10 times. This step must be performed gently because air trapped in the matrix while aspiration step interferes the binding efficiency of the peptides to the resin. After peptide binding, C-18 Zip Tips were washed with 10µl of 1% acetic acid, 5 times, to remove hydrophilic low molecular weight contaminants. Further, peptides were eluted with 5µl of 50% ACN, and followed by 5µl of 80% ACN, each in 1 % acetic acid. Both eluted fractions were pooled and dried in a speed vacuum concentrator. Afterwards, peptides were dissolved in appropriate buffer - usually 20µl of 2% ACN in 0.1 % acetic acid for mass spectrometry analysis.

2.4.7 Enrichment of phosphopeptides using polyMAC-Ti kits

Enrichment of phosphopeptides was performed using polyMAC kits ((Tymora Analytical, West Lafayette, IN, USA) with the protocol recommended by the manufacturer with slight modifications. Tryptic peptides were desalted and dried in a speed vacuum concentrator. Further, peptides were dissolved in 100µl of kit loading buffer, vortexed well and 10µl of PolyMAC reagent was added. This solution was mixed properly and shaken vigorously for 15 min at 1200 rpm so that phosphopeptides bind to the polyMAC Ti-beads. Consequently, 200µl of capture buffer was added to increase the pH (>6.5) of solution and vortexed briefly. The solution containing PolyMAC beads and peptides was added to 50 µl of washed capture gel in a spin column and shaken vigorously for 15 minutes at 1200 rpm. The solution was centrifuged at 2000rpm for 30 sec, and the flow through was removed. Furthermore, the gel pieces that were attached to the phosphopeptides and PolyMAC beads were incubated with 200 µl of loading buffer. Solution was shaken for 5min, spun down, and the gel was further washed twice with 200 µl of water. After washing, phosphopeptides were eluted with 150 µl of elution buffer two times. Both elutes were mixed and completely dried in speed vacuum concentrator. Lastly, dried peptides were re-suspended in 12 µl buffer containing 2% ACN and 0.1 % acetic acid for mass spectrometric analysis.

2.5 Workflows for mass spectrometric analysis of proteins

2.5.1 Label-free relative quantitation of proteins from tissue and plasma

2.5.1.1 Sample preparation

Four µg protein isolated from endomyocardial biopsies (n=33 before therapy, n=23 after therapy) and depleted plasma (n=34, R=23 and NR=11, before IA/IgG) of each DCM patient was tryptic digested with the above-mentioned trypsin digestion protocol. The acidified tryptic peptides were further purified using µC18-ZipTip column (2 µg). Peptides were eluted from the column, dried in

speed vacuum concentrator and dissolved in 20µl buffer containing 2% ACN and 0.1 % acetic acid for mass spectrometric analysis.

2.5.1.2 Mass spectrometric analysis

400ng tryptic peptides obtained from EMBs (before and after six months of IA/IgG) and plasma (after IA/IgG) was analyzed on a LTQ Orbitrap Velos mass spectrometer (Thermo Fisher Scientific, Bremen, Germany) coupled with a nanoAcquity UPLC system (Waters, Milford, MA, USA). Peptide mixtures were desalted on a trap column (C18, 2cm length, 180 µm inner diameter, 5 µm particle size, Waters) and further separated on a reversed-phase analytical column (C18, 10cm length, 100 µm internal diameter, 1.7 µm particle size, Waters) with a flow rate of 400nL/minute. The peptides were eluted with a non-linear gradient of 1-5% buffer B in 2 min, 5-25% B in 63 min, 25-60 % in 25 min, and 60-99% B in 2 min (buffer A-2% ACN with 0.1% acetic acid, buffer B-ACN with 0.1% acetic acid). The eluting peptides were ionized by electrospray at 1.6 KV in positive ion mode at a source temperature at 275^0C. The spectra (m/z 300-1700) of precursor ions (MS1) were acquired in Orbitrap (AGC target value 1x 10^6, resolution 30K, isolation width m/z- 1 and activation time 10 ms) whereas MS2 spectra of the 20 most intense ions were generated in the linear ion trap in data-dependent mode at collision induced dissociation energy of 35%. Dynamic exclusion (repeat count 1, repeat duration 30 s, exclusion list size 500, and exclusion duration 60s) was enabled to avoid repetitive MS/MS fragmentation and minimum ion signal for MS/MS was set to 2000. Only +2 and +3 charged precursor ions were probed for MS/MS fragmentation.

2.5.1.3 Data analysis

LC-MS/MS raw files generated by mass spectrometry were imported into Rosetta Elucidator software version 3.3 (Ceiba Solutions, Seattle, WA, USA) for feature extraction, peak alignment, database search and to extract protein intensities. MS/MS spectra were searched against a UniProt/SwissProt database confined to human entries (v2012-08, forward-reverse) using the

Sequest algorithm. Search parameters included oxidation on methionine as variable modification, carbamidomethylation on cysteine as a static modification, a precursor ion mass tolerance of 10 ppm and a fragment ion mass tolerance of 1 Da. Peptides were annotated at a false discovery rate < 1% (peptide teller probability > 0.84) using PeptideTellerTM algorithm. The resulting protein list was filtered for a ProteinTeller probability ≥0.9. Relative quantitation of differences was performed in Genedata Expressionist AnalystTM (Genedata AG, Basel, Switzerland). Protein raw intensities were transformed to log10 values with subsequent median normalization. Differentially abundant proteins between responders and non-responders were identified by Student's t-test. Proteins with a p-value ≤ 0.05 and a fold change (FC) ≥ │1.3│ were mapped for pathway analysis using Ingenuity Pathway Analysis (Ingenuity Systems, Redwood City, USA; http//www.ingenuity.com), and the PANTHER GO enrichment tool.

2.5.2 Relative quantitation of plasma proteins based on iTRAQ labeling

2.5.2.1 Sample preparation

For profiling of plasma from responder and non-responder DCM patients using iTRAQ approach, DCM patients were sub-grouped based on the inflammation status of myocardium as given below:

   (I) Responders - inflammation positive and presence of virus (R++) (n=5)

   (II) Responders - inflammation negative and no virus (R- -) (n=5)

   (III) Non-responders - inflammation positive and presence of virus (NR+ +) (n=5)

   (IV) Controls with normal LVEF (n=5)

50 µg depleted plasma protein (10 µg protein from five patients was pooled in each group) of each group was reduced, alkylated and tryptic digested as described above (section 2.4.5.). The obtained peptides were desalted using Sep-Pak tC18 cartridges (Waters, Wexford, Ireland). C-18 matrix of Sep-Pak column was activated with 1ml of 80% ACN in 1% acetic acid and further equilibrated with 1ml of 2.5%ACN in 1% acetic acid (three times). Subsequently, digested peptides were loaded

onto the column and flow through was reapplied to the column to ensure all peptides were bound to the C-18 matrix. Columns were further washed 3 times with 1ml of 2.5%ACN in 1% acetic acid. Peptides were eluted once with 200µl of 80% ACN in 1% acetic acid, and two additional times with 200µl of 50% ACN in 1% acetic acid. All three eluted fractions were pooled and dried using a speed vacuum concentrator. Further, peptides were dissolved in 30 µl triethylammonium bicarbonate (TEAB, 100 mM) for iTRAQ labeling.

2.5.2.2 Labeling of peptides by iTRAQ reagents (4-plex)

iTRAQ labeling was performed according to the manufacturer's protocol (Applied Biosystems, Foster City, CA, USA). Different iTRAQ tags were used for the various groups (114-R--, 115-R++, 116-NR++, and 117- control). One unit of iTRAQ reagent (reconstituted in 70 µl of ethanol) was added to each group of tryptic peptides (50 µg) and after incubation for 1 hour at room temperature, labeling was stopped by addition of 100µl de-ionized water for each reaction. After 30 minute incubation, peptides of all four groups were pooled (200µg) and desalted using Sep-Pak column to remove salts and unlabeled iTRAQ reagent. Eluted peptides were dried in a speed vacuum concentrator and reconstituted in 40 µl SCX "buffer A" (25% ACN, 10mM KH_2PO_4, pH ≤3) for strong cation exchange chromatography.

Note: iTRAQ experiment was performed in two technical replicates and the above protocol except tags were swiped (117-R--, 116 R++, 115 NR++, 114 healthy controls) in the second technical replicate to minimize the tag bias.

2.5.2.3 Strong cation exchange chromatography (SCX)

Strong cation exchange fractionation of iTRAQ tagged peptides was performed using Dionex HPLC (UltiChrom, Dionex, Idstein, Germany) to reduce the complexity of the peptide mixtures. 50µg pooled iTRAQ tagged peptides (10 µl) were loaded onto a polySULFOETHYL A™ column (300A, 50 X 1.0mm, PolyLC, Columbia, MD, USA) with buffer A at a flow rate of 50 µl/min.

Following sample injection, columns were washed with buffer A for 10 minutes to remove all contaminants. Peptides were eluted by buffer B (25% ACN, 10mM KH_2PO_4, and 1M KCl, pH $\leq$ 3) in ten different salt steps (25-1000mM KCl) for five minutes each and manually collected in tubes.

Peptides were dried in speed vacuum concentrator and reconstituted in 1% acetic acid. Desalting was performed using 5 µg C18-ZipTip columns (Merck Millipore, Darmstadt, Germany). Eluted peptides were dried and reconstituted in 20µl buffer containing 2% ACN and 0.1 % acetic acid for mass spectrometry analysis.

2.5.2.4 Mass spectrometric analysis

All ten fractions obtained from strong cation exchange fractionation were analyzed using a LTQ Orbitrap Velos mass spectrometry coupled with a nano UPLC system using the same LC parameters as described before (section 2.5.1.2). Mass spectrometric analysis was carried out again in a data dependent manner (see section 2.5.1.2) with the following changes: Full scans were recorded using the Orbitrap mass analyzer at a mass resolution of 60,000. For each MS cycle, the twelve most intense precursor ions were selected for MS/MS fragmentation. The fragmentation was carried out using high-energy collision dissociation (HCD) with 38% normalized collision energy. The ions selected for fragmentation were excluded for 30 sec. The automatic gain control for full FT-MS was set to 1 million ions and for FT MS/MS was set to 30,000 ions with a maximum time of accumulation of 500ms.

2.5.2.5 Data analysis

All ten raw files obtained from mass spectrometry were directly imported into Proteome Discoverer (PD) 1.4 software (Thermo Fisher Scientific) for identification and quantification of proteins. The data processing workflow of PD included five nodes, briefly; Node 0 (Spectrum files) for the selection of raw data files; Node 1 (Spectrum selector) for the spectrum extraction and selection of only those spectra which were produced by HCD fragmentation and detected in Orbitrap analyzer;

Node 2 (Sequest) where the search engine and search parameters were selected; Node 3 (Percolator), to calculate and apply false discovery rates; and Node 4 (Reporter Ion Quantifier) where the iTRAQ 4-plex analysis method was selected for quantification. Spectra were searched against a UniProt/SwissProt database confined to human entries (v2013 08, forward-reverse) and the following searched parameters were used in the workflow: two missed cleavages, peptide N-termini and lysine were set as +144.102 amu, carbamidomethylation of cysteine was defined as a fixed modification, and oxidation of methionine as variable modification. 1% FDR was applied on peptides. Precursor ion tolerance was 10 ppm, whereas fragment ion mass tolerance was 0.05 Da. Quantification was performed with different denominators for various group combinations like NR+/R+ (116/115), R+/Control (115/117) and NR+/Control (116/117), using the quantitation module of PD. The study was performed in two technical replicates with a similar workflow except that iTRAQ tags were swiped among different groups to minimize the tag bias. The results obtained from PD were exported to Microsoft Excel for further analysis. Differentially abundant proteins (FC $\lvert 1.3 \rvert$, variability $\leq$ 30%) present in both technical replicates were selected for further functional categorization using PANTHER and Ingenuity Pathway Analysis (Ingenuity Systems, Redwood City, USA; http//www.ingenuity.com).

2.5.3 Targeted peptide quantification by multiple reaction monitoring (MRM)

2.5.3.1 Sample Preparation

Proteins selected from the discovery phase experiments to distinguish responder and non-responder DCM patients at baseline in endomyocardial biopsies and plasma (EMBs n=17 proteins, plasma n=20 proteins) were further evaluated in a larger sample set using multiple reaction monitoring techniques. Only peptides fully tryptic and 7-25 amino acids in length were included in the study. Methionine containing peptides were excluded to avoid *in vitro* modifications. The uniqueness of peptides was confirmed using Peptide atlas (http://www.peptideatlas.org). Finally, peptides selected for MRM analysis were synthesized by JPT (JPT, Berlin, Germany) with a stable isotope

label containing 13C, and 15N Arg/Lys amino acids referred as "Spike TidesTM L". Lyophilized heavy peptides (approximately 20 nM each) were reconstituted in 80% v/v ammonium bicarbonate solution (100 mM) and 20% v/v ACN and were stored at -80°C until further use. Heavy standard peptides were spiked into the tryptic peptides of each sample (EMBs n=33, R n=19 NR n=14; depleted plasma n=93, R n=38, NR n=31, and healthy controls n=24) in different dilutions (1-100 fmol/µg protein) prior to mass spectrometric analysis.

2.5.3.2 Targeted mass spectrometric analysis

MRM was performed on a Triple Quadrupole mass spectrometer (TSQ VantageTM, Thermo Scientific) interfaced with a nano-LC (Easy-nLC, Thermo Scientific) or nano-Acquity UPLC system (Waters). Optimal tryptic peptides for the protein targets were selected based on the spectral library downloaded from NIST and an in-house built human peptide spectral library. Separation of peptides was performed by reversed phase chromatography (PepMap100, C18, 3µm, 100A 75 µm id X 150 mm, Dionex) with a binary non-linear 50-min gradient of 0-40% buffer B (100% v/v ACN, 0.1% acetic acid) at 300 nl/min flow rate (EASY-nLC) or with a non-linear 90 min gradient of 0-60% buffer B at 400nl/min flow rate with nano-Acquity UPLC system. The eluted peptides were ionized by electrospray (spray voltage 1600 to 1700 V, capillary temperature 250^0 C). The selectivity for both Q1 and Q3 were set to 0.7 Da (full-width half maximum). The collision gas pressure of Q2 was set to 1.5 mTorr and cycle time to 2 seconds. Collision energy was optimized for each precursor ion by factory default method. +2 and +3 charged precursor ions were selected for each peptide, and the 3-4 most abundant transitions were chosen for MRM acquisition. TSQ Vantage was operated in scheduled MRM mode with a retention time scanning window of 4 min for each precursor. Each sample was analyzed in duplicate.

2.5.3.3 Data analysis

The resultant raw files obtained from triple quadrupole data acquisition of EMBs and plasma proteins were analyzed independently by Skyline software version 2.6 and the ratio data obtained from co-eluting pairs of heavy and light peptides were exported. The ratio of each protein was calculated by taking an average of the individual peptide ratios from the same protein. Student's t-test was applied to assess the significantly different proteins between responder and non-responder DCM patients. Association between physiological parameters of DCM patients, and the protein ratios (light/heavy) of protein S100-A8 was determined by linear regression analysis embedded in the Expressionist Analyst software suite (GeneData, Basel, Switzerland).

Furthermore, the differentially abundant proteins obtained in plasma discriminating responders and non-responders at baseline were assessed for biomarker potential using Reciever Operating Characteristic (ROC) curve.

2.5.4 Analysis of phosphopeptides of HL-1 cardiomyocytes treated with TGF-β

2.5.4.1 Sample preparation and mass spectrometric analysis

200 µg protein of every sample (controls and TGF-β treated) was tryptic digested and desalted using C-18 matrix of Sep-Pak columns. Eluted peptides were completely dried in a speed vacuum concentrator and dissolved in loading buffer of the PolyMAC kit for the enrichment of phosphopeptides as described before. Enriched phosphopeptides were completely dried and dissolved in 2% ACN in 0.1 % acetic acid for mass spectrometry analysis which was carried on individual samples on a LTQ Orbitrap Velos mass spectrometer as described in the previous section 2.5.1.2.

2.5.4.2 Data analysis

All MS/MS raw files (n=18) were analyzed using special phosphoRS (PRS) node embedded in PD 1.4 software. Spectra were searched using Sequest against a Uniprot/SwissProt database confined

to mouse entries (v2014 03, forward) employing these parameters: two missed cleavages, carbamidomethylation of cysteine as a fixed modification, oxidation of methionine and phosphorylation at serine (S), threonine (T) and tyrosine (Y) as a variable modification. Only high confident phosphopeptides (1% FDR) were considered in the analysis. Precursor ion tolerance was 10ppm, whereas fragment ion mass tolerance was 0.05 Da. All search results were exported to Microsoft Excel for further manual curations. A non-redundant list of all phosphopeptides (≥50pRS score) was prepared and the area of phosphopeptides assigned as "0" (identified but close to the background signal), was replaced by the smallest phosphopeptides area (70,000) across all datasets. Also, the area of phosphopeptides was replaced by 35,000 if it is not available in the sample. Furthermore, area was summed if the phosphopeptides was present in two variable forms due to e.g. methionine oxidation. Finally, this manually curated list of phosphopeptides was exported to Genedata Expressionist AnalystTM (Genedata AG, Basel, Switzerland) software to obtain relative quantitative data for TGF-ß1 treated cells and controls at various time points. Raw intensities of phosphopeptides were transformed to log10 values and median normalization was performed. Student's t-test was applied to find differentially abundant phosphopeptides ($|FC| 1.3$, $p \le 0.05$). At last, the proteins related to the differentially abundant phosphopeptides were functionally enriched using the PANTHER GO online tool.

2.5.5 ELISA of protein S100-A8 and S100-A9

2.5.5.1 ELISA of Protein S100-A8

Plasma levels of human protein S100-A8 were determined using Circulex S100A8/MRP8 ELISA kits employing a sandwich enzyme immunoassay technique. ELISA microplates (96 wells) were pre-coated with specific antibody for human protein S100-A8. Assay procedure was followed as instructed by the manufacturer. Briefly, different concentrations of standard (5000 to 78.1 pg/ml) were prepared by serial dilution from master standard (50ng). Undepleted plasma samples (n=99, R n=44, NR n=38, and n=17 samples of healthy controls with preserved LVEF) were diluted 100

fold in dilution buffer provided with the kit. 100 µl of standard solutions, blank and diluted plasma of each sample was loaded into the precoated wells and incubated for 1 hour at room temperature on an orbital shaker at 300 rpm. Afterwards, each well was washed with 350 µl of wash buffer, four times. Subsequently, HRP conjugated detection antibody was added into each well and incubated for one hour on an orbital shaker at 350 rpm. Wells were washed again with 350 µl of wash buffer. Further, 100 µl substrate reagent (tetramethylbenzidine) was added to each well and plate was incubated for 20 min at room temperature. At last, 100 µl stop solution was added to stop the reaction, and absorbance was measured within 30 min using a VarioskanFlash spectrophotometer scanner (Thermo) at dual wavelengths of 450/540 nm. S100-A8 protein concentration of each sample was calculated in comparison with the standard curve. Furthermore, raw data were exported to Microsoft Excel, and the concentration of each sample was divided by its total protein concentration to obtain S100A8 amounts per µg protein.

2.5.5.2 ELISA of Protein S100-A9

Human plasma protein S100-A9 level was measured using CircuLex S100A9/MRP14 ELISA kit that principally work on sandwich enzyme immunoassay technique. ELISA microplates (96 wells) were precoated with the specific antibody of human protein S100-A9. Standard solutions were prepared in different concentrations (3200-50pg/ml) by serial dilution from master standard (64ng/ml). Undepleted plasma samples (n=46, R15, NR18, and 13 healthy controls with preserved LVEF) were diluted 25 fold in sample dilution buffer. 100 µl standards, blank and diluted plasma were pipetted into appropriate wells and incubated for one hour at room temperature on an orbital shaker (300rpm). Subsequently, wells were washed four times with 350 µl of wash buffer. Further, HRP conjugated detection antibody was added into each well and plate was incubated for one hour at room temperature. After four wash, 100 µl substrate reagent (tetramethylbenzidine) was added to each well and incubated for 20 min at room temperature. Finally, reaction was stopped by

addition of 100 µl stop solution, and absorbance was measured within 30 min using VarioskanFlash

spectrophotometer scanner at dual wavelengths of 450/540 nm.

3. Results

Analysis of the molecular alterations upon IA/IgG in DCM patients

The study aimed to characterize the molecular alterations in the heart initiated by immunoadsorption therapy (IA/IgG) in DCM patients and to distinguish the differences between patients with different therapy result not only after therapy but also before IA/IgG was applied. Dilated cardiomyopathy patients treated by immunoadsorption therapy were classified as responders (relative ΔLVEF $\geq$ 20%, and absolute ΔLVEF $\geq$ 5%) or non-responders according to the improvement of heart function. A proteome profiling of endomyocardial biopsies obtained from responder and non-responder DCM patients before and after six months of immunoadsorption therapy was performed. Protein patterns of myocardial tissues at baseline might disclose the molecular differences in the heart between responders and non-responders. Also, proteome profiling of EMBs after therapy might delineate the molecular alterations in the myocardium induced by immunoadsorption therapy in the patient subgroups. Additionally, proteome profiling of plasma was carried out to search for protein biomarkers that might be useful to distinguish responders and non-responders among DCM patients before immunoadsorption therapy to enable applications of personalized treatment strategies.

3.1 Results of endomyocardial tissue proteomic profiling at baseline in responder and non-responder

3.1.1 DCM patients

In a pilot study, the discovery phase proteome experiment was carried out on 16 DCM patients (responders n=7 and non-responders n=9) using shotgun proteomics (label-free quantitation). Furthermore, the study was extended to 33 DCM patients for a subset of differentially abundant proteins.

3.1.2 Clinical parameters of DCM patients at baseline

Dilated cardiomyopathy patients treated by immunoadsorption therapy were categorized into responders (n=7) and non-responders (n=9) as described before. Cardiac physiological parameters did not differ between responders and non-responders at baseline except disease duration, which was higher (p=0.08) in non-responder DCM patients (Fig. 4, Table 5).
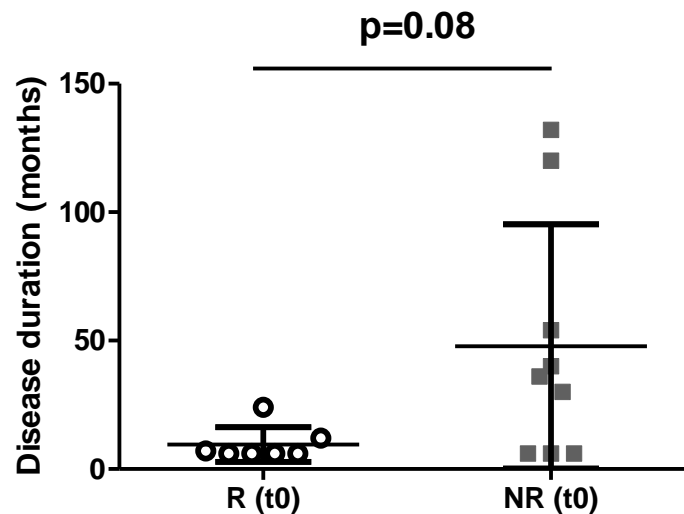
Fig. 4. Disease duration of responder and non-responder DCM patients at baseline

Self-reported disease periods of DCM patients (responders-white and non-responders-gray) with mean and the standard deviation of each group are represented.

In general, DCM patients with short disease period displayed improved cardiac functions after immunoadsorption therapy. However, also the non-responder groups included patients with short disease duration (Fig. 4). Therefore, disease duration cannot be used to discriminate responders and non-responders at baseline in general.

Table 5: Baseline characteristics of responder and non-responder DCM patients

	responders	non-responders	p-value
Age (years) ±SD[a]	44 ± 13	52 ± 9	0.14[b]
Gender (M/F)	3/4	8/1	0.10[c]
LVEF (%) ±SD[a]	33 ± 8	34 ± 8	0.67[b]
LVIDd (mm) ±SD[a]	66 ± 8	73 ± 8	0.14[b]
Inflammation (CD68+CD3(cells/mm^2) ±SD[a])	15.29 ± 6.31	23.67 ± 17	0.71[b]
Inflammation positive	4	5	1.00[c]
BMI	27 ± 5	28 ± 5	0.99[b]
Disease duration (months) ±SD[a]	10 ± 7	48 ± 47.6	0.08[b]
NYHA class (n)			1.00[c]
II	4	5	
III	3	4	
Medication			
β-Blockers	7	9	1.00[c]
ACE inhibitor	5	8	0.55[c]
AT1 antagonists	4	2	0.30[c]
Diuretics	7	9	1.00[c]
Digitalis	1	3	0.59[c]

[a] Mean values with standard deviation (SD), [b] Mann-Whitney test, two-tailed, [c] Fishers exact test, two-tailed, M/F-Male/Female; LVEF-Left ventricular ejection fraction, LVIDd-Left ventricular inner diameter at diastole, BMI-Body mass index, NYHA-New York Heart Association, AT1-Angiotensin 1.

Six months after immunoadsorption therapy in responders LVEF increased from 33 ± 8.4 to 44 ±

6.1 % (p=0.001) whereas LVIDd decreased in this patient subgroup from 65 ± 7.7 to 58 ± 6.1 mm

(p=0.006). LVEF and LVIDd did not change in non-responders after IA/IgG (Fig. 5).
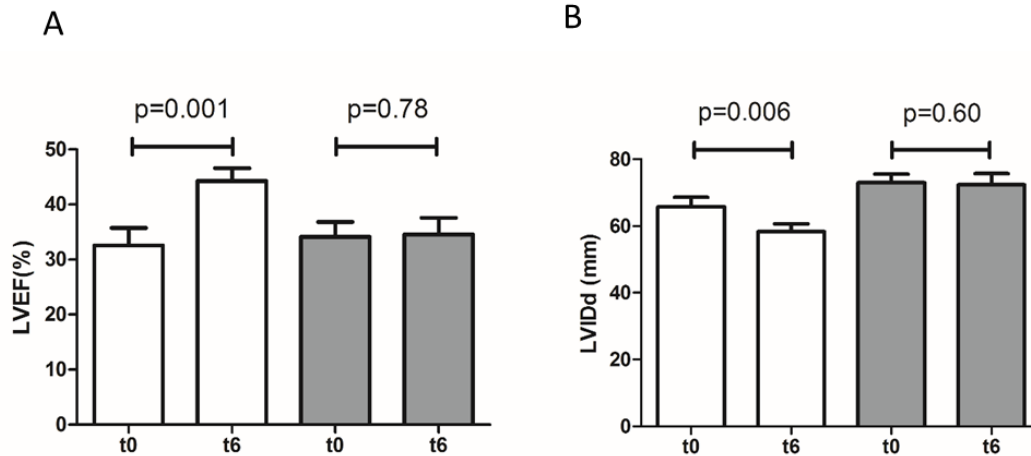
Fig. 5. Effect of immunoadsorption therapy on LVEF and LVIDd in DCM patients

The effect of immunoadsorption therapy (baseline-t0, after therapy-t6) in responders (white), and non-responders (gray) on (A) left ventricular ejection fraction and (B) left ventricular internal diameter at diastole is presented.

3.1.3 Protein coverage and quantification of proteins in human heart biopsy samples at baseline

Myocardial protein extracts of seven responders and nine non-responders were individually digested with trypsin and analyzed by LC-ESI-MS/MS. Alignment of all 16 raw files acquired by tandem mass spectrometry revealed 193,586 extracted features, 77,012 isotope groups and 8752 annotated peptides (FDR < 1%). After filtering for protein specific peptides, the number was reduced to 7639 peptides assigned to 1444 proteins identified in human heart biopsy tissue samples. Among them, 947 proteins were identified with at least two peptides and considered for subsequent analysis. Functional categorization of these proteins using PANTHER GO annotation revealed a high proportion of oxidoreductases, cytoskeletal proteins, hydrolases, transferases, enzyme modulators and structural proteins. Additionally, extracellular matrix proteins were also covered which play a pivotal role in the left ventricular remodeling in DCM patients [106]. A high proportion of proteins represented metabolic and cellular processes, which should allow a view on

the metabolic and cellular state of heart cells. Also, proteins crucial for adhesion, response to stimulus and apoptosis were covered.

Relative quantitation of summed up peptide intensities per protein revealed 54 proteins significantly different abundant (p≤0.05, FC │1.3│) in EMBs of responders and non-responders at baseline. Most of these proteins were predicted to be found in mitochondria, cytoplasm and nucleus while some were predicted to be found in the endoplasmic reticulum, lysosome, peroxisome, and membranes (Table 6).

Table 6. List differentially abundant proteins (54) between responders and non-responders at baseline

Swiss prot ID	Gene names	Protein Description	Squeeze Count	p-Value	FC (R/NR)
Mitochondria					
P48047	ATPO	ATP synthase subunit O	9	0.007	-1.51
Q96DV4	RM38	39S ribosomal protein L38	2	0.008	-1.75
P23368	MAOM	NAD-dependent malic enzyme	6	0.009	-1.38
P40939	ECHA	Trifunctional enzyme subunit alpha	27	0.011	-1.97
P55084	ECHB	Trifunctional enzyme subunit beta	18	0.012	-1.61
P51649	SSDH	Succinate-semialdehyde dehydrogenase	8	0.015	-1.33
P21912	DHSB	Succinate dehydrogenase [ubiquinone] iron-sulfur subunit	9	0.018	-1.32
O75251	NDUS7	NADH dehydrogenase [ubiquinone] iron-sulfur protein 7	4	0.019	-1.90
P07919	QCR6	Cytochrome b-c1 complex subunit 6	3	0.019	-3.03
P12235	ADT1	ADP/ATP translocase 1	4	0.022	-2.06
P24539	AT5F1	ATP synthase subunit b	10	0.026	-1.31

Swiss prot ID	Gene names	Protein Description	Squeeze Count	p-Value	FC (R/NR)
O75746	CMC1	Calcium-binding mitochondrial carrier protein Aralar1	12	0.038	-1.35
Q16798	MAON	NADP-dependent malic enzyme	3	0.039	-1.36
Q9P0S9	TM14C	Transmembrane protein 14C	2	0.039	-1.53
O95563	MPC2	Mitochondrial pyruvate carrier 2	2	0.044	-2.14
Q02978	M2OM	Mitochondrial 2-oxoglutarate/malate carrier protein	9	0.048	-1.92

Cytoplasm

Swiss prot ID	Gene names	Protein Description	Squeeze Count	p-Value	FC (R/NR)
O95336	6PGL	6-phosphogluconolactonase	2	0.001	1.34
P05109	S10A8	Protein S100-A8	2	0.003	3.02
P13639	EF2	Elongation factor 2	20	0.004	-1.36
P67936	TPM4	Tropomyosin alpha-4 chain	2	0.006	1.62
P08237	K6PF	6-phosphofructokinase, muscle type	19	0.015	-1.49
P31949	S10AB	Protein S100-A11	4	0.016	-1.49
P22694	KAPCB	cAMP-dependent protein kinase catalytic subunit beta	3	0.016	-1.34
P15924	DESP	Desmoplakin	41	0.016	-1.88
Q15075	EEA1	Early endosome antigen 1	3	0.016	-1.31
P33176	KINH	Kinesin-1 heavy chain	4	0.017	-1.39
P62081	RS7	40S ribosomal protein S7	2	0.022	-1.42
P23396	RS3	40S ribosomal protein S3	5	0.026	-1.39
P06753	TPM3	Tropomyosin alpha-3 chain	3	0.033	1.69
Q68DK2	ZFY26	Zinc finger FYVE domain-containing protein 26	2	0.039	-2.56
Q9ULP0	NDRG4	Protein NDRG4	2	0.039	-1.61
Q96AC1	FERM2	Fermitin family homolog 2	3	0.044	-1.48

Swiss prot ID	Gene names	Protein Description	Squeeze Count	p-Value	FC (R/NR)
O00303	EIF3F	Eukaryotic translation initiation factor 3	2	0.048	-1.44
P52907	CAZA1	F-actin-capping protein subunit alpha-1	2	0.048	1.56
Cytoplasm and Nucleus					
Q9Y224	CN166	UPF0568 protein C14orf166	4	0.009	-1.33
O60936	NOL3	Nucleolar protein 3	2	0.011	-1.30
O00159	MYO1C	Myosin-Ic	3	0.022	-2.38
O00410	IPO5	Importin-5	2	0.025	-1.42
P14618	KPYM	Pyruvate kinase isozymes M1/M2	20	0.035	-1.32
Endoplasmic reticulum					
O43852	CALU	Calumenin	4	0.015	1.34
P02462	CO4A1	Collagen alpha-1(IV) chain	2	0.030	-1.80
P07996	TSP1	Thrombospondin-1	5	0.035	3.08
Membrane					
Q96Q06	PLIN4	Perilipin-4	13	0.002	-1.98
Q16821	PPR3A	Protein phosphatase 1 regulatory subunit 3A	2	0.019	2.52
Lysosome					
P07602	SAP	Proactivator polypeptide	2	0.043	-1.65
Peroxisome					
Q6YN16	HSDL2	Hydroxysteroid dehydrogenase-like protein 2	11	0.050	-1.33
Secreted/extracellular space.					
P01042	KNG1	Kininogen-1	5	0.021	1.65
P00734	THRB	Prothrombin	3	0.027	1.93

Swiss prot ID	Gene names	Protein Description	Squeeze Count	p-Value	FC (R/NR)
P02452	CO1A1	Collagen alpha-1(I) chain	3	0.034	1.61
Q9GZM7	TINAL	Tubulointerstitial nephritis antigen-like	8	0.038	-1.32
Unclassified					
P15259	PGAM2	Phosphoglycerate mutase 2	7	0.003	-1.64
P60981	DEST	Destrin	2	0.028	-2.08
O43242	PSMD3	26S proteasome non-ATPase regulatory subunit 3	3	0.041	-1.45
O95861	BPNT1	3'(2'),5'-bisphosphate nucleotidase 1	2	0.047	-1.40

Among the 54 differentially abundant proteins, 11 proteins displayed higher abundance whereas 43 proteins revealed lower abundance in responder patients (Fig. 6). Differences between the groups ranged from 3.08 to -3.03 fold. Highest fold differences were observed for protein S100-A8 and thrombospondin-1 with higher abundance in the responder group, and cytochrome b-c1 complex subunit 6 and zinc finger FYVE domain-containing protein with higher abundance in the non-responder group.
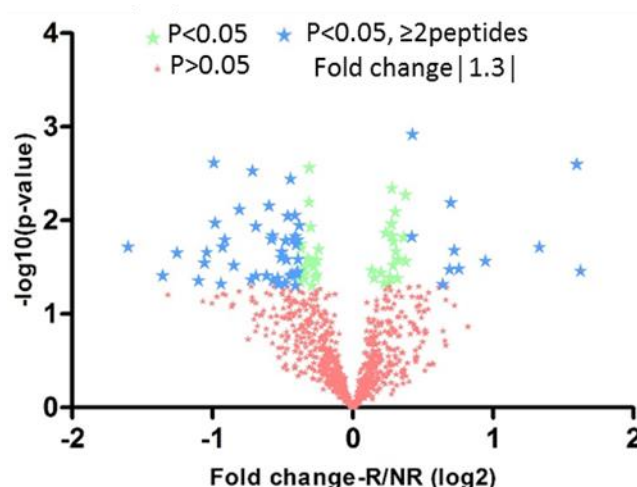
Fig. 6. Volcano plot of quantitative proteomics data

The difference in relative abundance (log2 fold change, x-axis) for all proteins (≥ 2 peptides) between responder and non-responders was plotted against the p-value (y-axis). Proteins with significantly lower and higher abundance (p< 0.05, ≥ 2peptides, fold change │1.3│) are labeled with blue stars.

3.1 4 Functional classification of proteins with different abundance in responders and non-responders at baseline

The 54 differently abundant proteins were examined for functional categorization using Ingenuity Pathway Analysis and PANTHER GO annotation tool. Differentially abundant proteins were assigned to various molecular functions (Fig. 7) in which responder and non-responder DCM patients seem to be different. Categories related to catalytic activity and binding were most influenced among molecular functions. Twenty three proteins of catalytic activity were different in responders and non-responders before immunoadsorption therapy, importantly including tropomyosin alpha-3 chain, kinesin-1 heavy chain, 6-phosphogluconolactonase, and prothrombin. Likewise, eighteen proteins were different in the functional class *binding*, in which some of them were of mitochondrial proteins like ADP/ATP translocase-1 and mitochondrial 2-oxoglutarate/malate carrier protein.
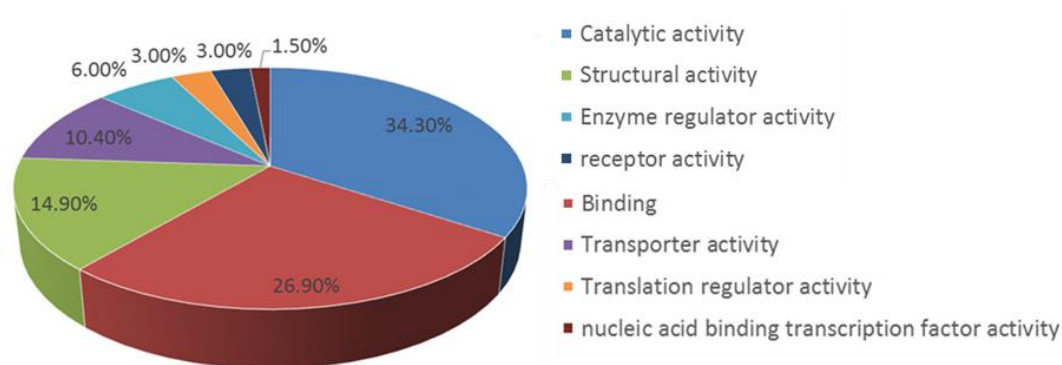
Fig. 7. Assignment of differentially abundant proteins to molecular functions using PANTHER GO annotation tool

Responder and non-responder DCM patients are different in the abundance of proteins that are majorly involved in catalytic, structural, binding, enzyme regulator, transport, and translation regulatory activities, as given.

Mitochondrial proteins pertained to several mitochondrial complexes (n=4) were lower in level in responder patients, such as NADH dehydrogenase [ubiquinone] iron-sulfur protein 7 (complex I), succinate dehydrogenase [ubiquinone] iron-sulfur subunit (complex II), cytochrome b-c1 complex subunit 6 (complex III), ATP synthase subunit O, and ATP synthase F (0) complex subunit B1 (complex V). Lower levels in the responder group were also observed for other mitochondrial proteins like ADP/ATP translocase-1 (inner membrane), 2-oxoglutarate/malate carrier protein, and pyruvate carrier-2. The same behavior was found for myosin-Ic and destrin as well as proteins related to apoptosis (26S proteasome non-ATPase regulatory subunit 3 and nucleolar protein 3) appearing to be lower abundant in responder patients. In contrast, cytoskeletal proteins like protein tropomyosin-4, tropomyosin alpha-3 chain and F-actin-capping protein subunit alpha-1 were higher in level in responders. Extracellular matrix proteins like collagen alpha-1(IV) chain (R/NR -1.80), collagen alpha-1(I) chain (R/NR 1.61), fermitin family homolog 2 (R/NR -1.48) and thrombospondin-1 (R/NR 3.08) that are important in the fibrotic remodeling also differed in the subgroups. Interestingly, the cardioprotective protein kininogen-1 was found to be present at higher abundance in responders. Additionally, perilipin – a protein that plays a significant role in the

biogenesis of lipid droplets was less abundant in responder patients. Differences were also observed for immune regulatory proteins such as S100-A8 (higher in responders), and S100-A11 (lower in responders).

Categorization of proteins regarding canonical pathways displayed differences between responders and non-responders in glycolysis (phosphofructokinase, phosphoglycerate mutase 2, and pyruvate kinase), gluconeogenesis (malic enzyme 2, malic enzyme 3, and phosphoglycerate mutase 2), mitochondrial dysfunction (ATP synthase, NADH dehydrogenase ubiquinone Fe-S protein 7, succinate dehydrogenase complex subunit B4, and ubiquinol-cytochrome c reductase protein) and beta-oxidation of fatty acids (hydroxyacyl-CoA dehydrogenase alpha subunit, hydroxyacyl-CoA dehydrogenase beta subunit). Furthermore, an upstream regulator analysis in IPA predicted the activation of PPAR-γ in non-responders based on the higher abundance of perilipin, trifunctional enzyme subunit alpha, trifunctional enzyme subunit beta, ATP synthase subunit O, as well as protein S100-A11 and collagen alpha-1(I) chain (lower in non-responders). This prediction was supported by higher PPAR- γ gene expression levels in non-responders than in responders (FC 1.33, p-value 0.01) derived from a prior EMB gene expression profiling (GEO ID: 200017800) of 12 of the 16 patients used in the current work.

Assignment of proteins to *Molecular and cellular function* by IPA (Fig. 8A) displayed enrichment of proteins in *Cellular function, maintenance and organization* (e.g. early endosome antigen 1, proactivator polypeptide, nucleolar protein 3, and destrin) as well as *Lipid metabolism and small molecule transport* (e.g. HADHA, HADHB, succinate dehydrogenase [ubiquinone] iron-sulfur subunit). Among *Physiological development and functional* categories (Fig. 8C) most interestingly, both subgroups seem to be different in *Cardiovascular system development and function* category based on ten differentially abundant proteins, e.g. kininogen-1, collagen alpha-1(IV) chain, collagen alpha-1(I) chain and ADP/ATP translocase 1.
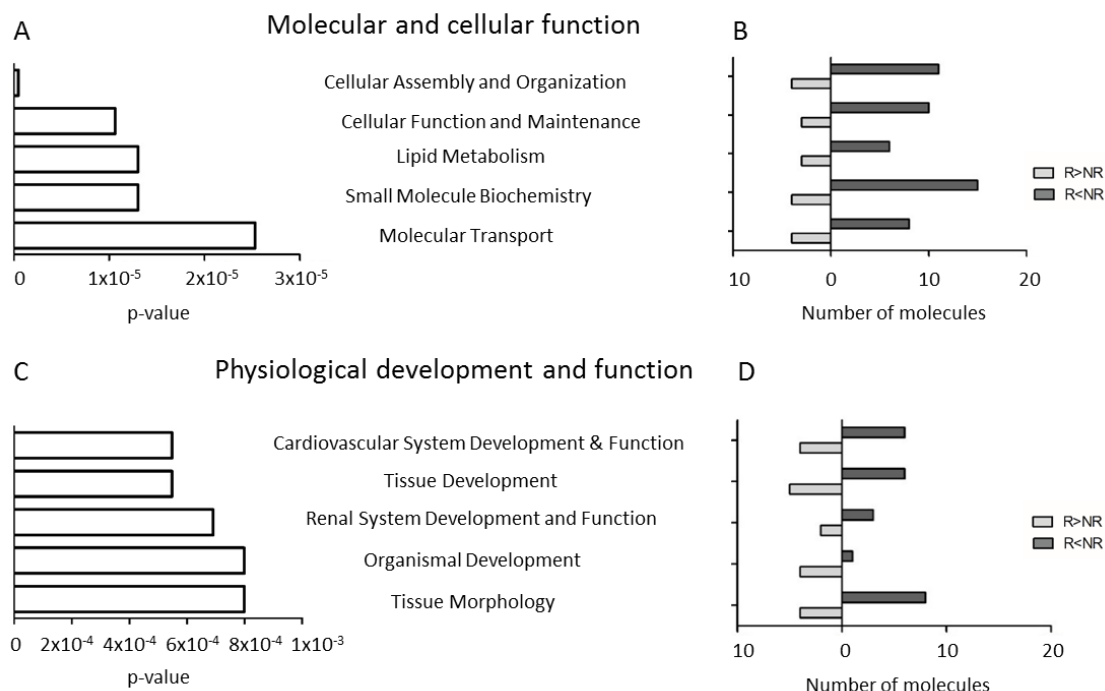
Fig. 8. Functional assignment of differentially abundant proteins in responders and non-responders at baseline

Top five enriched categories of (A) *Molecular and cellular function*, and (C) *Physiological development and function* along with protein abundance pattern (B and D) as well as significance of association (p-value) assigned by Ingenuity Pathway Analysis for canonical pathways are represented.

3.1.5 Validation of significantly different myocardial proteins using a MRM approach

Proteins discovered in shotgun proteomics were confirmed using multiple reaction monitoring. The MRM experiment was initially performed on the samples of the 16 DCM patients investigated in the discovery phase. Verification was focused on proteins with the most significant differences (lowest p-value) between responders and non-responders with relatively high abundance in the shotgun experiment. In total, 17 proteins were chosen for verification, comprising mitochondrial proteins (cytochrome b-c1 complex subunit 6, ADP/ATP translocase 1, ATP synthase subunit O, and ATP synthase subunit b), cytoskeletal proteins (destrin, kinesin-1 heavy chain, and desmoplakin), glycolytic proteins (phosphofructokinase, phosphoglycerate mutase 2, and pyruvate kinase), cardioprotective protein (kininogen-1), the immune regulatory protein S100-A8 and a

protein involved in triacylglycerol packaging (perilipin-4). Selected heavy peptides of all proteins were pooled and optimized for retention time and transitions. For every protein, 2-3 peptides were used for relative quantification. However, four proteins (S100A-8, cytochrome b-c1 complex subunit 6, cAMP-dependent protein kinase catalytic subunit beta, and tropomyosin alpha-3 chain) could be quantified only with one peptide because the other peptides chromatographic properties were not consistent across all DCM samples. Final MRM assays of 17 proteins consisted of 32 peptides with 123 transitions. For thirteen proteins, MRM results of the initially analyzed patient set confirmed the results of the shotgun experiment displaying similar relative ratios and low p-values. The results were most significant for the proteins kininogen-1, S100-A8, and perilipin-4 (Fig. 9A, B and C). MRM results of another three proteins (ADP/ATP translocase 1, ATP synthase subunit O, and 6-phosphofructokinase) corroborated the findings of the label-free analysis with p-values ≤ 0.1) (Fig. 9D, E and F). MRM data of another seven proteins (desmoplakin, kinesin-1 heavy chain, cytochrome b-c1 complex subunit 6, ATP synthase subunit b, destrin, tropomyosin and pyruvate kinase isozymes) displayed the same direction of the relative ratio with p-value≥0.1, whereas MRM data of four proteins (phosphoglycerate mutase 2, cAMP-dependent protein kinase catalytic subunit beta, importin-5, and protein NDRG4) was acquired and analysed but did not show any differences between the subgroups. Thus, for the majority of proteins label-free data was supported by MRM experiments, but p-values were slightly higher in MRM analysis than those of the shotgun approach.
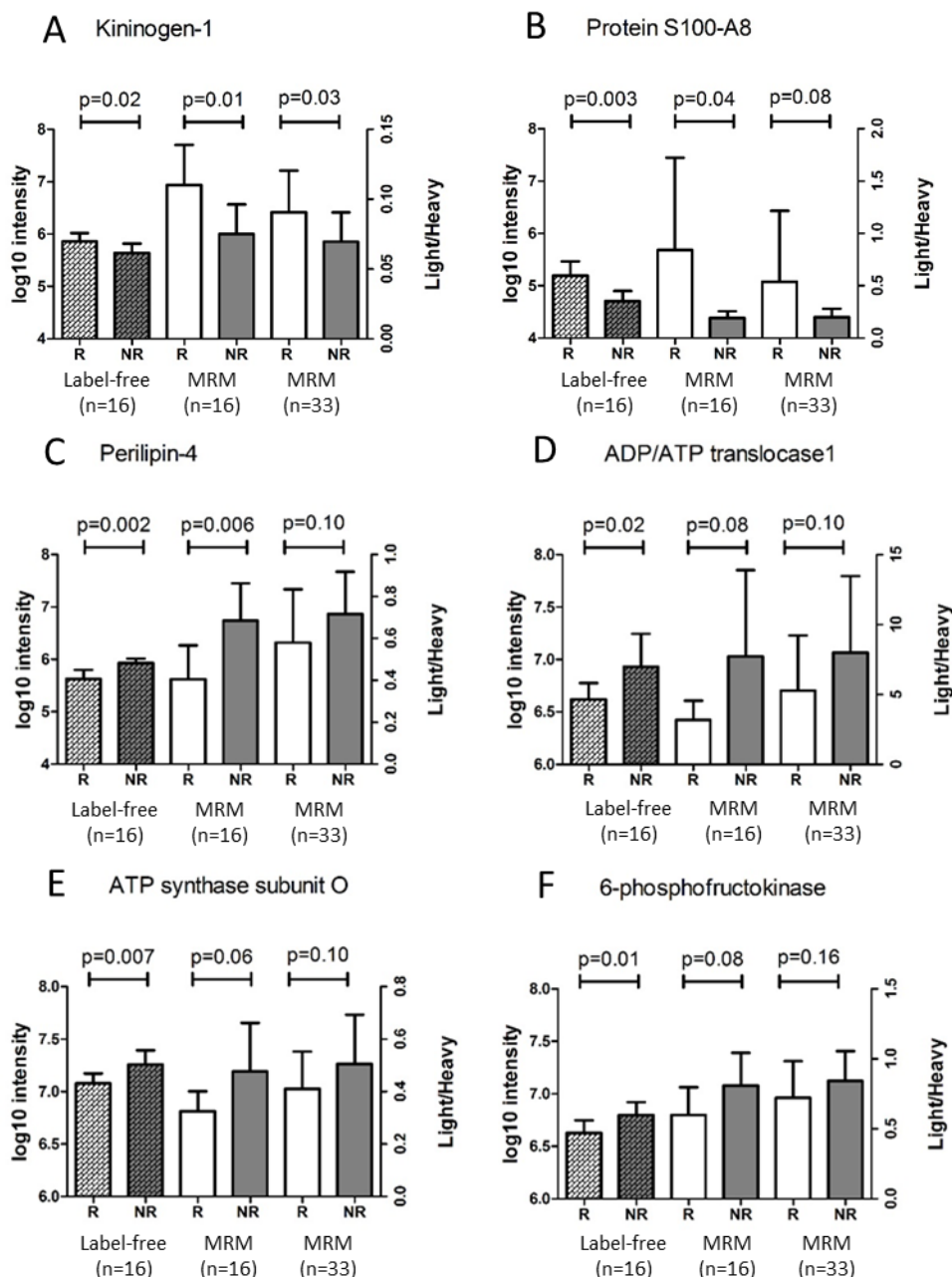
Fig. 9. Abundance of proteins with different levels in responders and non-responders at baseline in the shotgun approach (discovery phase) and in the MRM experiment (verification phase)

For six proteins (A) kininogen-1, (B) protein S100-A8, (C) perilipin-4, (D) ADP/ATP translocase1, (E) ATP synthase subunit O, and (F) 6-phosphofructosekinase, the abundance pattern obtained by mean signal intensities in label-free quantification (left y-axis, n=16) and by mean of light (sample)/heavy (standard) ratio in the MRM analyses (right y-axis, on n=16 and 33 DCM patients) with their standard deviation and significance (p-value) is displayed.

56

The verification phase was extended by including EMB protein extracts of another 17 DCM patients, representing 14 responders and 19 non-responders to 33 in total. 11 proteins displayed the same trend as observed in the shotgun approach. Among these 11 proteins, phosphoglycerate mutase 2, kinesin-1 heavy chain, and cytochrome b-c1 complex subunit 6 showed high variance (p-value > 0.4) whereas protein S100-A8 and kininogen-1 were the most significantly different protein between responders and non-responders. All MRM results for 17 proteins together with the shotgun proteomic results are summarized in Table 7.

Table 7. Summary of proteomics data obtained for 17 differentially abundant proteins between responders and non-responders.

Proteins are listed according to the p-value observed in the discovery phase in ascending order.

Swiss prot id	Protein Description	Label-free		MRM (n=16)		MRM (n=33)	
		R/NR	p*	R/NR	P*	R/NR	p*
Q96Q06	Perilipin-4	0.5	0.002	0.59	0.006	0.81	0.108
P05109	Protein S100-A8	3.02	0.003	4.39	0.043	2.68	0.076
P15259	Phosphoglycerate mutase 2	0.61	0.003	1.86	0.317	1.22	0.653
P48047	ATP synthase subunit O	0.66	0.007	0.68	0.062	0.81	0.108
P08237	6-phosphofructokinase	0.67	0.015	0.74	0.076	0.85	0.161
P22694	cAMP-dependent protein kinase beta	0.74	0.016	1.08	0.484	1.04	0.684
P15924	Desmoplakin	0.53	0.016	0.6	0.147	0.62	0.222
P33176	Kinesin-1 heavy chain	0.72	0.017	0.9	0.476	0.93	0.475
P07919	Cytochrome b-c1 complex subunit 6	0.33	0.019	0.47	0.439	0.84	0.691
P01042	Kininogen-1	1.65	0.021	1.47	0.013	1.3	0.031
P12235	ADP/ATP translocase 1	0.49	0.022	0.41	0.077	0.66	0.108
O00410	Importin-5	0.7	0.025	1.15	0.244	1.08	0.372
P24539	ATP synthase subunit b	0.76	0.026	0.82	0.156	0.87	0.165
P60981	Destrin	0.48	0.028	0.74	0.219	0.99	0.976
P06753	Tropomyosin alpha-3	1.69	0.033	1.3	0.247	1.2	0.318
P14618	Pyruvate kinase isozymes M1/M2	0.76	0.035	0.84	0.303	1.01	0.949
Q9ULP0	Protein NDRG4	0.62	0.039	1.00	0.994	1.00	0.966

*p – p-value

Protein S100-A8 plays a prominent role in the regulation of inflammatory processes and immune response. Therefore, the association of protein S100-A8 (MRM ratios) with the inflammation status (CD3 and CD68 positive cells) at baseline in responders and non-responders was checked, but was found to be very low (-0.06, p-value 0.4).

3.2 Endomyocardial proteomic profiling of responder and non-responder DCM patients before and after immunoadsorption therapy

To understand the immunoadsorption therapy induced molecular changes, global proteomic profiling of endomyocardial tissue before therapy (baseline, t0) and after six months (follow-up, FU, t6) was performed by label-free shotgun approach employing a LTQ-Orbitrap Velos mass spectrometer for responder (n=7) and non-responder (n=8) DCM patients. Previously, diploma student Michelle Goritzka analyzed the endomyocardial proteome of responders (n=5) and non-responders (3) before and after six months of therapy using a FTICR mass analyzer. Here, observations of both independent proteomic datasets were merged to find the proteomic differences between responders (n=12) and non-responders (n=11) induced by immunoadsorption therapy which might explain the different cardiac function in the patient subgroups.

3.2.1 Baseline characteristics of responder and non-responder DCM patients

Clinical parameters did not differ at baseline between responder and non-responder DCM patients as indicated in Table 8.

Table 8. Physiological characteristics of responders and non-responders at baseline

	responders (n=12)	non-responders (n=11)	responders vs. non-responders p-value
Age (years) ±SD[a]	52±9	49±13	0.35[e]
Gender (♂/♀)	6/6	9/2	0.19[f]
LVEF (%) ±SD[a]	35±8	32±8	0.38[e]
LVIDd (mm) ±SD[a]	72±8	66±6	0.10[e]

58

	responders (n=12)	non-responders (n=11)	responders vs. non-responders p-value
NYHA classification (n)	5	7	1.000[f]
II	7	4	
III			
NT-pro BNP (pg/ml) ±SD[a]	1001±1372	1081±992	0.95[e]
Disease duration (months)±SD[a]	17±21	39±45	0.20[e]
Inflammation positive (n)	8	7	1.00[f]
Fibrosis grade (n) 0/1/2/3	0/6/3/3	0/5/3/3	0.98[g]
Virus genomes			
PVB19/HSV1+HHV6/No virus	2/4/6	5/3/3	
Medication (n/total):			
β-Blocker	12/12	11/11	
ACE inhibitors	8/12	10/11	
AT1 antagonists	6/12	2/11	
Diuretics	12/12	11/11	
Digitalis	1/12	3/11	

LVEF- left ventricular ejection fraction, LVIDd – left ventricular internal diameter at diastole, NYHA – New York Heart association, nt-pro-BNP – n-terminal, pro-brain natriuretic peptide, ACE – angiotensin-converting enzyme, AT1 - angiotensin 1, [a]mean values with standard deviation (SD) are shown; (ACE- angiotensin-converting enzyme, AT1 - angiotensin-II-receptor-subtype-1, [e] Mann-Whitney test, two-tailed, [f] Fisher's Exact test, two-tailed, [g] Chi-squared test)

3.2.2 Clinical parameters after immunoadsorption therapy in responders and non-responders

Immunoadsorption followed by immunoglobulin substitution was well accepted by all 23 DCM patients that were included in this study. No physiological or clinical side effect of IA/IgG was observed in any of the DCM patients. Improved hemodynamic functions were observed in responders whereas non-responders did not show any benefit of therapy. In the responder group, left ventricular ejection fraction (LVEF) increased from $32 \pm 8\%$ at baseline to $45\pm7\%$ (p=0.002) after six months of IA/IgG (Fig. 10A). In responders, a significant decrease was observed in the left ventricular inner diameter at diastole (LVIDd) from 66 ± 6 at baseline to 60 ± 6 mm (p<0.040) after 6 months of therapy (Fig. 10B). The improvement became also obvious by a significant change in the New York Heart Association (NYHA) functional class (NYHA class III/II to II/I, p=0.02). In contrast, LVEF ($35\pm8\%$ at baseline to $36\pm9\%$ at FU) and LVIDd (72 ± 8 mm at baseline

to 71±10 mm at FU) did not change in non-responders after IA/IgG. Additionally, therapy associated advantages were also detected in myocardial inflammation as well as on the heart failure marker NT-proBNP in responders. Serum NT-proBNP levels were decreased (1081pg/ml to 532pg/ml, p<0.007) (Fig. 10C) in responders, whereas NT-proBNP level did not change in non-responders. All clinical data after therapy are summarized in Table 9.
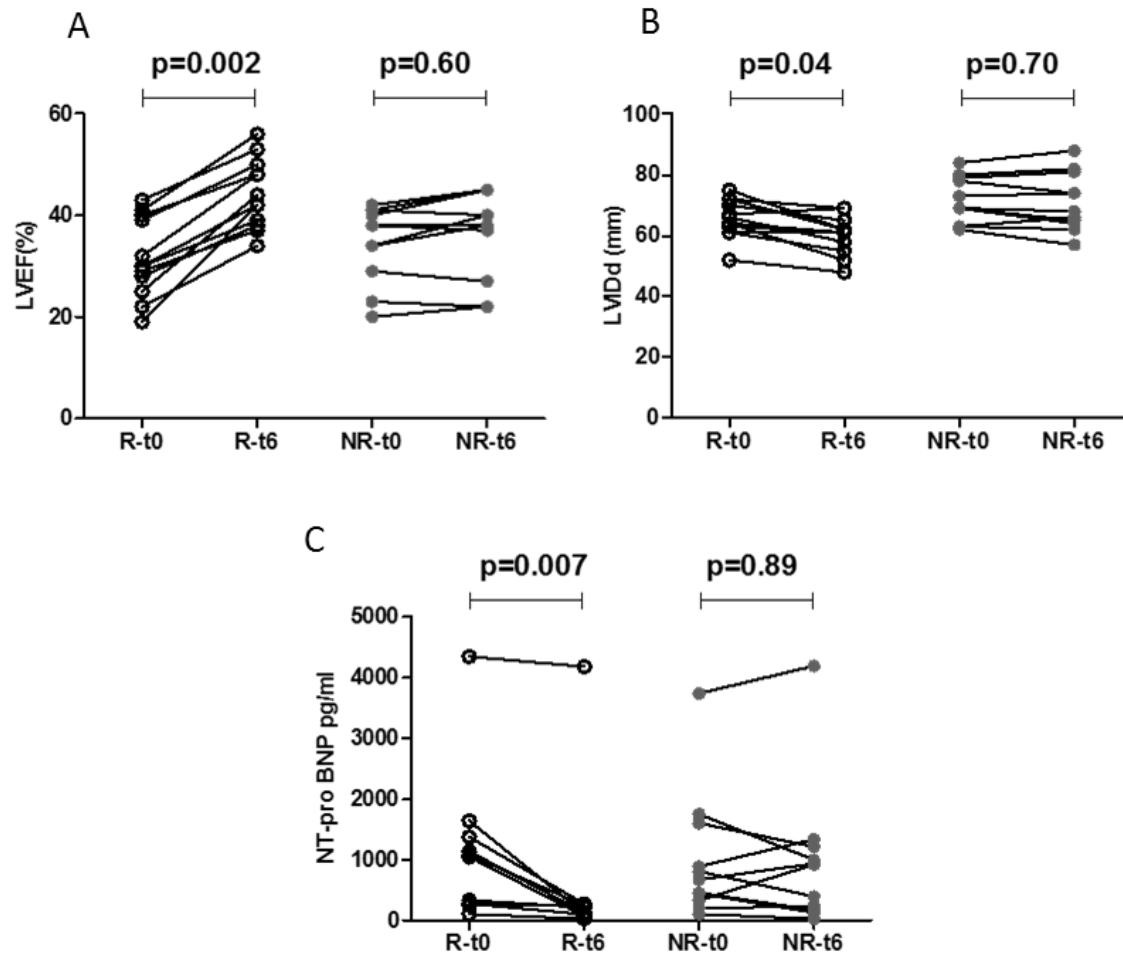
Fig. 10. Effect of immunoadsorption on LVEF (A), LVIDd (B), and NT-pro-BNP (C) in responders and non-responders

Data before (t0) and after six months (t6) of treatment is presented. P-value displays the significance of alterations upon IA/IgG. Responders displayed increased LVEF, decreased LVIDd and NT-proBNP after six months of therapy with p-value<0.05, whereas in non-responders, the effect of IA/IgG were not observed on these parameters.

Table 9. Longitudinal characteristics of DCM patient subgroups

	responders (n=12)			non-responders (n=11)		
	BL	FU	p-value	BL	FU	p-value
Subgroup-specific alterations upon IA/IgG						
LVEF (%) ±SD[a]	32 ± 8	45±7	<0.002	35 ± 8	36±9	0.60
LVIDd (mm) ±SD[a]	66 ± 6	60±6	<0.040	72 ± 8	71±10	0.90
Nt-pro BNP pg/ml ±SD[a]	1081±1205	532±1211	<0.007	1001±1051	962±1169	0.839
Inflammation positive (n)	8	4	0.413[d]	7	4	0.413[d]
NYHA I/II/III/IV (n)	0/5/7/0	5/4/3/0	0.02[e]	0/7/6/0	2/8/3/0	0.05[e]
Fibrosis grade[b] 0-0/1/2/3 (n)	0/6/3/3	0/5/4/4	0.80[e]	0/5/3/3	0/2/5/4	0.29[e]
Differences between subgroups after IA/IgG						
ΔLVEF (%) ±SD[a]		13±5			2±3	<0.0001[f]
ΔLVIDd (mm) ±SD[a]		-5±5			-1±3	0.032[f]

LVEF-left ventricular ejection fraction, LVIDd – left ventricular internal diameter at diastole, NYHA – New York Heart Association. Mean values with standard deviation (SD) are shown, [b] fibrosis in EMBs was determined and considered as grade 0 = no, grade 1= mild, grade 2 = moderate, grade 3 = severe. p-value baseline (BL) vs. follow-up (FU) calculated by [c]Wilcoxon signed rank test, [d] Fisher`s Exact test, two tailed, or [e] Chi-Square test, [f] p-value ΔLVEF, ΔLVIDd, Δnt-pro BNP (absolute change of LVEF, LVIDd or Nt-pro-BNP (FU-BL) of responders vs. non-responders was calculated by Mann-Whitney-test, two-tailed.

3.2.3 Proteomic changes induced by immunoadsorption therapy in responder and non-responder DCM patients

Proteomic alterations caused by immunoadsorption therapy were analyzed separately in responder and non-responder DCM patients by calculating the ratio of protein intensities at follow-up versus baseline (responder FU/BL, non-responder FU/BL). Along with this, the differences in the therapy response between the subgroups were addressed by comparing ratios of responders and non-responders (R FU/BL vs. NR FU/BL). Raw data of 23 DCM patients (Forty six raw files; 23 at BL and 23 at FU) obtained by mass spectrometry were analyzed with the Rosetta Elucidator software for feature extraction, peak alignment, and database search. In total, data of 669 proteins at BL and after IA/IgG were available for all patients. For those proteins, therapy effects in responders (R-

FU/BL), non-responders (NR-FU/BL) and the difference in the therapy effects (R-FU/BL vs NR-FU/BL) were calculated by applying rank product based statistics.

3.2.4 Effect of therapy on protein pattern in responder (R-FU/BL) DCM patients

Immunoadsorption therapy altered the expression of 16 proteins ($|$FC$|$ 1.3, $p \leq 0.05$, Table 10) in responders (R-FU/BL) of which, six were present at higher abundance, whereas ten proteins were detected at lower abundance at follow up.

Table 10. List of significantly altered proteins in responders (FU/BL) after IA/IgG

ID	Protein Name	FC (FU/BL)	p-val*
O75380	NADH dehydrogenase [ubiquinone] iron-sulfur protein	1.49	8.95E-13
Q01449	Myosin regulatory light chain 2	1.36	1.10E-12
P61457	Pterin-4-alpha-carbinolamine dehydratase	1.44	1.49E-12
P41222	Prostaglandin-H2 D-isomerase	1.35	9.70E-12
Q15056	Eukaryotic translation initiation factor 4H	1.41	2.56E-11
P55083	Microfibril-associated glycoprotein 4	1.31	3.84E-10
P02549	Spectrin alpha chain, erythrocytic 1	-1.36	1.90E-07
P00915	Carbonic anhydrase 1	-1.36	8.05E-07
P21333	Filamin-A	-1.36	1.96E-06
P00918	Carbonic anhydrase 2	-1.31	2.03E-06
Q8TEY5	Cyclic AMP-responsive element-binding protein 3-like protein 4	-1.60	6.81E-06
P02042	Hemoglobin subunit delta	-1.38	7.27E-06
P67936	Tropomyosin alpha-4 chain	-1.31	1.86E-04
P62805	Histone H4	-1.37	6.59E-04
O00232	26S proteasome non-ATPase regulatory subunit 12	-1.33	6.06E-03
P12814	Alpha-actinin-1	-1.32	7.13E-03

*p-val. – p-value, Rank product test

The differentially abundant proteins altered by therapy in responders were functionally categorized using PANTHER GO annotation tool. These proteins were assigned to several biological functions including metabolic process (10 proteins), cellular process (8 proteins), cellular organization (5 proteins) and development process (5 proteins). Five altered proteins were from cytoskeletal categories including spectrin alpha chain, myosin regulatory light chain, tropomyosin alpha-4

chain, filamin-A and alpha-actinin1. The highest fold change observed after therapy in responders was observed for protein NADH dehydrogenase [ubiquinone] iron-sulfur protein 6 (NDUFS6, FC 1.49) and Pterin-4-alpha-carbinolamine dehydratase (PCBD1, FC 1.44), whereas the strongest decrease was seen for protein cyclic AMP-responsive element-binding protein 3-like protein 4 (CREB3L4, FC -1.60) and hemoglobin subunit delta (HBD, FC -1.38). Furthermore, to get deeper insight at functional level, enrichment analysis was performed using Ingenuity Pathway Analysis (Fig. 11), but these analysis are of limited value due to a small number of molecules in each category.
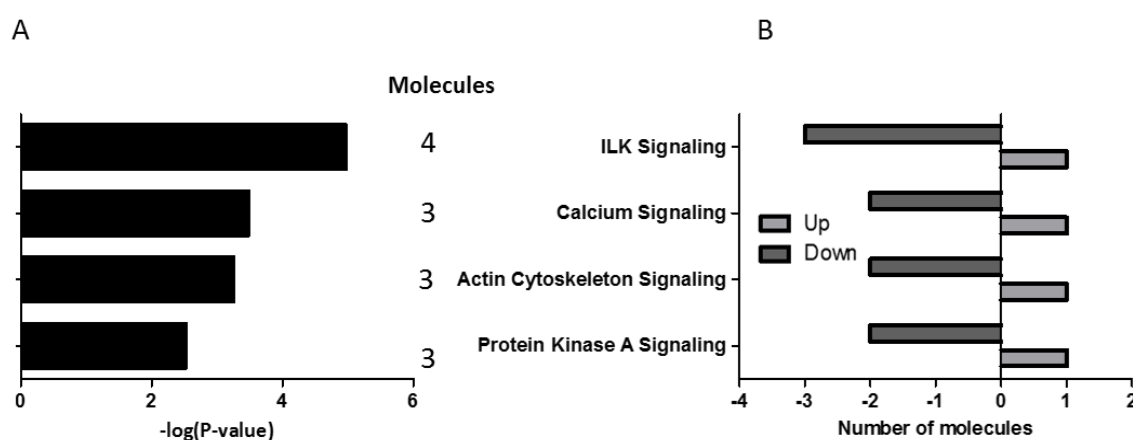
Fig. 11. Functional assignment of differential proteins to IPA canonical pathways

IPA categories for which the analysis revealed (A) an enrichment of differentially abundant proteins in responders upon therapy and (B) the number of higher (up) and lower (down) abundant proteins in each category. -log p-value: significance of association that is dependent on the number of proteins of each category.

3.2.5 Effect of immunoadsorption therapy on protein pattern in non-responder DCM patients

Concomitantly with the immunoadsorption therapy the abundance pattern of forty three proteins (Table 11) was altered in non-responders at FU. Among them, twenty seven were present at higher abundance, while sixteen were present at lower level. Differentially abundant proteins were from

diverse subcellular origins including mitochondria, extracellular matrix, cytosol, cytoskeleton, membrane and endoplasmic reticulum.

Table 11. Proteins altered by immunoadsorption therapy in non-responders at FU

ID	Protein Name	Fold change	p-val*
Mitochondria			
P14854	Cytochrome c oxidase subunit 6B1	1.96	4.19E-14
Q86SX6	Glutaredoxin-related protein 5	1.50	2.26E-11
Q00325	Phosphate carrier protein	1.36	3.59E-11
Q5JTJ3	Cytochrome c oxidase assembly factor 6 homolog	1.33	4.95E-09
P04040	Catalase	-1.47	6.78E-03
Extracellular matrix/space/region			
Q07507	Dermatopontin	2.44	9.72E-18
Q15063	Periostin	2.28	1.88E-19
P55083	Microfibril-associated glycoprotein 4	1.98	4.04E-16
P21810	Biglycan	1.89	1.79E-15
P51888	Prolargin	1.89	1.30E-15
P51884	Lumican	1.87	1.06E-15
P02452	Collagen alpha-1(I) chain	1.85	7.20E-15
P08123	Collagen alpha-2(I) chain	1.82	5.02E-15
P20774	Mimecan	1.74	1.94E-14
Q9UBX5	Fibulin-5	1.65	1.02E-11
P08603	Complement factor H	1.46	2.45E-10
P07585	Decorin	1.43	1.21E-10
P01834	Ig kappa chain C region	1.38	2.19E-09
P80748	Ig lambda chain V-III region LOI	1.35	2.08E-11

ID	Protein Name	Fold change	p-val*
P04004	Vitronectin	1.34	1.23E-09
P09382	Galectin-1	1.31	5.11E-09
P62805	Histone H4	1.30	3.60E-10
P35556	Fibrillin-2	-2.09	3.74E-03
Cytoskeleton			
Q9Y696	Chloride intracellular channel protein 4	1.40	6.17E-10
P60981	Destrin	1.36	1.25E-10
P47756	F-actin-capping protein subunit beta	1.34	4.08E-10
Q53GG5	PDZ and LIM domain protein 3	1.30	1.00E-09
Q01449	Myosin regulatory light chain 2	-1.47	7.57E-04
P11277	Spectrin beta chain	-1.56	1.10E-02
P02549	Spectrin alpha chain	-2.30	5.28E-03
Endoplasmic reticulum			
Q8TEY5	Cyclic AMP-responsive element-binding protein 3-like protein	-2.20	8.63E-02
Cytosol			
Q15056	Eukaryotic translation initiation factor 4H	1.44	1.59E-10
Q01995	Transgelin	1.31	2.34E-10
P13861	cAMP-dependent protein kinase II-alpha regulatory subunit	-1.40	2.28E-02
P68871	Hemoglobin subunit beta	-1.41	5.42E-03
P52758	Ribonuclease UK114	-1.43	1.47E-01
O00232	26S proteasome non-ATPase regulatory subunit 12	-1.46	9.41E-03
P69905	Hemoglobin subunit alpha	-1.47	3.88E-03
P02794	Ferritin heavy chain	-1.66	1.86E-02
P00918	Carbonic anhydrase 2	-1.67	1.34E-02
P00915	Carbonic anhydrase 1	-1.73	1.02E-02

ID	Protein Name	Fold change	p-val*
P02042	Hemoglobin subunit delta	-1.75	4.05E-03
Membrane			
Q9Y6E2	Basic leucine zipper and W2 domain-containing protein 2	-1.42	4.60E-04

*p-val. – p-value, Rank product test

The highest fold change was found for dermatopontin (DPT, FC 2.44) and periostin (POSTN, FC 2.28) while the strongest decrease was displayed by spectrin alpha chain (SPTA, FC -2.30) and cyclic AMP-responsive element-binding protein 3-like protein 4 (CREB3L4, FC -2.20). Altered proteins were from extracellular matrix, receptor, signaling, transfer, nucleic acid binding and cytoskeletal categories. Functional enrichment of altered proteins in non-responders after therapy revealed the canonical pathways *intrinsic prothrombin activation pathway*, *hepatic fibrosis*, *sertoli cell-sertoli cell junction signaling*, *dendritic cell maturation* and *calcium signaling* (Fig. 12). The number of proteins associated with each pathway was small (3-4 proteins), nevertheless results show that molecules related to fibrosis and calcium ion signaling were affected and suggested an ongoing progression of the cardiac disease. In contrast, *sertoli cell-sertoli cell junction signaling* has been related to germinal cells, and the related proteins (spectrin alpha chain-SPTA1, spectrin beta chain-SPTB, cAMP-dependent protein kinase type II-alpha regulatory subunit- PRKAR2A) of this pathway have also been associated to pathophysiological alterations in cardiomyocytes.
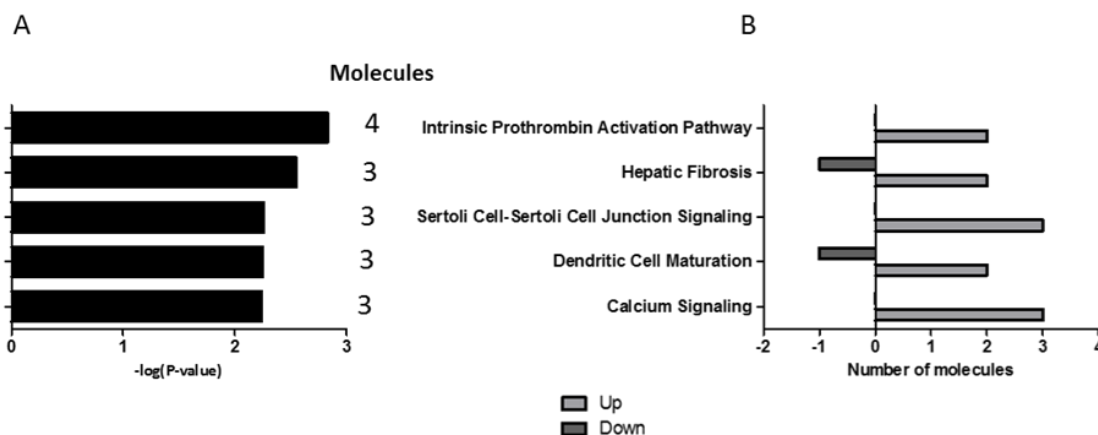
Fig. 12. Functional assignment of altered proteins in non-responders to IPA canonical pathways

(A) Pathways for which an enrichment of differentially abundant proteins was calculated; (B) the number of proteins of higher (up) and lower (down) abundance in each category is displayed. Significance of association (-log p-value) that depends on the associated proteins for each category is given.

3.2.6 Comparison of the immunoadsorption therapy effect on protein abundance in responders (R-FU/BL) and non-responders (NR-FU/BL)

The results described in the above sections show that different sets of proteins were altered by therapy in reponder and non-responder DCM patients. In total, only ten proteins displaying alterations during therapy were common in responders and non-responders (Fig. 13A). Among them, eight proteins (EIF4H, MFAP4, SPTA1, CA1, CA2, CREB3L4, HBD, and PSMD12) displayed the same regulation in both subgroups, whereas two proteins (H4 and MYL7) displayed opposite alteration between responders and non-responders (Fig. 13B). Myosin regulatory light chain 2 (MYL7) is a calcium binding protein, interacts with the tail of thick filament protein myosin to regulate myosin motility and function, and might be an interesting candidate for further evaluation in therapy response. In responders, during therapy MYL7 levels increased (R-FU/BL 1.36), whereas, in non-responders, its level decreased (NR-FU/BL 0.68). Apart from it, two proteins 26S proteasome non-ATPase regulatory subunit 12 (PSMD12) and cyclic AMP-

responsive element-binding protein 3-like protein 4 (CREB3L4) playing a vital role in protein turn over, were found decreased in both subgroups (responders, and non-responders) after therapy.
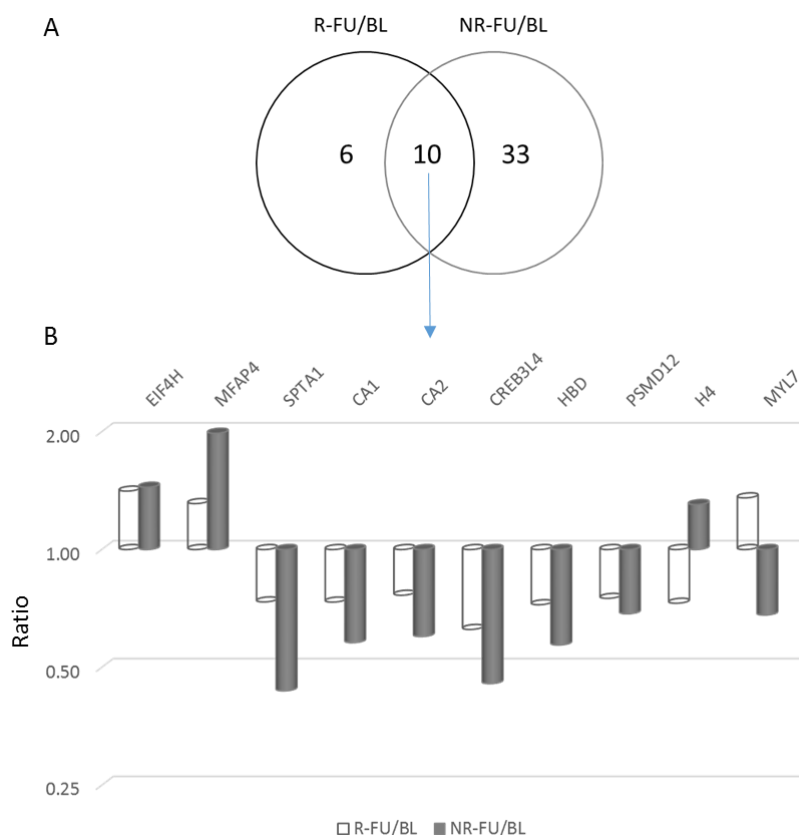
Fig. 13. Proteins affected by IA/IgG in both responders (R-FU/BL) and non-responders (NR-FU/BL)

(A) Overlap of altered proteins in responders and non-responders after therapy. In total, only ten proteins were affected by therapy in both patient subgroups and their abundance pattern is presented in (B). Among those proteins, two (EIF4H and MFAP4) were higher abundant, and six (SPTA1, CA1, CA2, CREB3L4, HBD, and PSMD12) were lower abundant in both subgroups after therapy, whereas two proteins (H4 and MYL7) displayed opposite regulation in responders and non-responders. (EIF4H- eukaryotic translation initiation factor 4H, MFAP4- microfibril-associated glycoprotein 4, SPTA1- spectrin alpha chain, CA1- carbonic anhydrase 1, CA2- carbonic anhydrase 2, CREB3L4- cyclic AMP-responsive element-binding protein 3-like protein 4, HBD- haemoglobin subunit delta, PSMD12- 26S proteasome non-ATPase regulatory subunit 12, H4- histone H4 and MYL7- myosin regulatory light chain 2).

3.2.7 Differential IA/IgG effect on proteins in the sub-groups (R-FU/BL vs NR-FU/BL)

To reveal the differences between the immunoadsorption therapy effect among the patient subgroups (R and NR), ratios of protein abundance before and after therapy (R-FU/BL vs NR-FU/BL) were compared. Comparison of FU over BL ratios of both subgroups revealed significantly different alterations for 57 proteins (p<0.05, FC ≥ |1.3|, Table 12). Most of these altered proteins except five (Collagen alpha-1, cAMP-dependent protein kinase catalytic subunit beta, Phosphoglycerate mutase 2, Transmembrane protein 14C, and Tropomyosin alpha-4 chain) were not found differentially abundant between responders and non-responders at baseline in the proteome analysis. Thus, predominantly the observed alterations were seen due to IA/IgG, rather than differences in proteins levels at baseline.

Table 12. List of proteins differentially altered in the DCM patient subgroups after IA/IgG

ID	Protein Description	FC (R/NR)	p-value*
Mitochondria			
Q9P0S9	Transmembrane protein 14C	1.47	1.07E-132
Q9Y241	HIG1 domain family member 1A, mitochondrial	1.38	1.50E-118
Q5JTJ3	Cytochrome c oxidase assembly factor 6 homolog	-1.34	3.61E-89
O95298	NADH dehydrogenase [ubiquinone] 1	-1.37	1.96E-97
Q00325	Phosphate carrier protein	-1.37	2.95E-105
Q86SX6	Glutaredoxin-related protein 5	-1.38	4.39E-107
P14406	Cytochrome c oxidase subunit 7A2	-1.40	2.55E-89
Q9Y696	Chloride intracellular channel protein 4	-1.44	2.57E-104
P14854	Cytochrome c oxidase subunit 6B1	-1.85	8.83E-155
Cytoplasm			
P02549	Spectrin alpha chain, erythrocytic 1	1.69	1.34E-166
P61457	Pterin-4-alpha-carbinolamine dehydratase	1.46	3.01E-112
Q8TEY5	Cyclic AMP-responsive element-binding protein 3-like protein 4	1.38	1.57E-149
P52758	Ribonuclease UK114	1.36	3.09E-89
P22694	cAMP-dependent protein kinase catalytic subunit beta	1.35	5.87E-100
P36871	Phosphoglucomutase-1	1.30	8.17E-85
P04080	Cystatin-B	-1.31	2.65E-94
O43768	Alpha-endosulfine	-1.32	6.53E-97
Q15149	Plectin	-1.32	3.53E-102
Q00610	Clathrin heavy chain 1	-1.32	3.34E-88
P52566	Rho GDP-dissociation inhibitor 2	-1.39	1.15E-100

ID	Protein Description	FC (R/NR)	p-value*
P12814	Alpha-actinin-1	-1.43	1.09E-104
P08670	Vimentin	-1.43	1.24E-102
P67936	Tropomyosin alpha-4 chain	-1.44	1.27E-101
Q32MK0	Myosin light chain kinase 3	-1.46	1.45E-107
Q53GG5	PDZ and LIM domain protein 3	-1.51	1.64E-115
P63261	Actin, cytoplasmic 2	-1.57	4.46E-110
Q01469	Fatty acid-binding protein	-1.62	6.86E-116
Secreted/extracellular matrix			
P35556	Fibrillin-2	2.27	1.44E-167
P00751	Complement factor B	-1.30	1.59E-86
P02751	Fibronectin	-1.32	6.51E-88
P04004	Vitronectin	-1.33	4.24E-101
P12109	Collagen alpha-1	-1.34	3.31E-96
P01857	Ig gamma-1 chain C region	-1.35	7.06E-88
P09382	Galectin-1	-1.35	5.63E-94
P20774	Mimecan	-1.44	1.25E-116
P55083	Microfibril-associated glycoprotein 4	-1.51	5.93E-124
P51884	Lumican	-1.63	3.41E-129
P51888	Prolargin	-1.66	2.49E-131
P08123	Collagen alpha-2	-1.71	1.66E-135
Q9UBX5	Fibulin-5	-1.85	6.12E-142
P21810	Biglycan	-2.02	6.32E-157
Q15063	Periostin	-2.12	8.91E-172
P02452	Collagen alpha-1	-2.13	1.55E-173
Q07507	Dermatopontin	-2.23	2.36E-173
Nucleus			
Q00577	Transcriptional activator protein Pur-alpha	1.31	8.94E-83
P31943	Heterogeneous nuclear ribonucleoprotein H	-1.44	5.03E-103
Q99879	Histone H2B type 1-M	-1.66	1.62E-127
P62805	Histone H4	-1.79	8.14E-141
Unclassified			
Q01449	Myosin regulatory light chain 2, atrial isoform	1.99	4.41E-165
P02794	Ferritin heavy chain	1.55	1.01E-127
P15259	Phosphoglycerate mutase 2	1.49	3.31E-124
Q9Y6E2	Basic leucine zipper and W2 domain-containing protein 2	1.41	2.62E-97
O75368	SH3 domain-binding glutamic acid-rich-like protein	-1.31	1.22E-89
P24844	Myosin regulatory light polypeptide 9	-1.34	5.13E-97
P01834	Ig kappa chain C region	-1.43	1.26E-100
P48681	Nestin	-1.43	1.71E-112

ID	Protein Description	FC (R/NR)	p-value*
P35749	Myosin-11	-1.61	1.84E-132

*p-val. – p-value, Rank product test

Among the 57 differentially abundant proteins, 14 proteins were present in higher abundance, while 43 proteins displayed lower levels in responders than in non-responders after follow-up. Functional classification of altered proteins revealed differences in the therapy response of responders and non-responders in cytoskeletal, extracellular matrix, signaling, and nucleic acid binding proteins. Also, both subgroups were different in proteins involved in various biological processes, most importantly cellular and metabolic processes. Furthermore, functional classification of altered proteins highlighted the following categories of molecular and cellular function: *cellular assembly and organization* (19 proteins), *cellular function and maintenance* (18 proteins), and *cell morphology* (21 proteins). Likewise, in disease and disorder categories the difference in *cardiovascular disease* (17 proteins) was most prominent. Among canonical pathways, differences were more prominent for proteins associated with *ILK signaling, actin cytoskeleton signaling, fibrosis*, and *calcium signaling* (Fig. 14).
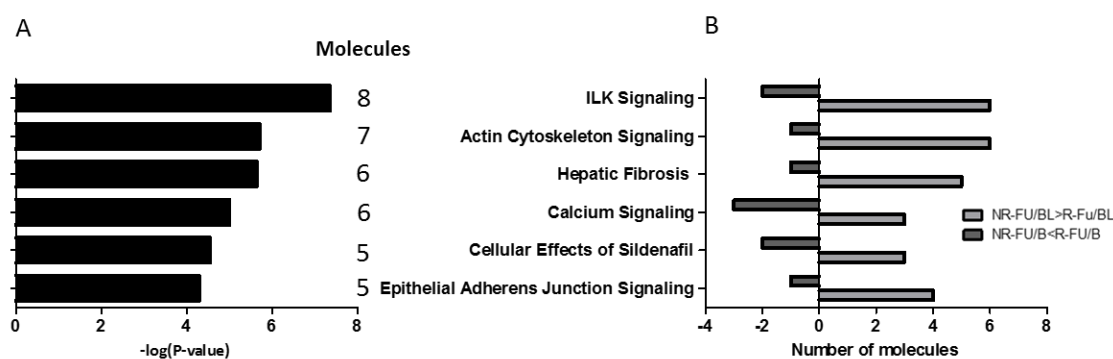
Fig. 14. Canonical pathways differentially affected upon therapy in the patient subgroups

Proteins differentially affected upon therapy in responders and non-responders (R-BL/FU vs NR-BL/FU) were subjected to enrichment analysis in IPA and the results for canonical pathways are shown. (A) Significance of enrichment (-log p-value) and number of associated proteins. (B) Differential effect of therapy in the patient subgroups per category.

Seven proteins related to actin cytoskeleton signaling displayed a differential pattern of alteration (R-FU/BL vs NR-FU/BL). Among them, six proteins (MYL9, MYH11, MYLK3, FN1, ACTG1, and ACTN1) displayed lower abundance, while protein myosin regulatory light chain-2, atrial isoform (MYL7) was more abundant in responders at FU in comparison to non-responders (Fig. 15). Myosin regulatory light chain-2, atrial isoform (MYL7) and myosin regulatory light polypeptide 9 (MYL9) are calcium binding proteins, whereas myosin-11 (MYH11) helps in cardiac muscle fibre development, hence regulates the contraction of muscles. Fibronectin (FN1), an extracellular matrix protein was found less abundant in responders (FC 0.77) and has been shown to be involved in cell adhesion, cell motility, and maintenance of cell shape. Actin, cytoplasmic 2 (ACTG1) was found at lower level in responders, and has functions in sarcomere organization, cell junction assembly, and it also contributes to the structural integrity of cytoskeletal structures. Also, another protein alpha-actinin-1 (ACTN1) was found at lower level in responders in comparison to non-responders after six months of immunoadsorption therapy, and it is an F-actin cross linking protein that helps actin to anchor to a variety of intercellular structures.
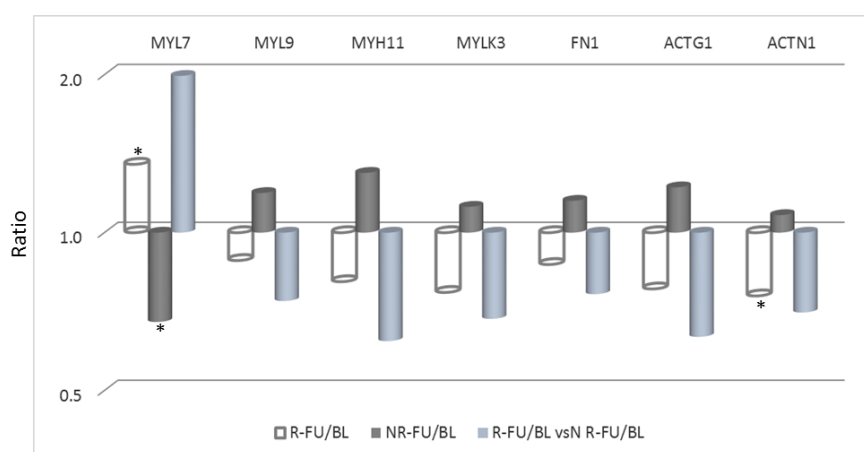

Fig. 15. Differential alterations of actin cytoskeleton signaling associated proteins upon IA/IgG in responders and non-responders

MYL7- myosin regulatory light chain 2, MYL9- myosin regulatory light polypeptide 9, FN1- fibronectin, MYH11- myosin-11, ACTG1- actin cytoplasmic 2, MYLK3- myosin light chain kinase 3 and ACTN1- alpha-actinin-1. (* significant in R-FU/BL, and NR-FU/BL)

Besides the actin cytoskeleton, therapy seemed to significantly influence the level of proteins associated with fibrosis. In responders, therapy was accompanied with a decrease of five proteins involved in fibrotic remodeling -myosin regulatory light polypeptide 9, fibronectin, collagen alpha-1(I) chain, myosin 11 and collagen alpha-2 (I) chain. In contrast, protein myosin regulatory light chain 7 was found at higher levels in responders than non-responders at FU (Fig. 16).
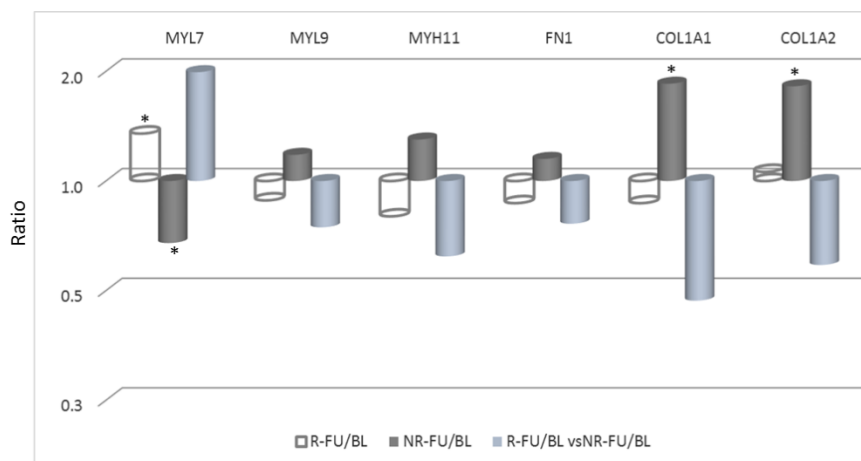

Fig. 16. Differential alteration of proteins associated with fibrosis upon IA/IgG in responders and non-responders

MYL9- myosin regulatory light polypeptide 9, FN1- fibronectin, COL1A1- collagen alpha-1(I) chain, MYH11- myosin-11, MYL7- myosin regulatory light chain 7 and COL1A2- collagen alpha-2(I) chain. (* significant in R-FU/BL, and NR-FU/BL)

Furthermore, the lower level of fibrotic proteins in responders at FU suggesting a lower degree of fibrosis in this patient subgroup in comparison to non-responders was supported by the lower abundance of extracellular matrix proteins (mimecan, biglycan, prolargin, and dermatopontin) indicating the differences among subgroups in extracellular matrix remodeling processes after IA/IgG.

Moreover, based on the alterations observed for proteins upon IA/IgG, Ingenuity Pathway Analysis predicted a lower activity of transforming growth factor beta in responders than in non-responders after immunoadsorption therapy. The lower activity of TGF-β was predicted based on the ratios of 15 proteins (VIM, POSTN, MYH11, MFAP4, HNRNPH1, FTH1, FN1, FBLN5, FABP5,

COL6A1, COL1A2, COL1A1, CLIC4, BGN and ACTN1) which displayed a differential alteration upon IA/IgG in responders and non-responders. In responders, those proteins displayed in general a lower abundance after therapy (Fig. 17) whereas in non-responders the change was smaller or the level was even higher.
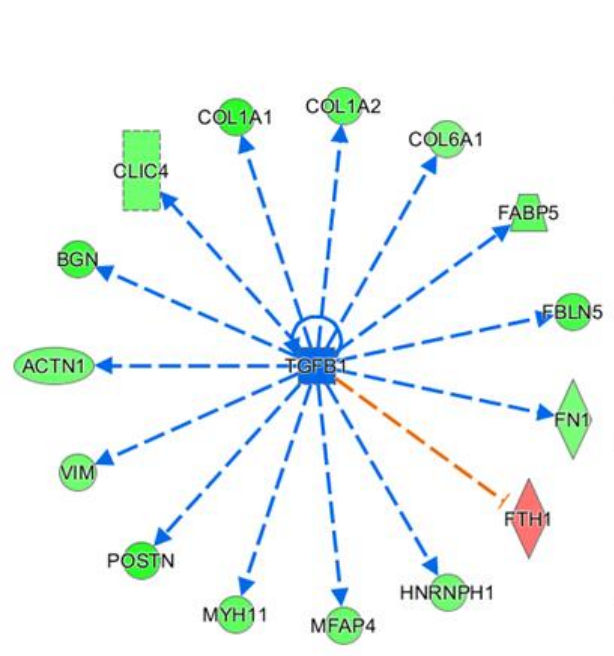

Fig. 17. Differential abundance pattern of TGFβ associated proteins upon IA/IgG in the DCM patient subgroups (R-FU/BL vs NR-FU/BL)

Out of fifteen proteins associated with TGF-ß activity, for 14 R-FU/BL vs NR-FU/BL ratios were < 1, which led to prediction of a lower activity of the cytokine in responders after six months after IA/IgG. Blue dotted line- low TGF-ß activity leads to lower abundance of dependent molecules. (POSTN- periostin, MYH11- myosin-11, MFAP4- microfibril-associated glycoprotein 4, HNRNPH1- heterogeneous nuclear ribonucleoprotein H, FTH1- ferritin heavy chain, FN1- fibronectin, FBLN5- fibulin-5, FABP5- fatty acid-binding protein, COL6A1- collagen alpha-1(VI) chain, COL1A2- collagen alpha-2(I) chain, COL1A1- collagen alpha-1(I) chain- CLIC4,chloride intracellular channel protein 4, BGN- biglycan, ACTN1- alpha-actinin-1)

Additionally, in line with this finding, Ingenuity Pathway Analysis predicted a lower expression/activity of SMAD3 signaling in responders based on lower abundance of seven different proteins including lumican, fibronectin, collagen alpha-1(VI) chain, collagen alpha-2(I) chain (alpha-2 type I collagen), collagen alpha-1(I) chain (alpha-1 type I collagen) and biglycan. SMAD3

signaling is directly related to TGF-β signaling and seemed to be reduced in responders after therapy.

3.3 Results of plasma proteomic profiling by implementing Isobaric Tag for Relative and Absolute Quantitation (iTRAQ) technology

In the previous section, efforts were made to disclose the myocardial proteomic differences between responder and non-responder DCM patients before immunoadsorption therapy to predict the therapy outcome. In general, endomyocardial proteomic profiling of responders and non-responders revealed many proteins displaying different levels in both patient subgroups mainly involved in carbohydrate and lipid metabolism. More specifically, differences were observed in proteins related to mitochondrial functions, immune regulation, and cardioprotection. However, the proteins discovered in EMBs are difficult to use as a classifier to discriminate responders and non-responders in the routine clinical practice because biopsy extractions require complex surgical interventions that are not feasible in every case. In this regards, blood plasma might be a better choice as it is easily and almost non-invasively obtained. Biochemical plasma tests can easily be performed in clinics as well as in analytical laboratories. Thus, in this study efforts were made to screen for plasma proteomic biomarkers that might be useful for clinicians to identify and select the subgroup of DCM patients, who could benefit from immunoadsorption therapy. Along with this, plasma profiling of healthy controls (LVEF ≥45) was also performed to compare the plasma proteome of responders and non-responders to healthy controls.

3.3.1 Plasma proteome analysis pipeline

To dig deeper into the plasma proteome, complementary techniques such as iTRAQ and label-free quantification were used and furthermore a subset of proteins displaying different levels during the initial screening was subjected to validation using multiple reaction monitoring and ELISA. The workflow used in the plasma proteome study has been summarized in Fig. 18.
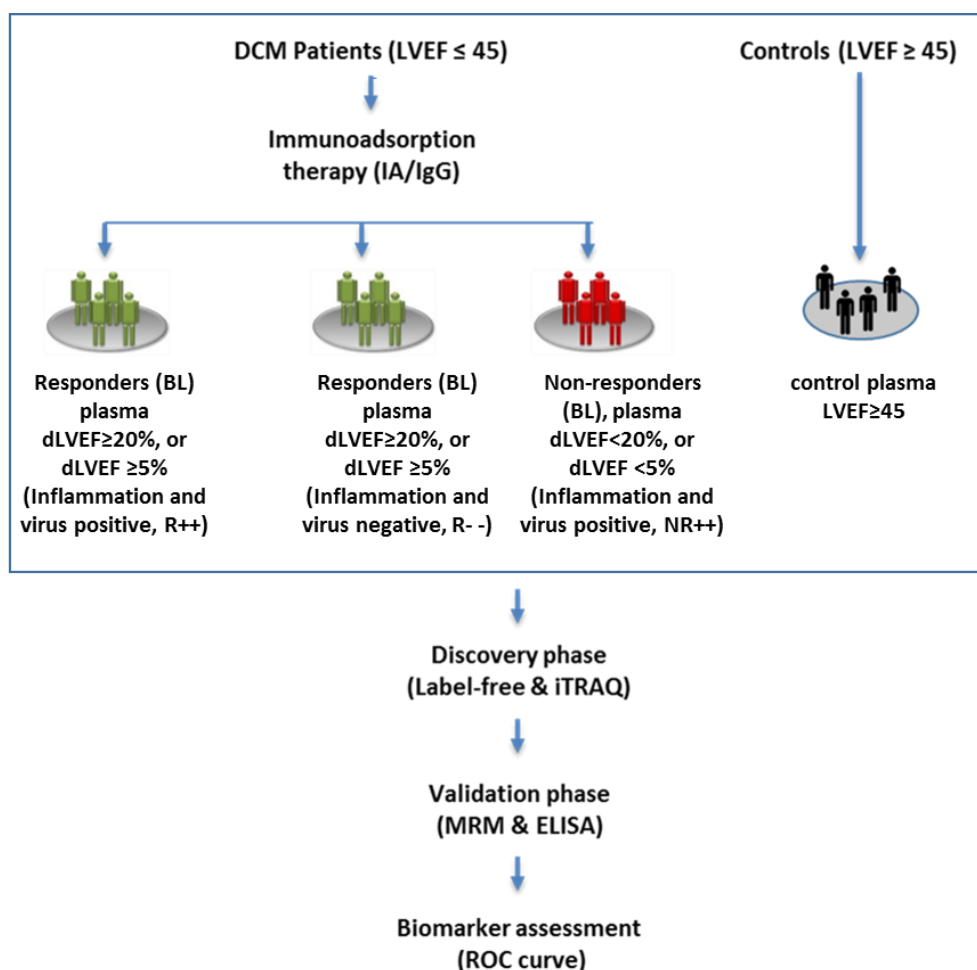
Fig. 18. Summary of plasma proteomic workflow

Dilated cardiomyopathy patients treated by immunoadsorption therapy were grouped as responders or non-responders retrospectively according to LVEF improvement. Plasma that was collected from each patient at baseline was depleted for six high abundant plasma proteins using MARS-6 immunoaffinity columns. Biomarker candidates were derived from discovery phase experiments carried out via a label-free (n=34) and an iTRAQ (n=20) workflow, and reviewed in a validation phase applying MRM (n=93 samples, N=proteins) and ELISA (n=99 samples, n= proteins) techniques. Furthermore, the potential of differentially abundant proteins to classify DCM patient subgroups was assessed using Receiver Operating Characteristic curves (ROC).

3.3.2 Clinical parameters of patients at baseline whose plasma samples were analyzed in the discovery and the validation phase

Clinical parameters at baseline did not differ in responders and non-responders except disease duration and LVIDd that were significantly higher in non-responder DCM patients (Table 13).

Table 13.Baseline characteristics of R and NR dilated cardiomyopathy patients

	R (33)	NR (16)	p-value
Age (years) ±SD[a]	50 ± 11	53 ± 9	0.20[b]
Gender (M/F)	23/10	12/4	1.00[c]
LVEF (%) ±SD[a]	32 ± 6	34 ± 8	0.38[b]
LVIDd (mm) ±SD[a]	69 ± 8	74 ± 7	0.04[b]
Inflammation CD68+CD3(cells/mm2) ±SD[a]	22 ± 25	19 ± 10	0.76[b]
Inflammation positive	22	10	1.00[c]
BMI	28 ± 4	27 ± 4	0.40[b]
Disease duration (months) ±SD[a]	22 ± 33	44 ± 41	0.03[b]
NYHA class (n)			0.76[c]
II	14	8	
III	19	8	
Medication			
β-Blockers	33	16	1.00[c]
ACE inhibitor	25	14	0.46[c]
AT1 antagonists	13	5	0.76[c]
Diuretics	33	16	1.00[c]
Digitalis	4	6	0.06[c]

[a] Mean values with standard deviation (SD), [b] The Mann-Whitney test, two-tailed, [c] Fishers exact test, two-tailed, M/F-Male/Female, LVEF-Left ventricular ejection fraction, LVIDd-Left ventricular inner diameter at diastole, BMI-Body mass index, NYHA-New York Heart Association, AT1-Angiotensin 1.

As mentioned in the previous sections (myocardial tissues), in responders therapy has a significant influence not only on LVEF but also on LVIDd. Thus, six months after immunoadsorption therapy in responders LVEF increased from 32 ± 5.9 to 46 ± 6.7 % (p<0.0001) whereas LVIDd decreased from 69 ± 8.1 to 63 ± 8.2 mm (p=0.002). LVEF (33.7 ± 7.4 to 33.8 ± 8.9, p=0.97) and LVIDd (73.6 ± 7.4 to 73.4 ± 8.8, p=0.97) did not change in non-responders in response to IA/IgG.

3.3.3 Plasma proteome screening using a iTRAQ labeling approach

For the iTRAQ experiment pools of very well characterized patient samples were used. Inflammation and virus persistence might influence not only the myocardial proteome but also plasma protein composition. Therefore, DCM patients were grouped not only by therapy response but also sorted into virus and inflammation positive or negative. Because of the low number of non-

responders with virus and inflammation negative diagnosis, no pool of such patients could be analyzed. Thus, three patient pools (responders with inflammation and virus R++, responders without inflammation and virus R--, and non-responders with inflammation and virus NR++) and a plasma pool of patients with normal heart function were investigated and the corresponding paired ratios of all groups were calculated. The whole experiment was performed twice (two technical replicates) and the combined analysis of both replicates identified 363 non-redundant plasma proteins across the four pools representing 5 individual samples each. Proteins with peptide variability ≤30% and fold change ≥│1.2│) present in both technical replicates with similar directions were considered as differentially abundant. In general, a large number of proteins (nearly 25% of all identified proteins) were found differentially abundant with relatively small fold changes among various group comparisons (Fig. 19).

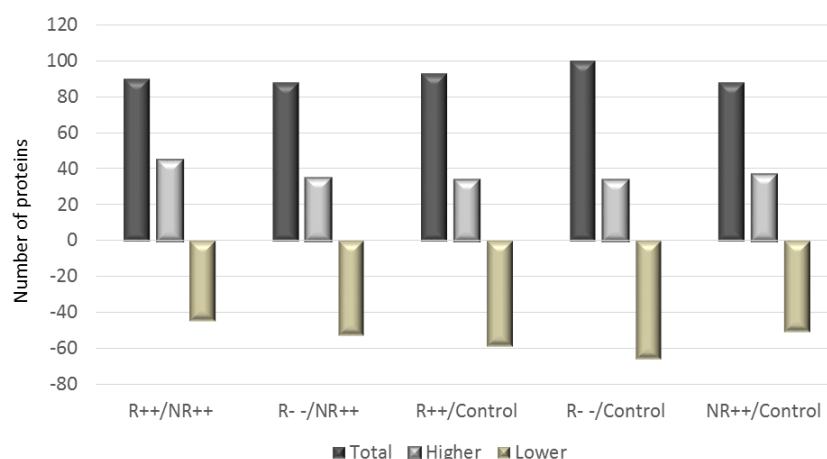**Fig. 19. Number of differentially abundant plasma proteins in the pairwise comparison of groups**

Along with the number of differentially abundant plasma proteins in each comparison, number of higher and lower abundant proteins are also given.

3.3.4 Differentially abundant plasma proteins between dilated cardiomyopathy (responders and non-responders) patients and healthy controls obtained by the iTRAQ approach

Responder and non-responder DCM patients were subgrouped according to presence of inflammation and virus status into R++, R-- and NR++, and their plasma proteome was compared to the one of controls with normal ejection fraction. Comparative analysis of the differentially abundant plasma proteins among the three groups can point to general differences between DCM patients and controls independent of inflammation status and virus presence and revealed thirty-six common proteins (Fig. 20, Table 14). Among those, five proteins (ficolin-2, putative WAS protein family homolog 3, endoplasmic reticulum resident protein 44, serotonin N-acetyltransferase, and dopamine beta-hydroxylase) were more abundant, whereas twenty five proteins displayed lower abundance in DCM patients in all three (R++/controls, R--/controls, and NR++/controls) group comparisons. In addition, for six proteins (Nik-related protein kinase, transcobalamin-1, teneurin-1, conserved oligomeric Golgi complex subunit 3, GON-4-like protein, and alpha-amylase 1) abundance pattern were not consistent across all three group comparisons (R++/controls, R--/controls, and NR++/controls) (Table 14).

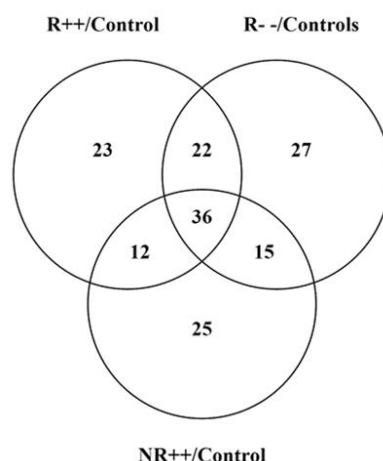**Fig. 20. Comparison of proteins with different abundance in DCM patient subgroups (R++, R- -, and NR++) and controls**

Table 14. List of 36 differentially abundant plasma proteins common among R++/control, R--/control and NR++/control comparison

Swiss prot ID	Description	R++/Co (Ratio)	R- /Co (Ratio)	NR++/Co (Ratio)
Q15485	Ficolin-2	2.05	2.17	1.68
C4AMC7	Putative WAS protein family homolog 3	1.88	1.89	1.80
Q9BS26	Endoplasmic reticulum resident protein 44	1.77	1.32	1.25
Q7Z2Y5	Nik-related protein kinase	1.54	1.28	0.73
Q16613	Serotonin N-acetyltransferase	1.51	1.97	1.44
P09172	Dopamine beta-hydroxylase	1.56	1.47	1.69
P05090	Apolipoprotein D	0.80	0.67	0.78
P20061	Transcobalamin-1	0.83	0.83	1.35
Q9UKZ4	Teneurin-1	0.78	0.62	1.35
Q9HDC9	Adipocyte plasma membrane-associated protein	0.74	0.59	0.81
P24592	Insulin-like growth factor-binding protein 6	0.67	0.43	0.50
P02144	Myoglobin OS=Homo sapiens	0.66	0.47	0.82
P01814	Ig heavy chain V-II region OU	0.63	0.28	0.46
P02768	Serum albumin	0.57	0.74	0.78
P20742	Pregnancy zone protein	0.61	0.61	0.67
P01777	Ig heavy chain V-III region TEI	0.60	0.65	0.71
P40121	Macrophage-capping protein	0.59	0.80	0.66
P11226	Mannose-binding protein C	0.49	1.69	1.46
Q96JB2	Conserved oligomeric Golgi complex subunit 3	0.56	10.96	0.25
B9A064	Immunoglobulin lambda-like polypeptide 5	0.55	0.39	0.49
Q3T8J9	GON-4-like protein	0.53	1.53	0.79
P04745	Alpha-amylase 1	0.50	1.73	1.41
P01764	Ig heavy chain V-III region VH26	0.45	0.41	0.55
P04208	Ig lambda chain V-I region WAH	0.33	0.31	0.44
P01781	Ig heavy chain V-III region GAL	0.32	0.22	0.40
P01617	Ig kappa chain V-II region TEW	0.31	0.17	0.34
P01765	Ig heavy chain V-III region TIL	0.30	0.18	0.42
P01860	Ig gamma-3 chain C region	0.27	0.36	0.43
P01880	Ig delta chain C region	0.30	0.28	0.18
P01625	Ig kappa chain V-IV region Len	0.25	0.18	0.35
P80748	Ig lambda chain V-III region LOI	0.30	0.27	0.42
P01596	Ig kappa chain V-I region CAR	0.26	0.21	0.26
P01743	Ig heavy chain V-I region HG3	0.25	0.20	0.33
P01593	Ig kappa chain V-I region AG	0.23	0.12	0.24
P01876	Ig alpha-1 chain C region	0.17	0.20	0.41
P01861	Ig gamma-4 chain C region	0.08	0.08	0.15

*Co (Control)

Many immunoglobulin chains, albumin, myoglobin, apolipoprotein D, and macrophage capping

protein found lower abundant in the plasma of dilated cardiomyopathy patients in comparison to

the healthy controls. In contrast, ficolin-2, Serotonin N-acetyltransferase, Endoplasmic reticulum resident protein 44 and Dopamine beta-hydroxylase were found higher abundant in the plasma of DCM patients.

3.3.5 Differentially abundant plasma proteins between responders and non-responders extracted from the iTRAQ data

Analysis revealed ninety differentially abundant plasma proteins (present in both the technical replicates in identical direction, ranged between 3.88 to -2.95) between responder and non-responder DCM patients with inflammation and virus persistence. The strongest differences were seen for protein haptoglobin with higher abundance (FC 3.88) and mannose-binding protein C (FC -2.95) with lower levels in responders.

Likewise, when the plasma proteome of responders without inflammation and virus persistence was compared to non-responders with inflammation and virus proof, eighty-eight differentially abundant plasma proteins (present in both the technical replicates with identical directions) were observed. The strongest differences with higher abundance in responders were seen for protein conserved oligomeric Golgi complex subunit 3 (FC 44.96) and C-reactive protein (FC 2.25), whereas lower levels in responders were observed for protein poly [ADP-ribose] polymerase 1 (FC -3.70) and Ig gamma-1 chain C region (FC -2.5).

Out of those proteins, forty-five were found common between R++/NR++ and R--/NR++ groups (Fig. 21A). Among the 45 common proteins, ten proteins displayed the opposite pattern of abundance between R++/NR++ and R--/NR++ groups (Supplemental Table 1), while 13 proteins were higher (Fig.21 B) and 22 proteins were lower abundant (Fig.21 C) between R++/NR++ and R--/NR++ groups. In addition, forty-five (Supplemental Table 2) and forty-three (Supplemental Table 3) proteins were found to be different only in the responder group with inflammation and virus (R++) or responders without inflammation and virus (R--) in comparison to non-responders

respectively. Thus, virus persistence and inflammation of myocardium seems to be associated to the levels of plasma proteome in DCM subgroups.
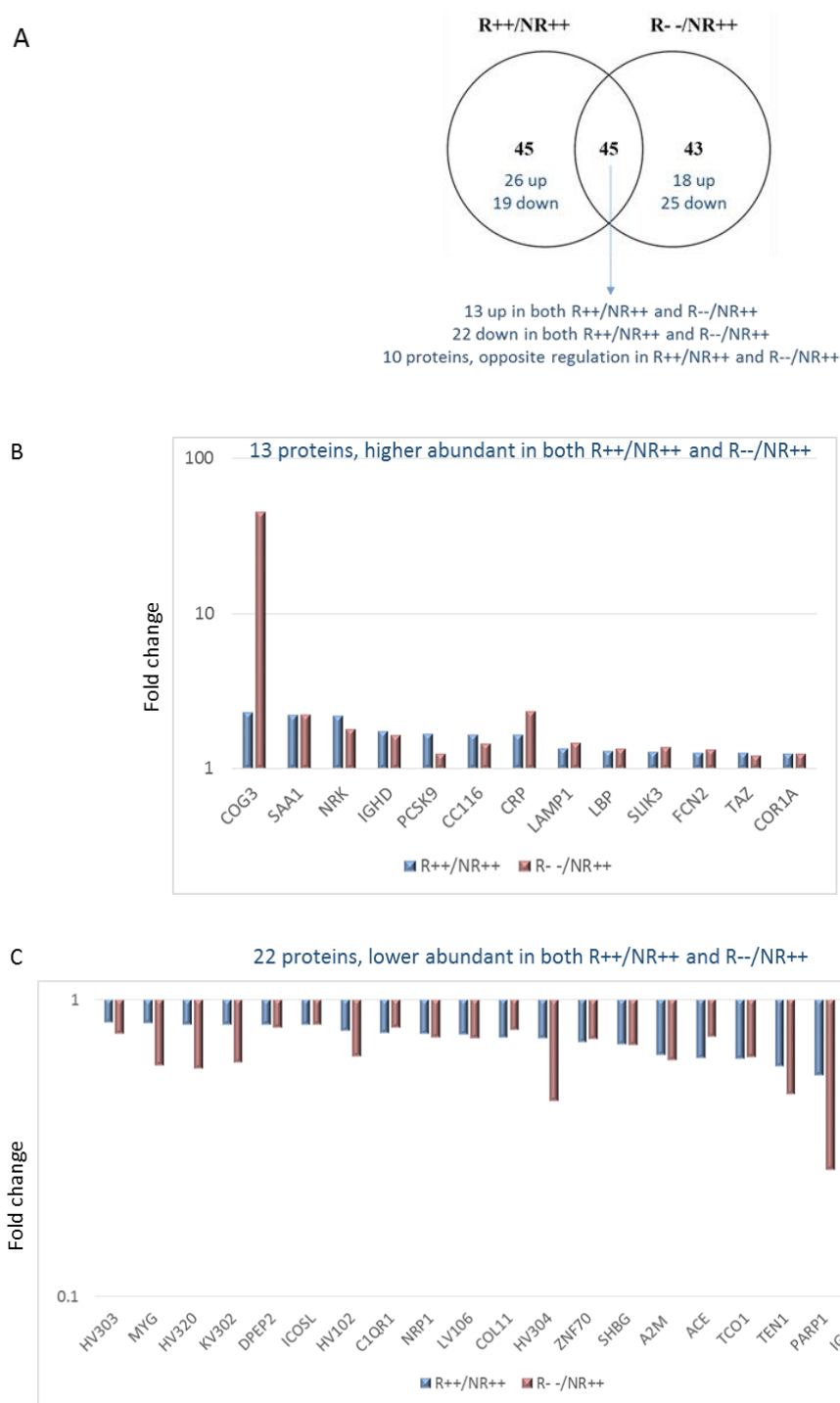
A

R++/NR++   R- -/NR++

45   45   43
26 up   18 up
19 down   25 down

13 up in both R++/NR++ and R--/NR++
22 down in both R++/NR++ and R--/NR++
10 proteins, opposite regulation in R++/NR++ and R--/NR++

B

13 proteins, higher abundant in both R++/NR++ and R--/NR++

Fold change

COG3 SAA1 NRK IGHD PCSK9 CC116 CRP LAMP1 LBP SLIK3 FCN2 TAZ COR1A

■ R++/NR++   ■ R- -/NR++

C

22 proteins, lower abundant in both R++/NR++ and R--/NR++

Fold change

HV303 MYG HV320 KV302 DPEP2 ICOSL HV102 C1QR1 NRP1 LV106 COL11 HV304 ZNF70 SHBG A2M ACE TCO1 TEN1 PARP1 IGHG2 MFAP4 IGHA1

■ R++/NR++   ■ R- -/NR++

Fig. 21. Differentially abundant plasma proteins between responders and non-responders obtained from the iTRAQ approach

Venn diagram (A) for the comparisons R++/NR++ and R--/NR++ displaying common and group specific proteins. Out of 45 common proteins, 13 (B) displayed higher abundance while 22 (C)

displayed lower abundance in both the groups. Also, an independent set of proteins (R++/NR++ 45, R--/NR++ 43) in each group was identified.

3.3.6 Comparison of iTRAQ experiment results with those of a label-free approach

A label-free plasma proteome experiment using individual patient plasma samples of responders and non-responders at baseline was carried out by Martin Feig within the scope of his medical doctoral thesis. Since within the thesis of Martin Feig, proteins with differential abundance obtained from the discovery phase was not validated, therefore, protein candidates were selected and included in the verification experiments. In the next paragraph the results of both experimental setups are compared to highlight advantages and disadvantages of each method.

In summary, profiling of 34 DCM patients (R 23, NR 11) using a label-free method covered 271 non-redundant plasma proteins, of which 137 proteins were identified with at least two peptides. Stringent data analysis revealed 20 differentially (FC $\lvert 1.2 \rvert$, and $p \leq 0.05$) abundant plasma proteins between responder and non-responder DCM patients. Due to the pre-fractionation of iTRAQ labelled peptides prior to mass spectrometric analyses, identification increased to 363 proteins, covering clearly more proteins than the label-free analysis. The combination of the data sets of the label-free and iTRAQ approach identified a total of 467 non-redundant plasma proteins. Among them, approximately 34 % proteins (161) were common in both label-free and iTRAQ methods, but an independent set of proteins (Label-free 104, iTRAQ 202 proteins) was also identified and quantified in each experimental workflow. The major advantage of using the label-free analysis was to explore individual patient data that was not obtained in iTRAQ experiments as samples were pooled before iTRAQ labeling prior to mass spectrometric analysis. However, the iTRAQ method provided a higher number of identified and quantified proteins probably because peptide complexity was reduced by strong cation exchange fractionation before mass spectrometric analysis. In general, the number of quantified peptides per protein was higher in the iTRAQ method (Fig. 22).
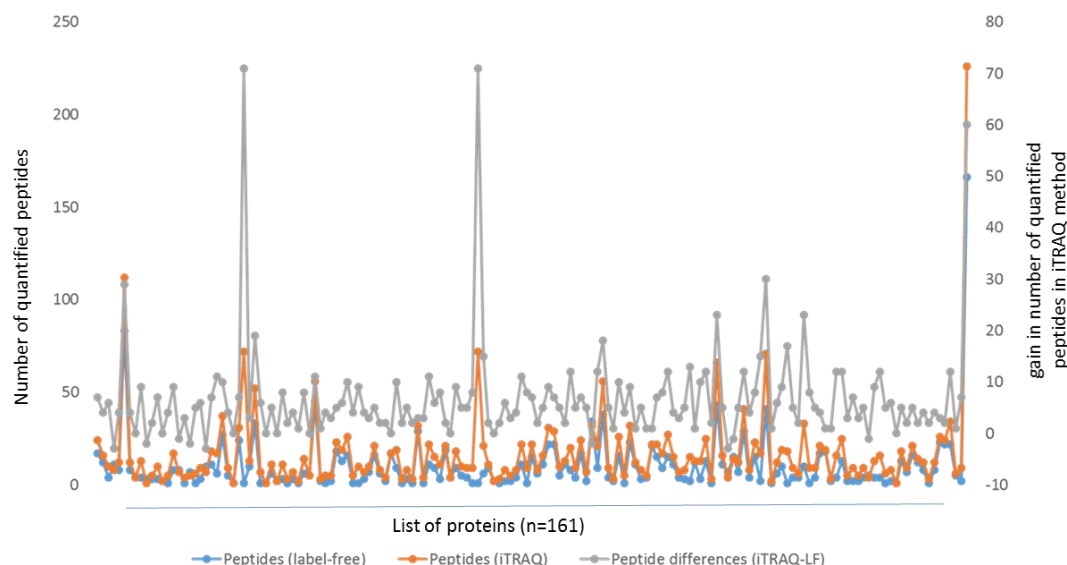
Fig. 22. Number of quantified peptides per protein in the label-free and the iTRAQ experiment

The number of unique peptides (left y-axis) identified and quantified in label-free (blue dots) and iTRAQ (red dots) method for the 161 proteins identified by both methods are represented. Gray dots (right y-axis) represent the gain in the number of quantified peptides for each protein in the iTRAQ method.

The plasma proteins covered in the present study span more than seven orders of magnitude in concentration, ranging from 6 pg/ml (CRISP3-Cysteine-rich secretory protein 3) to 40mg/L (HPR-haptoglobin related protein) (http://plasmaproteomedatabase.org/). The plasma proteome covered in our analysis included approximately 50% (231) classical plasma proteins, whereas the rest can be assigned to a cellular origin (Fig. 23).
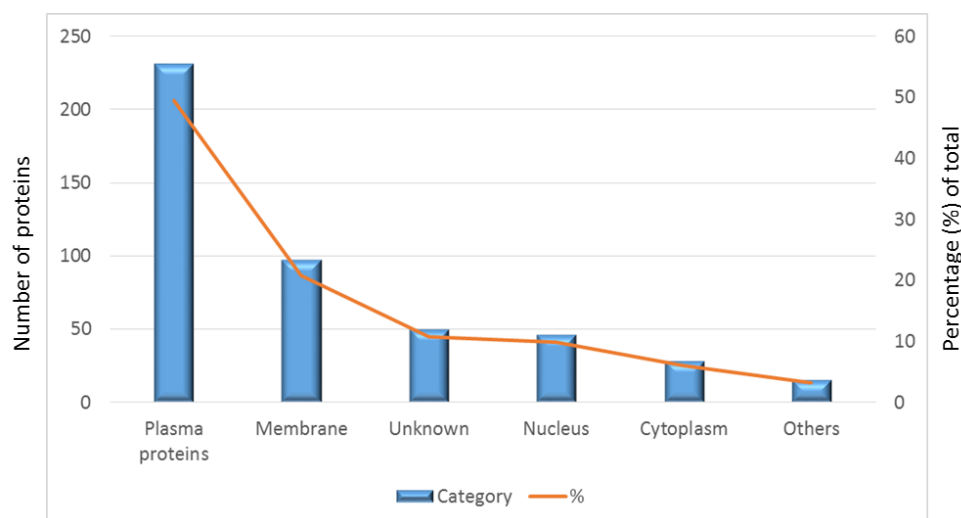
Fig. 23. Various categories of proteins detected in human plasma in the current study

Number of proteins in each category (left y-axis) and their percentage (right y-axis) of total identified plasma proteins are plotted. (Others; endoplasmic reticulum, lysosome, mitochondrion matrix, peroxisomes and cell projection-cilium)

In total, 154 plasma proteins were differentially abundant (p-value≤0.05, FC≥│1.2│) between responders and non-responders, highlighted at least by one of the methods either label-free or one of the technical replicate of iTRAQ method (Fig. 24). Some of these differentially abundant proteins might be potential biomarkers to distinguish responders and non-responders at baseline. 74 proteins were more abundant (FC, 3.88 to 1.22) whereas 80 proteins were less abundant (FC, -2.91 to -1.20) in the plasma of responders. These differentially abundant plasma proteins have various biological functions related to metabolism, immune regulation, cellular process, localization, and developmental processes. A large proportion of immune proteins seem to be present at different levels in plasma of responders and non-responders, importantly complement factor B, complement component C1Q receptor, L-selectin, cysteine rich secretory protein-3, collectin-11, galectin-3-binding protein, lipopolysaccharide-binding-protein, haptoglobin related protein, proteins S100-A7, S100-A8 and S100-A9. Also, many cytoskeletal proteins like coronin-1A, actin binding LIM protein-1, actin cytoplasmic-1, and transgelin-2, which play an important role in heart biology, might have the potential to distinguish responder and non-responder DCM

patient before immunoadsorption therapy. Extracellular matrix proteins play an important role in cardiac remodeling and in our study vasorin, a disintegrin and metalloproteinase with thrombospondin motifs-13, and leucine rich alpha-2-glycoprotein was found differentially abundant in both subgroups. Apart from these, enzyme modulator proteins like ribonuclease-4, endothelial protein C receptor, and various transcription factors like myelin transcription factor -1, zinc finger protein basonuclin-2, GON-4-like protein, and zinc finger protein-70 differed in level in both subgroups. The levels of cell adhesion molecules (cadherin-2, and desmocollin-1) and many transporter proteins (serum amyloid A-1 protein, transcobalamin-1, apolipoprotein C-II, apolipoprotein L1, and caprin-1) were also different in responder and non-responder DCM patients.
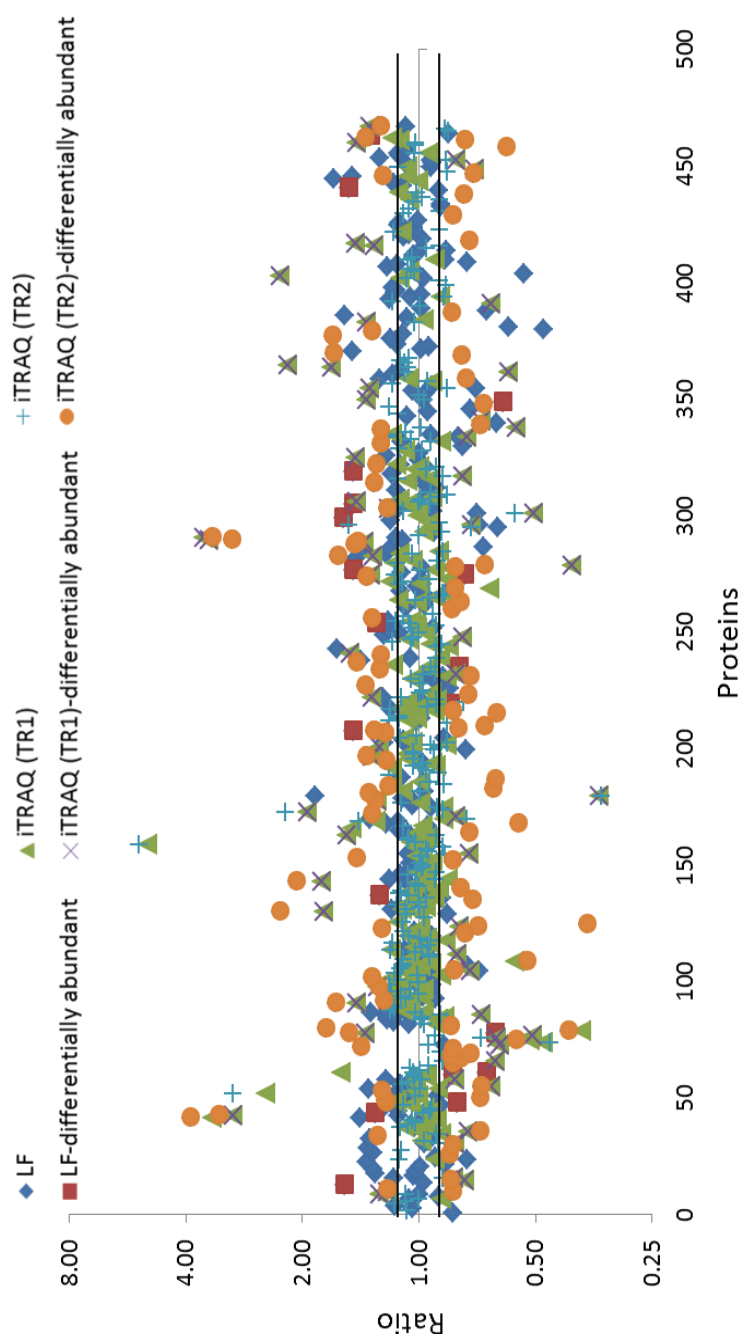
Fig. 24. Fold change (R/NR) of all plasma proteins identified and quantified by the label-free and the iTRAQ approach

All plasma proteins identified and quantified in label-free (LF-diamond shape) and iTRAQ (TR1- triangle shape, and TR2-plus symbol) data are plotted against fold change (y-axis). Differentially abundant plasma proteins are shown with separate labels (rectangle shaped, label-free approach FC │1.2│, p ≤ 0.05; cross symbol - iTRAQ technical replicate-1; circle shades - iTRAQ technical replicates2, FC │1.2│, peptide variability ≤30%).

Furthermore, functional categorization of differentially abundant plasma proteins revealed differences between responders and non-responders in many aspects including LXR activation,

Legend: LF · LF-differentially abundant · iTRAQ (TR1) · iTRAQ (TR1)-differentially abundant · iTRAQ (TR2) · iTRAQ (TR2)-differentially abundant

Axis labels: Ratio (y-axis): 8.00, 4.00, 2.00, 1.00, 0.50, 0.25 — Proteins (x-axis): 0, 50, 100, 150, 200, 250, 300, 350, 400, 450, 500

immune response, hematopoiesis, and coagulation system (Fig. 25). The list of proteins involved

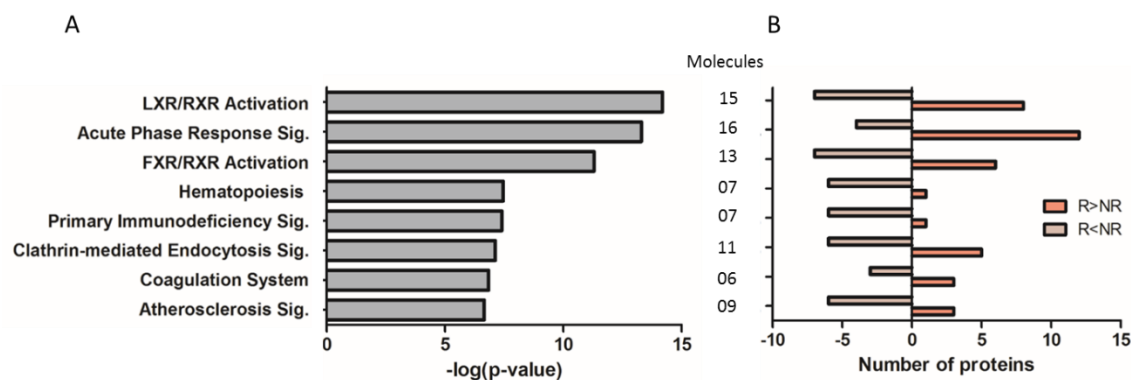in each canonical pathway is given in Table 15.

Fig. 25. Categorization of plasma proteins with different abundance in responders and non-responders

Functional assessment of differentially abundant plasma proteins points to differences in various canonical pathways (A) between responders and non-responders, as represented with significance of enrichment (-log p-value). (B) Number of proteins higher or lower abundant in responders linked to each pathway.

The Liver X receptors (LXR) are transcription factors and thereby important regulators of lipid and

glucose homeostasis, while retinoid X receptors (RXR) binds to retinoid and also control lipid

metabolism. The levels of several plasma proteins (Table 15) involved in LXR and RXR pathways

were found in different levels in responder and non-responder DCM patients.

Table 15. List of plasma proteins assigned to canonical pathway

Ingenuity Canonical Pathways	Associated proteins
LXR/RXR Activation	PON1, ITIH4, S100A8, TF, SERPINF1, PCYOX1, LBP, SAA1, APOC2, ORM1, APOC4, HPR, PLTP, APOL1, ALB
Acute Phase Response Signaling	MBL2, ITIH4, CFB, TF, SERPINF1, ITIH3, SERPINA3, LBP, CRP, A2M, SAA1, HP, APCS, ORM1, VWF, ALB
Hematopoiesis/ primary Immunodeficiency Signaling	IGLC1, IGHG2, IGHM, IGHG3, IGHD, IGHA1, IGHG4
Clathrin-mediated Endocytosis Signaling	PON1, APOC2, S100A8, TF, ORM1, ACTB, PCYOX1, APOC4, APOL1, ACTG2, ALB
Coagulation System	F9, A2M, F12, F7, F11, VWF
Atherosclerosis Signaling	PON1, APOC2, S100A8, ORM1, PCYOX1, APOC4, ICAM, APOL1, ALB

Additionally, a number of proteins whose levels were different in responders and non-responders, is involved in various cardiac disorders like heart failure and myocardial infarction. Important proteins discovered in these categories are C-reactive protein (R/NR, 1.54), serotransferrin (R/NR, -1.77), carbonic anhydrase-1 (R/NR, -1.44), angiotensin-converting enzyme (R/NR, -1.58), von Willebrand factor (R/NR, 1.25), and adiponectin (R/NR, -1.27).

3.3.7 Validation of plasma proteins using Multiple Reaction Monitoring (MRM)

The results obtained in the discovery phase experiments were further confirmed using multiple reaction monitoring. Differentially abundant plasma proteins were selected from both iTRAQ and label-free data. In total, 20 differentially abundant plasma proteins involved in various functional classes like cytoskeletal proteins (actin binding LIM protein-1), calcium binding proteins (protein S100-A9, protein S100-A8), blood coagulation proteins (coagulation factor XII, coagulation factor IX), cell adhesion molecules (desmocollin-1, neural cell adhesion molecule L1-like protein, neurophilin-1), and immune proteins (cysteine-rich secretory protein 3, serum amyloid A-1 protein, C-reactive protein, lipopolysaccharide-binding protein, mannose-binding protein) were selected. 2-3 unique peptides per protein were chosen for relative quantitation, and their corresponding heavy

labeled peptides were synthesized with stable isotope label containing 13C and 15N Arg/Lys amino acids. In total, 55 heavy labeled peptides were pooled and optimized for retention time and collision energy in the triple quadrupole mass spectrometer. Heavy labeled peptides were spiked into a test plasma protein digest in five different concentrations (0.1-500fmol/µg) and the response of heavy peptides was evaluated by linearity curve (Fig. 26).
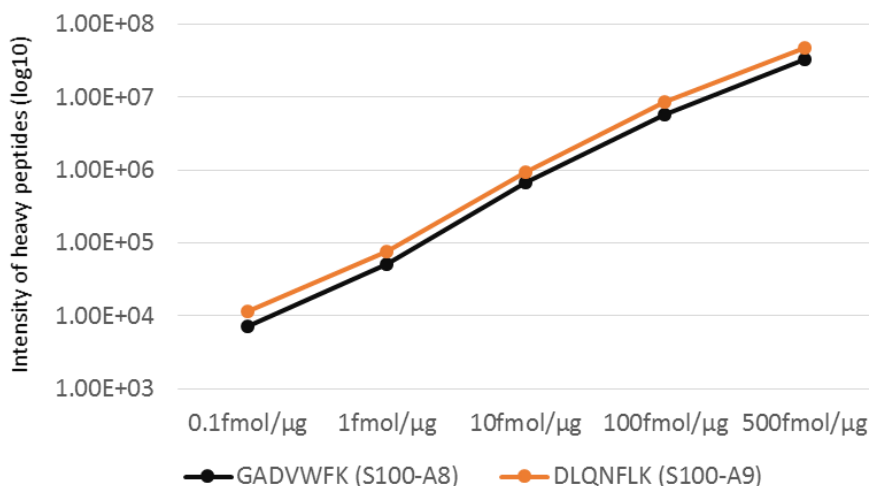

Fig. 26. Linearity curve of heavy peptides

The response of heavy peptides is plotted (y-axis) for five different concentrations (x-axis) spiked into the plasma protein digest. Data show that the curves are linear up to 100fmol/µg for all peptides, but the MS signal starts to get saturated at 500fmol/µg. Only data for two heavy peptides are shown.

From the linearly curve, one concentration of each heavy peptide was selected (Fig. 27) for final spike-in into the real plasma samples used in this study.

As described in the previous section the discovery phase experiments was performed in a limited number of plasma samples (label-free n=34, and iTRAQ n=20, pooled in pools of 5 each), while in the validation phase (MRM), the number of samples was increased to ninety three (R 38, NR 31, and healthy controls 24). Suitable concentrations of heavy labeled peptides were mixed into four µg of protein digest of each depleted plasma sample and measured in triple quadrupole mass

spectrometer. Each sample was measured twice. Raw MS data was analyzed in skyline software

and exported to an excel sheet for further quantitative analysis of various subgroups.

A
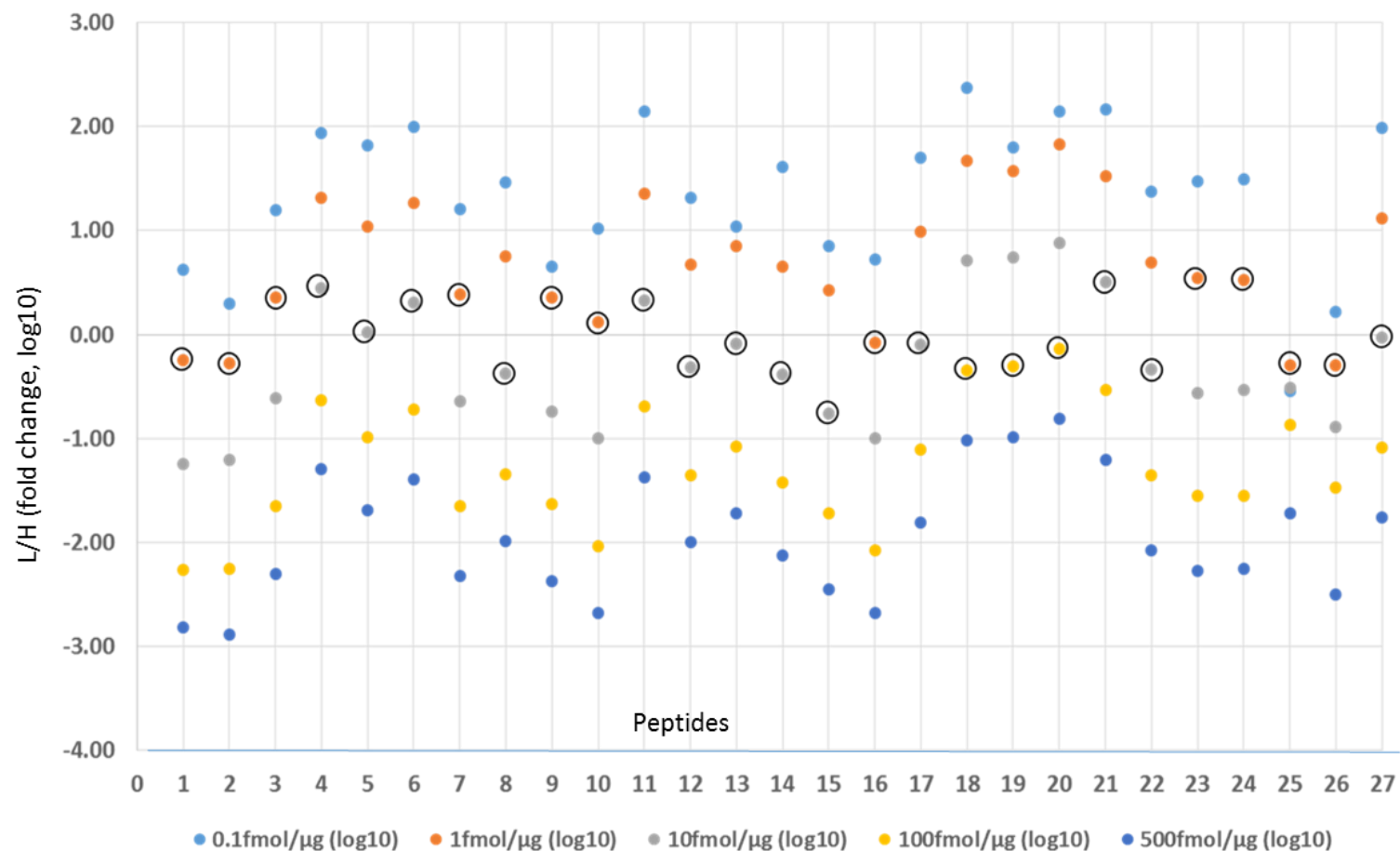
1. GADVWFK (S100-A8), 2.DLQNFLK (S100-A9), 3. ESDTSYVSLK (CRP), 4. NCELDVTCNIK (FA9), 5. NWGLGGHAFCR (FA12), 6. VVGGLVALR (FA12), 7. FQASVATPR (MBL2), 8. WLTFSLGK (MBL2), 9. GYQINWWK (NCHL1), 10. TTVILPLAPFVR (NCHL1), 11. AWFLESK (APOC4), 12. AVDTWSWGER (LG3BP), 13. ELSEALGQIFDSQR (LG3BP), 14. YSSDYFQAPSDYR (LG3BP), 15. EWIQVDLGLLR (NRP1), 16. SFEGNNNYDTPELR (NRP1), 17. FFGHGAEDSLADQAANEWGR (SAA1), 18. ELLDTVTAPQK (PEDF), 19. TVQAVLTVPK (PEDF), 20. SCDLALLETYCATPAK (IGF2), 21. GIVEECCFR (IGF2), 22. ITLPDFTGDLR (LBP), 23. LAEGFPLPLLK (LBP), 24. VQLYDLGLQIHK (LBP), 25. VPSHLQAETLVGK (DSC1), 26. YEDLYSNCK (CRIS3), 27. YYYVCQYCPAGNWANR (CRIS3)
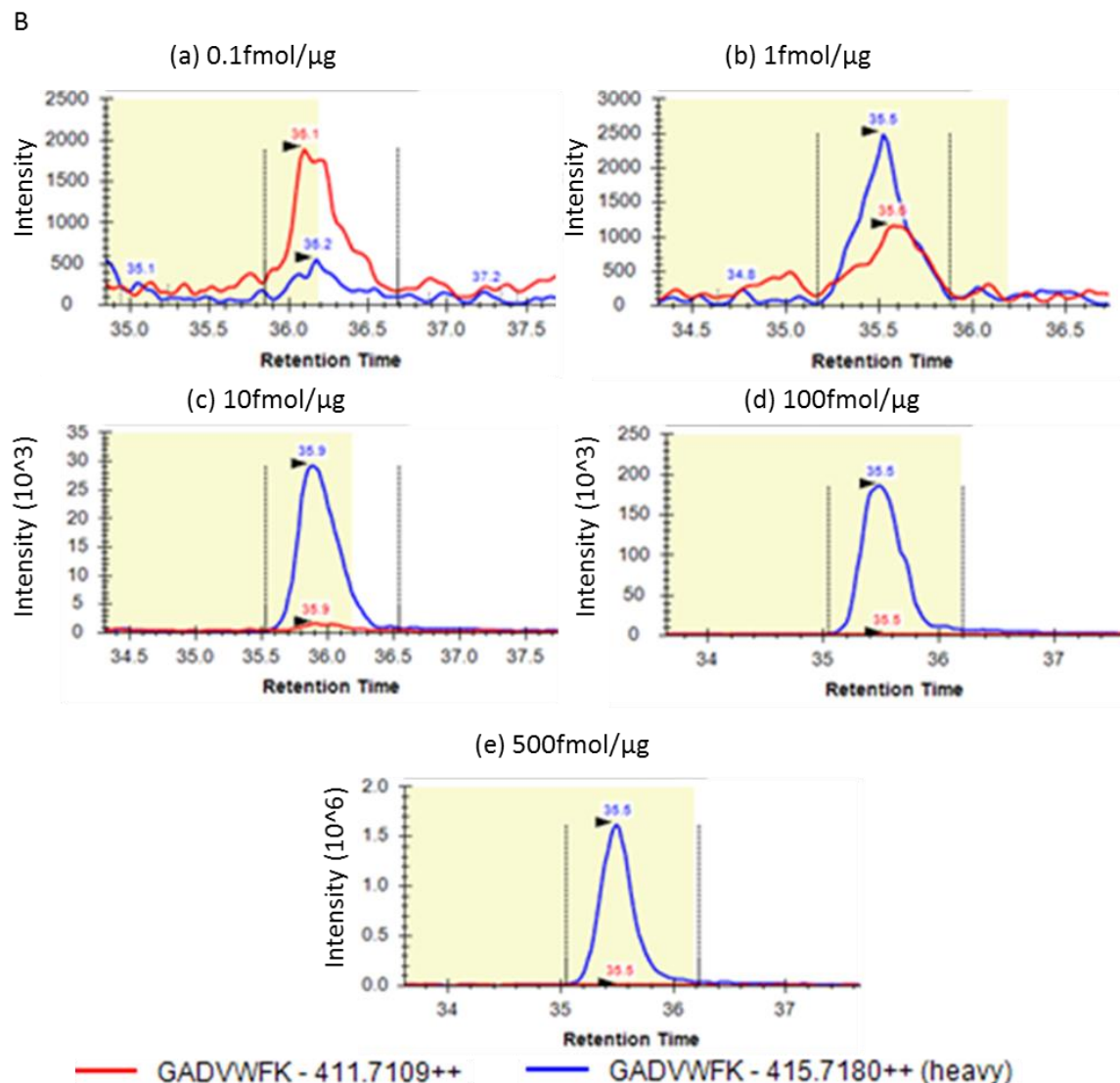
B

(a) 0.1fmol/µg

(b) 1fmol/µg

(c) 10fmol/µg

(d) 100fmol/µg

(e) 500fmol/µg

GADVWFK - 411.7109++   GADVWFK - 415.7180++ (heavy)

Fig. 27. Selection of heavy peptide concentrations

Five different concentrations (0.1, 1, 10, 100 and 500 fmol/µl) of heavy peptides were mixed with plasma protein digests of equal amount prior to triple quadrupole mass spectrometric measurement and the obtained fold change (light/heavy) of each peptide are plotted on the y-axis (A). The concentration of each peptide was selected (shown as a circles) based on the equal intensity of light and the heavy peptide. Data of 27 peptides are shown here, as they were used in the final quantitation of proteins. (B) MRM result for peptide GADVWFK (red-heavy, blue-light) of protein S100-A8 at five different concentrations (a-e) of the heavy standard peptide. Heavy to light ratio was closest to 1 at 1fmol/µg. Therefore, this concentration was chosen for further spike-in for this peptide.

Among the twenty target proteins, relative quantitative data of sixteen proteins (of 27 unique peptides) could be calculated whereas light peptides corresponding to four proteins (caprin-1, actin-binding LIM protein 1, myelin transcription factor, and microfibril-associated glycoprotein-4) either were not detected or not consistent across all samples. Among the sixteen proteins, the relative quantitative result for ten proteins had the same trend as that obtained in the discovery phase experiments. MRM results were most significant for five proteins (protein S100-A8, protein S100-A9, C-reactive protein, cysteine-rich secretory protein and lipopolysaccharide-binding protein) that corroborated the finding of discovery phase displaying similar ratios and a low p-value ≤ 0.05 between responders and non-responders (Fig. 28). Three additional proteins (insulin-like growth factor II, neural cell adhesion molecule L1-like protein and galectin-3-binding protein) displayed similar ratios with slightly higher p-value $=0.07$. Additionally, MRM results of two proteins (mannose-binding lectin protein C and serum amyloid A-1 protein) showed the same trend in ratios as in the discovery phase but at p-value >0.1. The MRM findings of six proteins (pigment epithelium-derived factor, neuropilin-1, coagulation factor IX, coagulation factor XII, apolipoprotein C-IV, and desmocollin-1) did not match with the discovery phase results. Thus, in conclusion, validation of discovery phase results in a larger sample size using MRM could confirm results of 10 proteins but other 6 were not confirmed because of the high variation of the patients within the sub-groups (R/or NR) (Fig. 29).
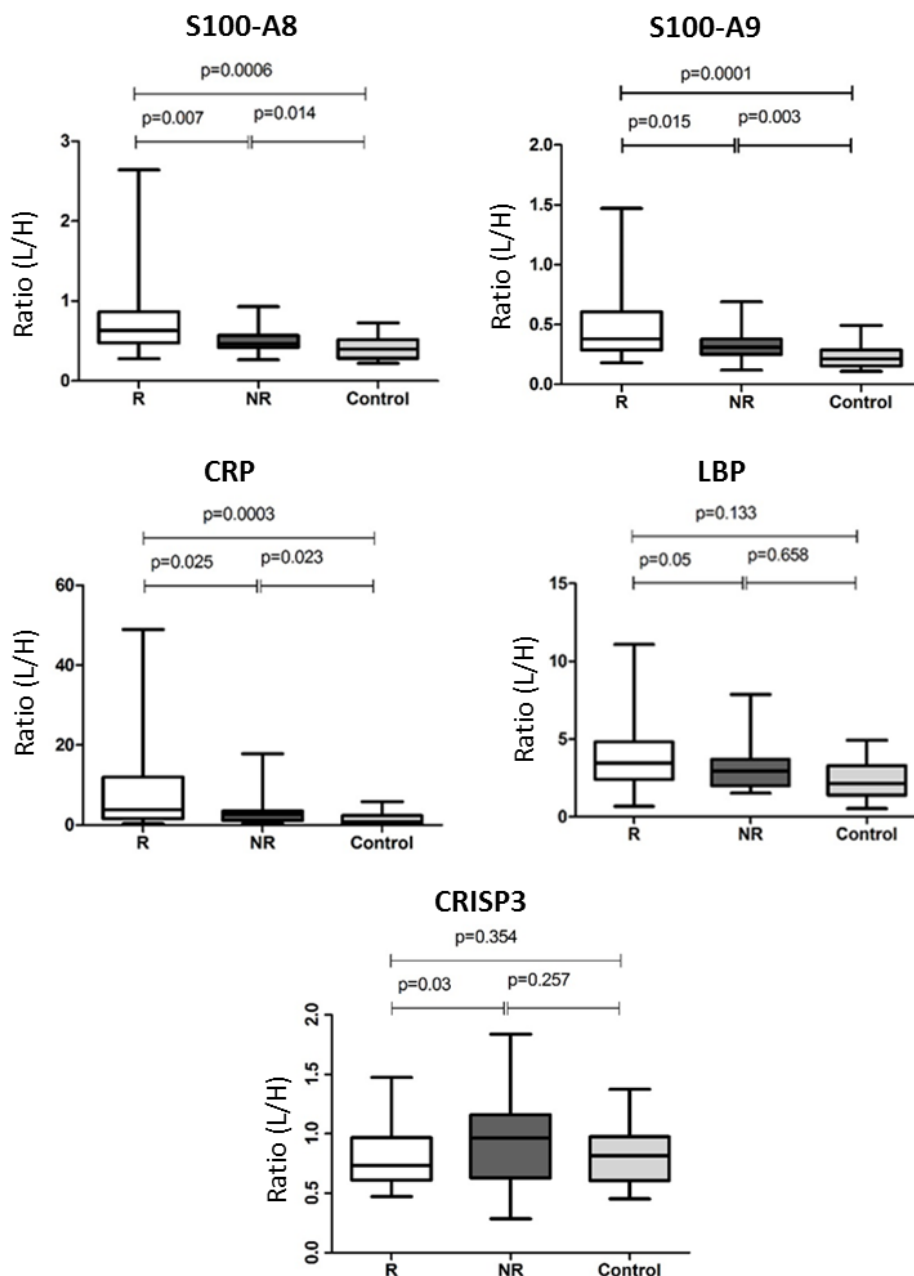
Fig. 28. Box plots showing the distribution of intensity ratios (Light/Heavy) of five proteins with the most significant difference between responders and non-responders

Box plot illustrating the distribution of average intensity ratios of proteins among responders (R), non-responders (NR) and healthy controls along with significance of differences (p-value) between the groups. (protein S100-A8, S100-A8; protein S100-A9, S100-A9, C-reactive protein, CRP; neural cell adhesion molecule L1-like protein, CHL1; cysteine-rich secretory protein, CRISP3; and lipopolysaccharide-binding protein, LBP).
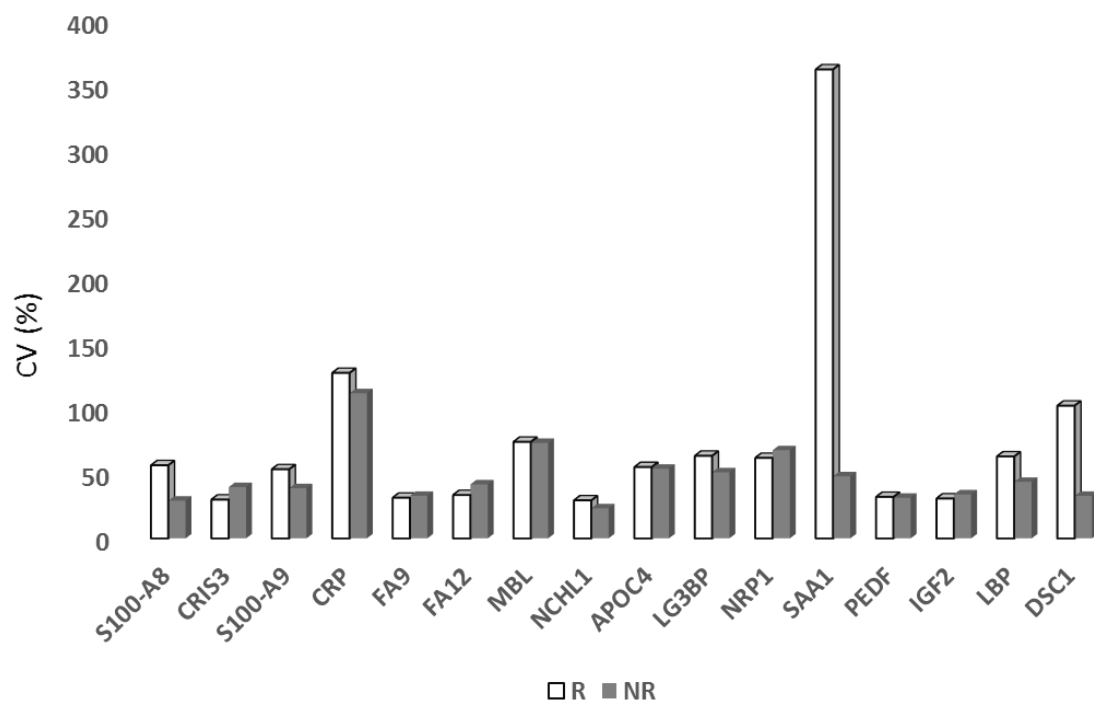
Fig. 29. The coefficient of variation (CV %) among responders and non-responders for sixteen proteins validated in MRM

For all sixteen proteins, the coefficient of variation is plotted (y-axis) for all responder and non-responder DCM patients. In general, the CV is very high for all proteins indicating large inter individual variation of protein levels within the groups.

The relative quantitative value for each protein in responder and non-responder DCM patients was also calculated in comparison to healthy controls. All MRM results of 20 proteins together with the label-free and iTRAQ results are summarized in Table 16.

Table 16. Summary of the quantitative data for the twenty proteins analyzed by label-free, iTRAQ and MRM approaches

ID	Description	Label-free		iTRAQ				MRM			
		R/NR	P-value	R/NR-TR1	R/NR-TR2	R/NR	P-value	R/Co	P-value	NR/Co	P-value
P05109	Protein S100-A8	*	*	1.76	2.29	1.42	0.0070	1.77	0.0006	1.24	0.0141
P06702	Protein S100-A9	*	*	1.79	2.07	1.36	0.0150	1.95	0.0001	1.43	0.0027
P02741	C-reactive protein	*	*	1.45	1.64	2.26	0.0250	5.18	0.0033	2.30	0.0235
O00533	Neural cell adhesion molecule L1-like protein	*	*	1.21	-1.22	-1.15	0.0300	-1.27	0.0063	-1.13	0.1527
P18428	Lipopolysaccharide-binding protein	1.47	0.039	1.26	1.30	1.33	0.0500	1.27	0.1330	-1.05	0.6589
Q08380	Galectin-3-binding protein	1.48	0.004	1.07	-1.07	1.31	0.0700	1.06	0.7210	-1.24	0.1006
P01344	Insulin-like growth factor II	-1.22	0.017	-1.04	1.02	-1.15	0.0700	-1.99	0.1810	-1.73	0.3073
P11226	Mannose-binding protein C	1.85	0.05	-2.91	-2.95	1.30	0.1100	1.26	0.2569	-1.07	0.7387
P36955	Pigment epithelium-derived factor	1.29	0.004	1.02	1.06	-1.10	0.2200	-1.08	0.2933	1.02	0.8431
P0DJI8	Serum amyloid A-1 protein	*	*	1.94	2.21	3.36	0.2800	4.72	0.2928	1.40	0.4645
P00740	Coagulation factor IX	1.30	0.004	-1.04	-1.03	1.04	0.6500	1.03	0.7346	-1.01	0.9146
O14786	Neuropilin-1	*	*	-1.31	-1.21	1.07	0.6500	-1.26	0.1432	-1.38	0.0630
P00748	Coagulation factor XII	-1.25	0.014	1.14	1.21	1.06	0.7090	-1.20	0.1911	-1.27	0.1763
P55056	Apolipoprotein C-IV	1.47	0.028	-1.10	1.00	-1.03	0.8300	1.18	0.2360	1.21	0.1710
Q08554	Desmocollin-1	*	*	1.45	1.00	1.01	0.9200	-1.13	0.6766	-1.16	0.5800
Q14444	Caprin-1	1.48	0.01	*	*	*	*	*	*	*	*
Q01538	Myelin transcription factor 1	1.56	0.011	*	*	*	*	*	*	*	*
O14639	Actin-binding LIM protein 1	1.56	0.018	*	*	*	*	*	*	*	*
P55083	Microfibril-associated glycoprotein 4	*	*	-2.49	-1.47	*	*	*	*	*	*

*not detected, Co- control

3.3.8 Validation of findings by ELISA

3.3.8.1 ELISA assay for protein S100-A8

Mean and standard deviation (SD) for protein S100-A8 was calculated for the three groups (R n=44, NR n=38, healthy controls n=17) (Fig. 30). Plasma concentration of protein S100-A8 was higher in responders than in non-responders (68.8 ± 42.7 vs 46.23 ± 34.5 ng/ml or 660.3 ± 410.3 vs 420.3 ± 293.6 pg/mg, FC 1.57, p=0.004; Student's t-test). In both responders and non-responders, standard deviation is high, representing a high variation within the subgroups. Also, in comparison to healthy controls, responders displayed higher level (FC 1.96, p=0.002) of S100-A8, while non-responders did not show significant differences (FC 1.25, p=0.27). Additionally, higher abundance of plasma S100-A8 was found in plasma of dilated cardiomyopathy patients in comparison to healthy controls (FC 1.63, p=0.03). Plasma concentrations of S100-A8 of healthy controls in our data were found approximately 15-60 ng/ml (26.45 ± 10.62 ng/ml), which is comparable to the data of healthy controls as given by the manufacturer ($\approx$2-50ng/ml). Taken together, ELISA data of protein S100-A8 corroborated the finding of MRM and iTRAQ analyses, which confirms the reliability of our proteomic study.
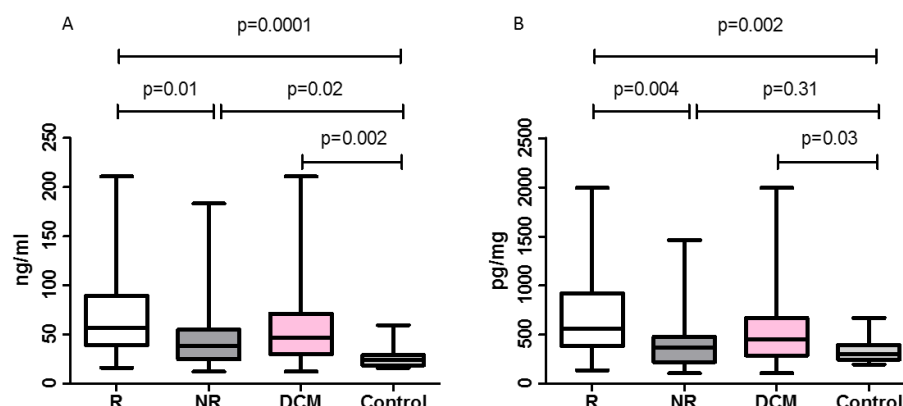
Fig. 30. ELISA results of protein S100-A8

Concentrations (A.ng/ml, and B.pg/mg, Y-axis) of plasma protein S100-A8 in various groups (X-axis) are illustrated. Level of protein S100-A8 was 1.57 fold higher in responders than in non-responders. Likewise, responders displayed higher abundance of S100-A8 in comparison to healthy controls. Also, higher level of S100-A8 was seen when all DCM patient values were compared with those of healthy controls. Data are shown as mean ± SD and significance was tested using Student's t-test.

3.3.8.2 ELISA assay for protein S100-A9

The ELISA plate was prepared as instructed by the manufacturer and absorbance was measured at wavelengths of 450/540 nm. Unfortunately, most of the samples (R n=15, NR n=18, healthy controls n=13) used for the measurement in this experiment displayed very low absorbance which fits into the lowest region of standard curve. Therefore, accurate relative quantification was not expected with this data and an assay with higher sensitivity would be necessary. Nevertheless, absorbance of all samples was plotted to get a rough idea of the mean in each group and the differences between the groups (Fig. 31). Mean absorbance in responders was 1.26 fold higher (p=0.038) than in non-responders. Also responders displayed 1.7 fold higher value (p=0.001) and non-responders displayed 1.35 fold higher value (p=0.039) than healthy controls.
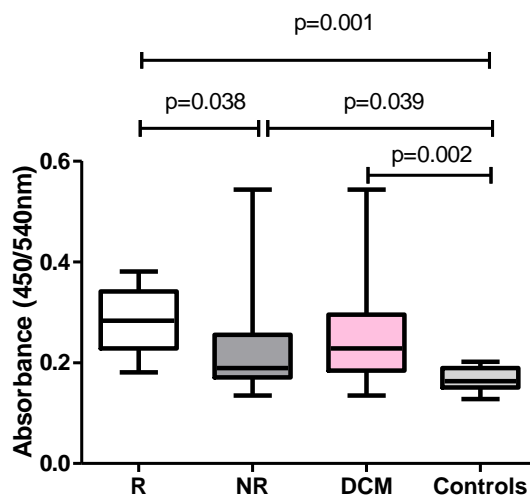
Fig. 31. Plasma levels of protein S100-A9 in responders, non-responders, and healthy controls

Mean absorbance of each group is plotted (responders, non-responders, and healthy controls), and the statistical significance is given based on two-tailed Students t-test.

3.3.9 Assessment of biomarker potential using Receiver Operating Characteristic (ROC) curves

To evaluate the potential of the five proteins with the strongest difference between the patient subgroups (protein S100-A8, S100-A9, CRP, LBP, and CRISP3) to differentiate responders and non-responders before immunoadsorption therapy, a receiver operating characteristic curve was plotted using ratio data (light/heavy) of MRM for DCM patients (Fig. 32).
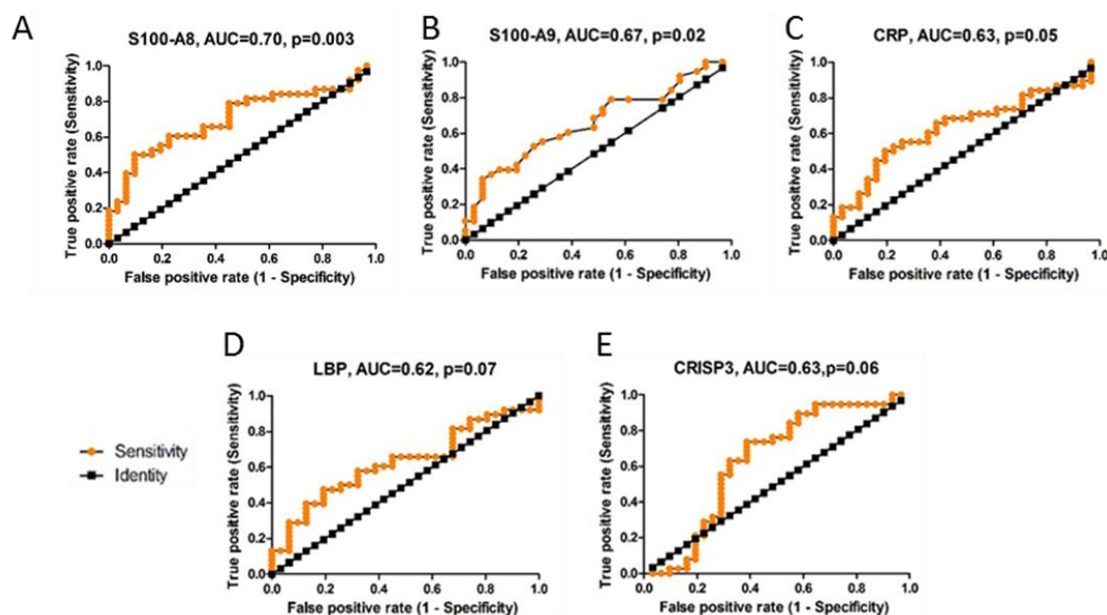
Fig. 32. Receiver operating characteristic (ROC) plot of proteins with different abundance in plasma of responders and non-responders

ROC curve of sensitivity (True positive rate, Y-axis) versus 1-specificity (False positive rate, X-axis) are plotted for protein S100-A8 (A), S100-A9 (B), CRP (C), LBP (D), and CRISP3 (E). The calculated area under the receiver operating characteristic curve (AUC) at 95% confidence interval (CI) along with the significance (p-value) for each protein is shown.

3.3.10 Comparison of proteome in endomyocardial biopsies and plasma in DCM patients at baseline

Myocardial and plasma proteomes of responders and non-responders were compared at baseline. Approximately 10 % (145) of all proteins identified in endomyocardial tissues were also observed in the plasma of DCM patients (Fig. 33A). These proteins were mainly of the extracellular matrix, membrane, organelle, and cellular origin, and might be secreted or leaked from myocardial tissue into blood plasma. Additionally, comparison of differentially abundant proteins (p≤0.05, Fold Change │1.2│, Fig. 33B) revealed protein S100-A8, and proactivator polypeptide, that were common in myocardial tissues and plasma of responders and non-responders. Protein S100-A8 has an important role in immune regulation, whereas proactivator polypeptide plays a vital role in sphingolipid metabolic processes. Protein S100-A8 was significantly higher (EMBs 3.02, p=0.002,

and plasma 2.29), whereas protein proactivator polypeptide was lower abundant (EMBs -1.65, p=0.002, and plasma -1.22) in responder DCM patients.
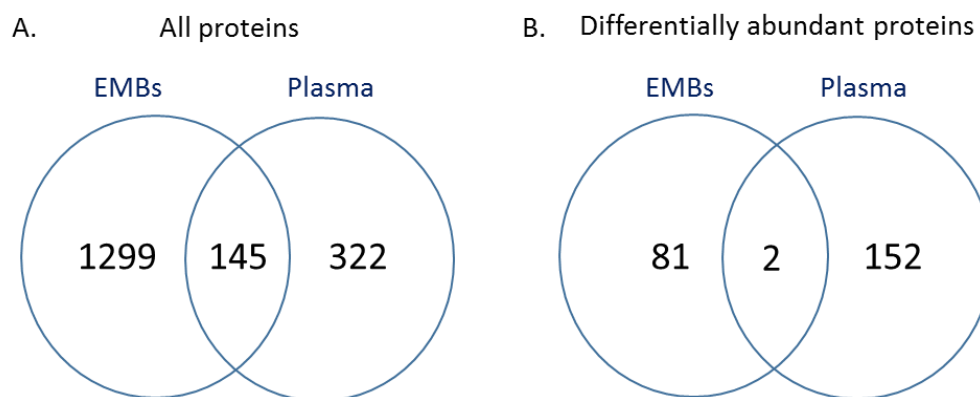
A.   All proteins   B.   Differentially abundant proteins

EMBs   Plasma   EMBs   Plasma

1299   145   322   81   2   152

Fig. 33. Venn diagram of proteins common between endomyocardial tissues and plasma at baseline

Overlapping of proteins between endomyocardial biopsies and plasma (A) All identified and quantified proteins, (B) differentially abundant proteins.

Furthermore, the abundance pattern of protein S100-A8 and proactivator polypeptide were evaluated in gene expression data of myocardial biopsies (R 24 and NR 16) at baseline (provided by Sabine Ameling). The higher abundance of protein S100-A8 in EMBs and plasma was further supported by the higher transcript levels (FC 2.82, p=0.02) in endomyocardial biopsies. In addition, mRNA expression of proactivator polypeptide (FC -1.18, p=0.17) in EMBs displayed a similar trend as the protein pattern at baseline, but with slightly higher p-value.

In conclusion, abundance of protein S100-A8 was higher in responder DCM patients than non-responders across different studies and supported by mRNA data (Fig. 34).
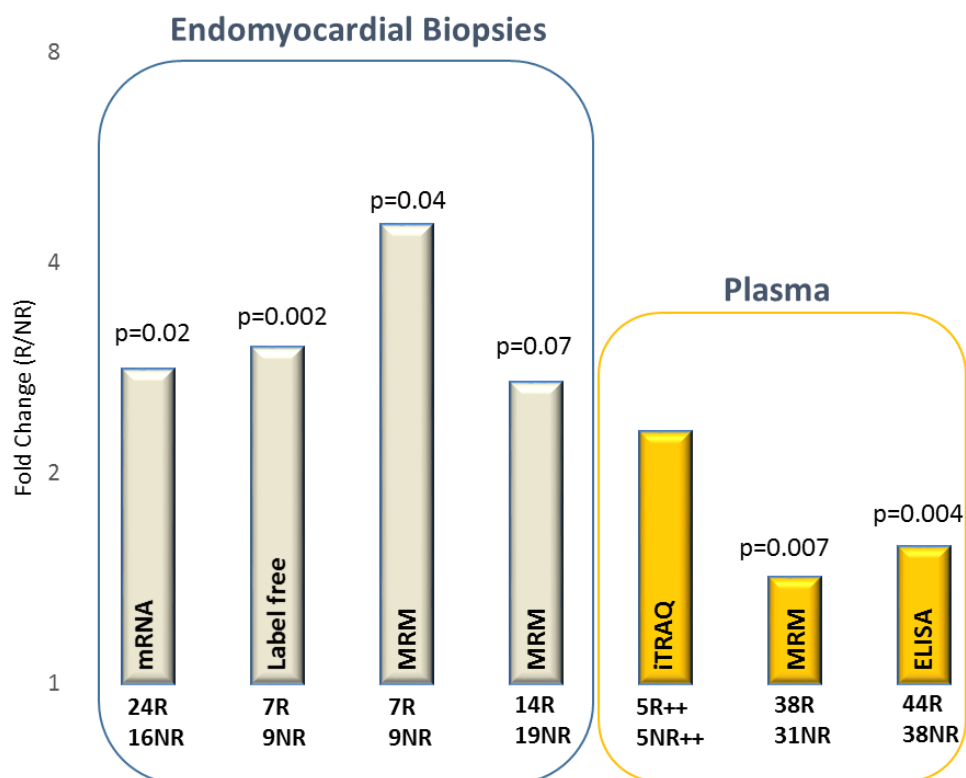
Fig. 34. Abundance pattern of protein S100-A8 across different studies

Higher abundance of protein S100-A8 in responders in endomyocardial biopsies and plasma with significance (p-value), and the number of samples used across different studies are shown.

3.4 Results of phosphoproteomic analysis of TGF-β treated HL-1 cardiomyocytes

The complete workflow used in the HL-1 cardiomyocytes phosphopeptide analysis is represented in Fig. 35. Briefly, HL-1 cardiomyocytes were incubated with medium containing TGF-β1 (10ng/ml) for 1, 6 and 24 hours, while respective controls were incubated with normal media. Proteins were isolated and digested with trypsin and phosphopeptides were enriched using a polyMAC kit. Furthermore, enriched fractions of phosphopeptides were measured on an LTQ Orbitrab Velos mass spectrometer.

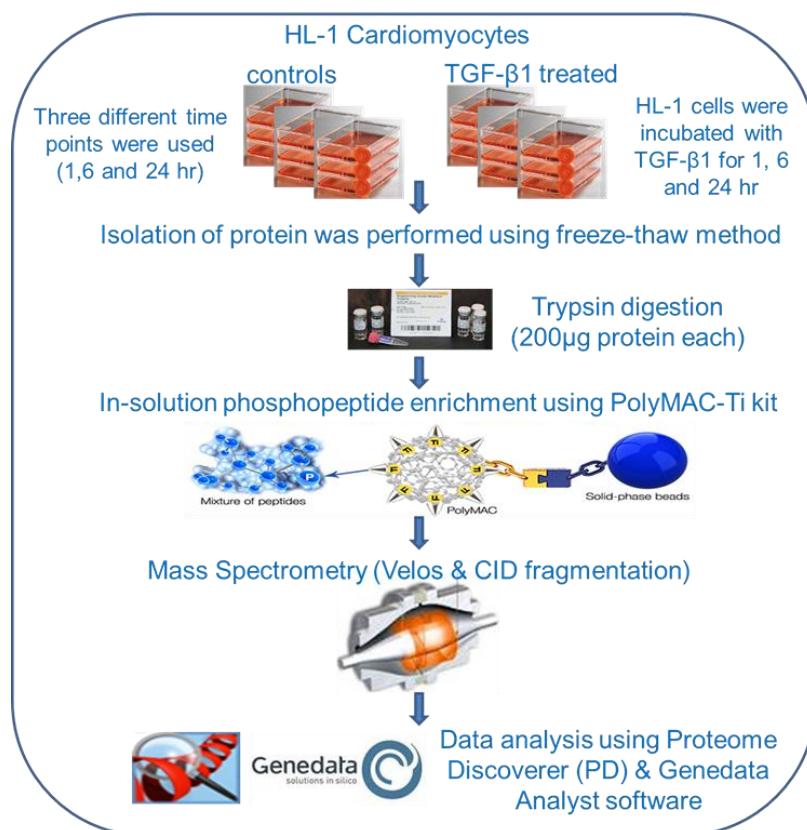**Fig. 35. Overview of the HL-1 phosphoproteome analysis**

All acquired data was analyzed in Proteome Discoverer software and individually evaluated for quality assessment by analyzing the total number of phosphopeptides and the total ion intensity of each chromatogram (Fig. 36).
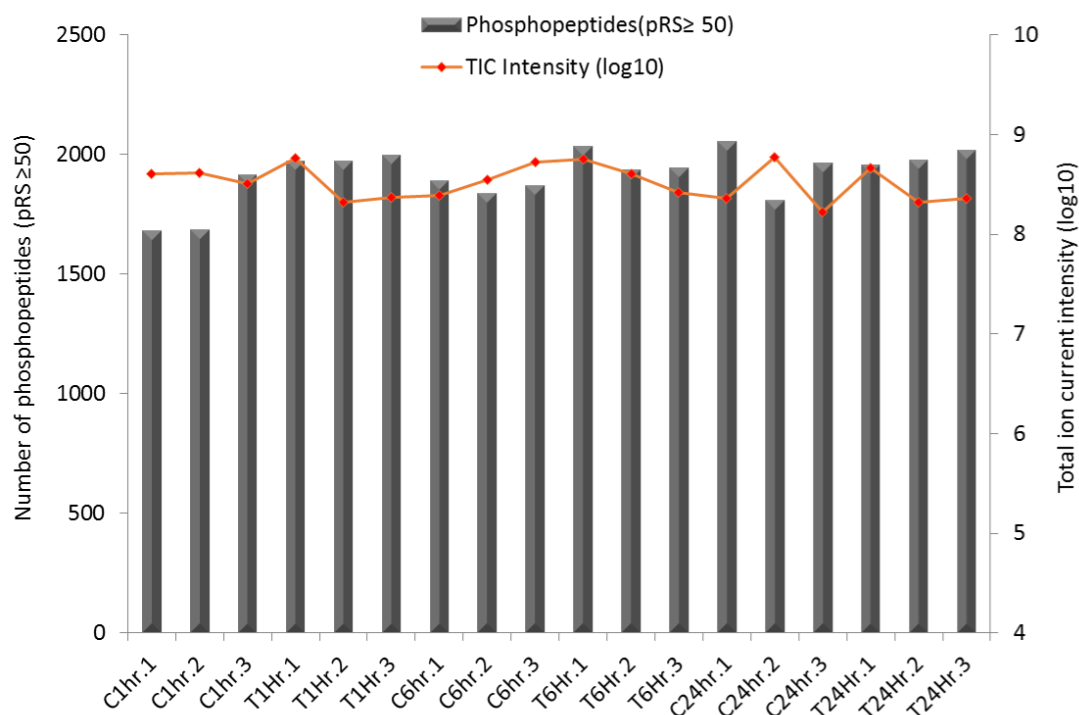
Fig. 36. Distribution of total ion current intensity (TIC) and number of identified phosphopeptides among bioreplicates

Total number of identified phosphopeptides (bars, left y-axis) and total ion intensity (dots, right y-axis) obtained in each chromatogram is given. (C1-control-1 hour, T1-TGF-β1 treated-1 hour, C6-control- 6 hour, T6-TGF-β1 treated-6 hour,   C24-control-24 hour, T24-TGF-β1 treated-24 hour)

The number of identified phosphopeptides and total ion current of every sample was very similar across all bioreplicates, representing the consistency and reproducibility of phosphopeptide enrichment in the sample sets. In addition, the percentage area of phosphopeptides of each sample in our datasets was approximately 97-98 %, representing the good enrichment efficiency of phosphopeptides (Fig. 37). Furthermore, in-depth analysis of phosphopeptides identified approximately 3000 phosphosites in each sample. For example, in replicate one of control of 1 hour (C1hr.1), 2932 phosphosites were identified, among them 2571 were at serine, 341 at threonine, and 20 were at tyrosine amino acid.
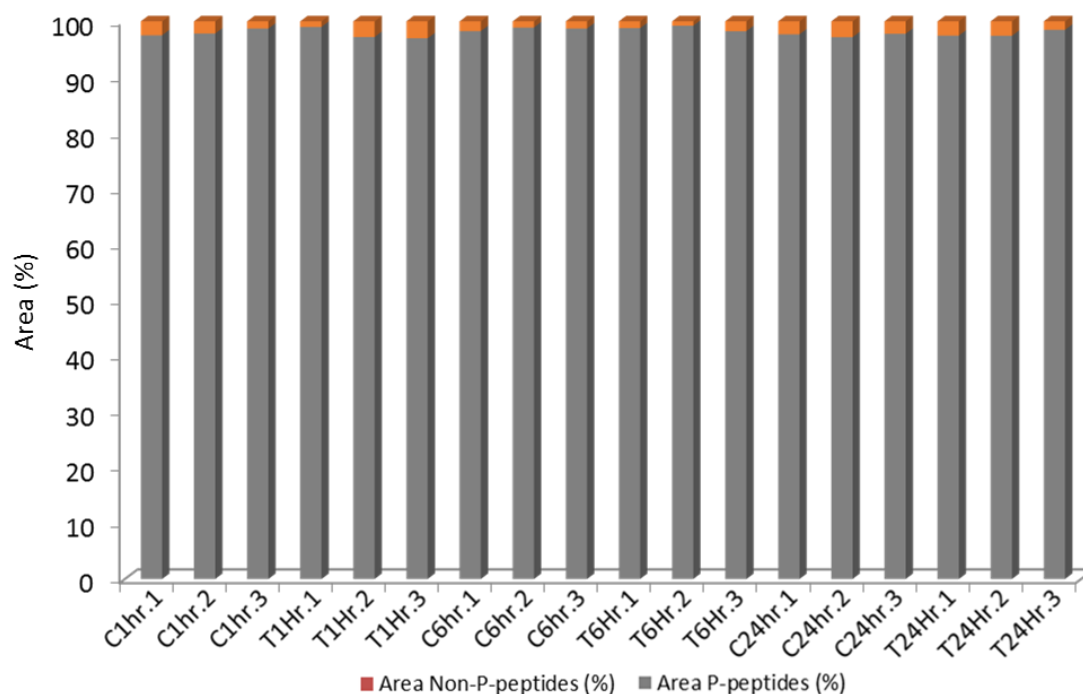
Fig. 37. Area of phosphopeptides and non-phosphopeptides across all bioreplicates

Percentage area of phosphopeptides (gray bars) and the area of non-phosphopeptides (red bars) for each bioreplicate is given.

Furthermore, approximately 50% of the phosphopeptides were identified across all biological replicates (Fig. 38) and the overlap was reduced (<50%) when replicates were compared at various time points. Comprehensive analysis of all 18 samples revealed 5256 (pRS ≥50) non-redundant phosphopeptides belonging to 1495 proteins. Stringent analysis of phosphopeptides (present at least with two quantitative values in one condition) revealed 2795 phosphopeptides entangled with 1102 non-redundant proteins. These phosphopeptides were further used for relative quantitative analysis using the Genedata Expressionist Analyst software.

Fig. 38. Identification of phosphopeptides among bioreplicates

Overlapping of phosphopeptides (pRS ≥ 50) among three bioreplicates of one hour controls (A) and TGF-β1 treated HL-1 cardiomyocytes (B) are given.

The label-free analysis for relative quantitation of phosphopeptides becomes very tedious as many of the identified phosphopeptides either were absent or had no intensity across various replicates. This issue can be addressed in the future by performi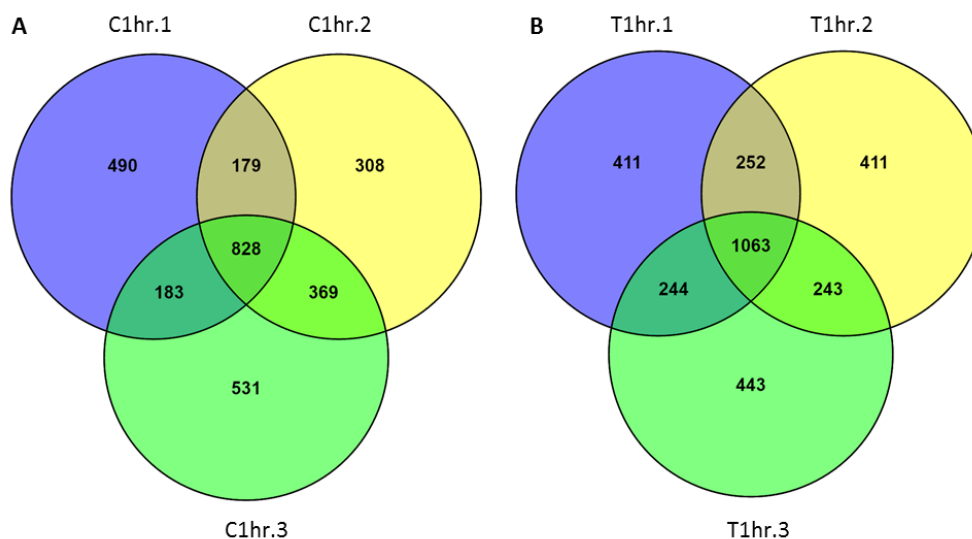ng experiments with more bioreplicates. Furthermore, the quantification appeared more challenging due to observation of many phosphopeptides with missed cleavages. We addressed some of these issues using rigorous quantitative analysis, and could identify 214, 92 and 53 non-redundant altered phosphopeptides (p-value≤ 0.05, |FC| 2.0) upon TGF- β1 incubation for 1, 6, and 24 hours, respectively. Thus, the immediate effect of TGF-β1 on the phosphopeptides was visible at 1 hour as a large number of phosphopeptides was altered, and this effect decreased at 6 and 24 hours. In addition, none of the altered phosphopeptides were found at all time points, when differentially altered phosphopeptides of the three incubation periods (1, 6 and 24 hours) were compared. In total, analysis of all three groups revealed 342 non-redundant altered phosphopeptides, assigned to 264 non-redundant proteins. Differentially altered proteins (represented by phosphopeptides) were functionally assigned to various protein classes and pathways and importantly included ubiquitin-proteasome

pathway, cytoskeletal regulation by Rho GTPase, calcium signaling, and TGF-β signaling. Examples of phosphopeptides related to TGF-β signaling and cytoskeletal regulation, altered by TGF-β1 incubation are shown (Fig.39).
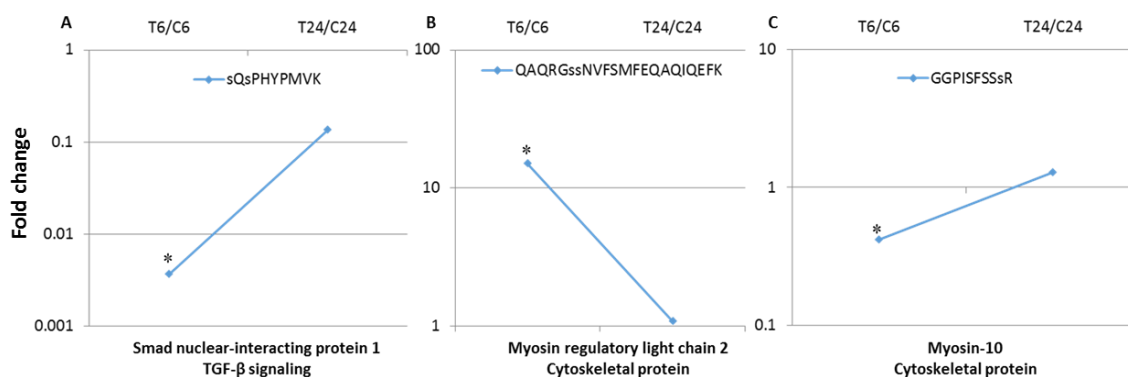
Fig. 39. Effect of TGF-β1 on phosphopeptide abundance at various time points

Effect of TGF-β1 incubation after 6 and 24 hours on the phosphopeptides related to protein (A) Smad nuclear interacting protein 1 (B) myosin regulatory light chain 2, atrial isoform, and (C) myosin 10. (* p<0.05).

TGF-beta signaling pathway might be interesting for further TGF- β1 induced cardiac signaling in cardiomyocytes. More specifically, phosphopeptide sQsPHYPMVK of Smad nuclear interacting protein-1 was reduced after TGF- β1 incubation in all three condition (1, 6 and 24 hours) but was significant (p=1.71E-05) after six hours treatment. Phosphorylation on the phosphopeptide, sQsPHYPMVK, at serine amino acid on position 89 and 91 seem to be decreased upon TGF- β1 stimulation.

4. Discussion

Dilated cardiomyopathy (DCM) is a myocardial impairment of the left or both ventricles with diminished cardiac functions [1]. Many cases of DCM are idiopathic (≈40%), although genetic predisposition, virus infection, inflammation and humoral and cellular immune system are known to play a causal role in its progression and pathogenesis [4]. Clinical studies have proven the presence of viral particles in the endomyocardial biopsies and their pivotal role in initiating an immune response [20, 21]. With regard to immunity, the appearance of autoantibodies against various cardiac proteins and their adverse impact on heart physiology is well established [32–34]. Thus, removal of antibodies from the blood of dilated cardiomyopathy patients was expected to improve the hemodynamics in these patients. Therefore, removal of antibodies via immunoadsorption (IA) and subsequent immunoglobulin (IgG) substitution (Ig/IgG) from the plasma of DCM patients has been shown to be associated with improved cardiac functions like left ventricular ejection fraction, left ventricular inner diameter at diastole, and endothelial dysfunction [48, 49, 51, 51]. But in general the response of immunoadsorption therapy differs among DCM patients, but the reasons for differential outcome have not been disclosed. Only approximately 60% of the DCM patients benefit from immunoadsorption therapy, and these were called as responders (LVEF ≥ 20% relative to the baseline value, and ≥ 5% in the absolute LVEF value) whereas those DCM patients who did not recover after therapy were called as non-responders. Interestingly, the benefits of therapy are known, but the molecular changes induced by therapy in the myocardium of DCM patients have not been disclosed yet. Immunoadsorption therapy is an invasive and extremely costly intervention, and so far, protein bio-signatures are not available to predict the therapy response. Nevertheless, clinicians are obligated to treat DCM patients by IA/IgG without prior understanding of the treatment outcome to prevent the deterioration of myocardial function. In this direction, research findings suggested a Fcγ -receptor polymorphism, disease duration, and the presence of cardio-depressant antibodies may affect the outcome of therapy [59, 61]. But,

hitherto, none of the studies could discover a potential biomarker/or biosignatures with clinical utility to distinguish responders and non-responders for the selective treatment of DCM patients before IA/IgG therapy.

Thus, in the current study, the objectives were to understand the proteome changes induced by immunoadsorption therapy in myocardial tissues in responder and non-responder DCM patients employing a shotgun proteome approach. Also, biochemical pathways induced by IA/IgG in the subgroups were evaluated. In addition, another major goal of the present study was to find protein predictors to differentiate responder and non-responder DCM patients before IA/IgG for a potential selective treatment of a subgroup of patients. To address this question, proteome profiling of endomyocardial biopsies and plasma of DCM patients at baseline was performed employing shotgun and targeted proteomic approaches.

Proteome profiling of human heart tissues is a challenging task due to the limited number and the small amount of human biopsies as well as the presence of the relatively high abundance of contractile and mitochondrial proteins in comparison to other metabolic and regulatory proteins [107]. 2-D gel electrophoresis along with mass spectrometry was the starting point to decipher the cardiac proteome [107, 108]. In general, 2-D gel electrophoresis can resolve >2000 proteins routinely in complex cell lysates [108], but in the heart, this high number of identification is difficult to achieve due to many limitations predominantly due to the large numbers and abundance of protein species of the contractile apparatus (1). Previously, proteome analysis of left ventricular tissues from DCM patients and controls (normal LVEF) was performed using 2-D gel electrophoresis that revealed differences in more than 100 proteins, broadly confined to cytoskeletal and myofibrillar proteins, mitochondrial proteins, and proteins associated to stress response [107–109]. Also, 2-D analysis of twenty-four explanted human hearts revealed many differentially regulated proteins in ischemic and dilated cardiomyopathy hearts in comparison to non-diseased hearts, of which some proteins were involved in cell death and apoptotic processes [110]. Although

111

2-D gel electrophoresis is efficient for resolving a large number of protein species, gel based approaches are limited in resolving hydrophobic, high and low molecular weight, or extremely acidic and basic proteins [111, 112]. However, the aforesaid limitations could partly be resolved using LC-MS/MS centered methods, and their implementation covered a broad spectrum of myocardial proteins with reliable relative protein quantification based on small amount of protein digest. Label-free proteomic analysis of endomyocardial biopsies from inflammatory dilated cardiomyopathy patients (n=10) and controls (n=7) revealed 174 differentially abundant proteins, mainly involved in carbohydrate metabolism, actin cytoskeleton, and extracellular matrix remodeling [94]. Furthermore, during the last ten years, massive efforts were made to develop new and innovative technologies along with improved sample preparation protocols to increase the coverage of the proteome. Many groups implemented labeling methods (iTRAQ, and SILAC), fractionation strategies (cation exchange, anion exchange, and OFFGEL fractionation), and sub-cellular fractionation to reduce the sample complexity, which in general, increases the number of identified proteins also improving quantitation [113].

In this study presented here, a label-free proteome approach (shotgun proteomics) was used to find differences in the myocardial proteome of responder and non-responder DCM patients before and after immunoadsorption therapy. In this label-free method, peptide quantification was based on the intensity of precursor ion signals obtained during MS1, whereas the identification relied on the fragment spectra (MS/MS). The complex mixture of peptides was separated on a C-18 hydrophobic reverse phase column by a liquid chromatography prior to mass spectrometry. The retention times across all LC-MS/MS run were reproducible and consistent in our data (chromatographic shift < 0.4 min), that is a prerequisite for precursor based label-free quantitation [114]. In the current myocardial proteome analysis, the number of identified and quantified proteins (954 proteins at t0, with at least 2 peptides) was approximately twice as high as previously reported by Hammer et al. (485 proteins with at least 2 peptides) [94], when the myocardial proteome of DCM patients was

compared with healthy controls. This higher number of protein identifications is likely due to the advancement in mass spectrometer development as LTQ Orbitrap Velos was used in the current study which is faster and more sensitive than the LTQ-FTCIR employed by Hammer et al. in the previous study.

The number of identified and quantified proteins in myocardial tissues might be increased even further by implementing fractionation methods like cation or anion exchange chromatography prior to MS/MS measurement, but such prefractionation is still a further challenge in the label-free quantitation.

Differences in the myocardial proteome of responder and non-responder DCM patients at baseline

In this pilot study, myocardial label-free proteome analysis of sixteen DCM patients (R 7, NR 9) at baseline revealed a total of 954 proteins (≥ 2 peptide). Among them only roughly 5 % were differentially abundant in the DCM patient subgroups analyzed. The rather low proportion of differences found is in line with the results of the gene expression study performed on EMBs of 24 responders and 16 non-responders by Ameling et al, [62] and most likely at least partially caused by large interindividual variations in the protein pattern.

Functional classification of proteins differentially abundant in responders and non-responders at baseline revealed differences in the carbohydrate, energy, and lipid metabolism. These functions have also been shown to be impaired in DCM and other heart failure patients in comparison with subjects with normal heart function [115, 116]. Glycolysis and particularly the enzyme 6-phosphofructokinase were found to be reduced in the cardiomyopathic heart of hamsters by a NMR and surface fluorometry study [117]. However, glycolysis in patients with different response to IA/IgG seem to be differentially impaired. Our study revealed lower abundance in therapy responders for three proteins of glycolytic pathways of which two, 6-phosphofructokinase and

pyruvate kinase, are regulatory enzymes. However, no difference between responders and non-responders regarding glycolytic gene expression or mRNA levels of other metabolic pathways were reported by Ameling et al. [62], which might be due to the fact that protein abundance might have been modulated at posttranscriptional level. When myocardial proteome analysis on ten (5 responders and 5 nonresponders) DCM patients was performed (diploma thesis Michelle Goritzka) many mitochondrial proteins were found at higher level in responders. In contrast, in the present study, lower abundance of mitochondrial proteins in responders was detected for a number of mitochondrial proteins of the electron transport chain (one protein of each complex except complex IV). The reason for such contrary results might probably be the strict limitation of the former study to patients with inflammation and virus persistence (inflammatory DCM) whereas the current study included DCM patients irrespective of inflammation or virus presence (responders- in only 3 out of 7 inflammation and virus were proven, and in only 2 out of 9 non-responders inflammation and virus were detected). Furthermore, the current study included a higher number of DCM patients. The lower abundance of mitochondrial proteins in responders hints towards lower energy states in responders than in non-responders. The speculation of lower energy state in responders was further supported by the lower abundance of other mitochondrial proteins including ADP/ATP translocase 1, mitochondrial 2-oxoglutarate/malate carrier protein, and mitochondrial pyruvate carrier 2. The nucleotide-transporting protein of the inner mitochondrial membrane - ADP-ATP translocase has also been identified as an autoantigen in myocarditis and DCM patients [118]. The presence of such autoantibodies may even more influence myocardial energy metabolism by hampering the transport of ATP/ADP across inner mitochondrial membrane. The harmful effect of human cardiodepressant antibodies has been proven when rat cardiomyocytes were incubated with plasma or enriched IgG3 fraction from DCM patients and reduced contractility, and Ca^{+2} ratios were observed [119]. *In-vivo* studies of guinea pig immunized with ADP-ATP carrier developed DCM and have proven the reduction in mitochondrial-cytosolic nucleotide transport as well as diminished cardiac functions (stroke volume and mean aortic pressure) based on the imbalance between energy supply and

demand [120]. It is possible that removal of antibodies targeted to ATP-ADP translocase by immunoadsorption therapy might be linked with reduction of their influence on energy metabolism and improved hemodynamics in responder DCM patients. A detailed analysis of the targets of cardiac autoantibodies was not within the scope of the present study. However, previous studies have shown an association between the presence of autoantibodies with negative inotropic effects and the responder status of patients [22, 61, 62].

As mentioned above, responders and non-responders displayed differences also in beta-oxidation of fatty acid and lipid metabolic pathways. Proteins involved in ß-oxidation of fatty acids (trifunctional enzyme subunit alpha and beta), and perilipin-4 were lower in the responder group. Perilipin-4 is a member of the perilipin family that coats the surface of lipid droplets and regulates the lipid turnover. Inactivation of perilipin-4 reduces the lipid accumulation in the heart by inhibiting triacylglycerol (TAG) packaging in mice [121] and is linked to mitochondrial ß-oxidation and energy production as well as controls lipolysis by modulating several signaling pathways [122]. Many studies have shown the direct regulation of perilipin, carbohydrate and lipid metabolism by peroxisome proliferator-activated receptor gamma (PPAR-γ or PPARG), which was predicted as an upstream activator in non-responders in this proteomic analysis. Using MRM, efforts were made to verify the expression pattern of PPAR gamma on protein level, but peptides of PPAR-gamma could not be detected in myocardial tissue samples (data not shown).

Cytoskeletal proteins distinguishing patient subgroups were either present at higher levels (tropomyosin alpha-3 chain, tropomyosin alpha-4 chain and F-actin-capping protein subunit alpha-1) or at lower levels (myosin-Ic, and destrin) in responders compared to non-responders. Tropomyosin protein plays a central role in Ca^{+2} signaling and contractility in the heart [123]. Mutations in the tropomyosin gene leading to imbalanced protein levels have been linked to dilated cardiomyopathy patients [124]. Tropomyosin alpha-3 chain and tropomyosin alpha-4 chain have been shown associated with the troponin complex and help to stabilize cytoskeletal actin filaments

in non-muscles, but their precise role in dilated cardiomyopathy has not been well evaluated yet. In the current study different levels of both tropomyosin alpha-3 chain and tropomyosin alpha-4 chain in responders might explain the differences in Ca^{+2} signaling and stability of actin filaments among both the subgroups. Likewise, different levels were also observed for protein F-actin-capping protein subunit alpha-1, that binds the fast growing end of actin filaments in a calcium independent manner. Furthermore, the protein destrin has been shown as actin-depolymerizing protein [125] whereas, protein myosin-Ic supports intracellular movements and links the actin cytoskeleton to the cellular membrane. The different levels of destrin and myosin-Ic in responders and non-responders point to a differential regulation of proteins with impact on the contractility of the myocardium. Moreover, further proteomic data suggests differences in the Ca^{2+} homeostasis directly linked to contractility. Thus, higher values of the calcium binding protein calumenin together with lower abundance of sarcoplasmic/ endoplasmic reticulum calcium ATPase 2 (SERCA2) in responders (FC -1.6, p-value 0.1) were observed. It was shown that calumenin interact with SERCA2 in the sarcoplasmic reticulum (SR) and that overexpression leads to decreased SR Ca^{2+} uptake and decreased fractional Ca^{2+} release [126].

On the other hand, kininogen 1 was found to be more abundant in responders. The protein has its strongest impact by affecting coagulation and the complement system. But it is also associated with cardioprotective effects via the vasodilator bradykinin produced by proteolytic processing [127]. Furthermore, extracellular matrix proteins (collagen alpha-1(I) chain and collagen alpha-1(IV) chain) were found to differ in level in responders and non-responders, pointing to a different ventricular remodeling.

Immune response and inflammatory processes play a vital role in development and progression of dilated cardiomyopathy. Notably, an immune protein -protein S100-A8 -was significantly higher abundant in responders. Protein S100-A8 (also known as calgranulin A or MRP8) is an acute phase Ca^{+2} binding protein and is associated with a variety of pro- and anti-inflammatory processes. The

116

potential utility of this protein as a biomarker has been claimed in several diseases including cancer, acute myocardial infarction, and cardiovascular events [128–130]. In a recent study, blood plasma and platelet level of protein S100-A8 were found to be higher in heart failure patients with preserved ejection fraction in comparison to healthy controls. Furthermore, Ca^{+2} concentration and action potential adversely affected when recombinant S100-A8 was added to iPSC-derived cardiomyocytes [131]. In our proteome study, higher abundance of protein S100-A8 in the responder group was supported by gene expression data of endomyocardial tissues with a 2.82 fold higher transcript level in responders, p-value 0.019 [62] which promotes this molecule for further investigations.

In general, Western blotting and ELISA are the most applied technologies in most of the research laboratories for the targeted semi-quantitative analysis of proteins in bio-fluids and cell extracts. However, the sensitivity of Western blot experiments depends on the availability of highly specific antibodies and has limitations regarding reproducibility across the large numbers of samples. Furthermore, high amounts of protein are required which are frequently not available when human biopsies are analyzed [132]. Although new immunolabeling systems (e.g. Odyssey, LiCOr Biosciences) have improved the quantitation of results of Western blotting experiments, these systems are still inflexible as they depend on high-quality antibodies. In comparison to Western blot, ELISAs allow better quantification, and are less time consuming, but are less specific as no information about the size of protein presenting the epitope is obtained. However, again this method depends on the availability of high-quality antibodies. Additionally, multiplexed antibody-based methods (ELISA, Luminex) for cardiac proteins have not been extensively developed so far or are rather expensive. The innovative progress and improvements in mass spectrometry technologies provided a competitor i.e. MRM to the classical techniques, which can overcome some of the limitations of the above-mentioned experimental techniques [132, 133]. In addition, MRM provides robust and accurate quantitative data to verify multiple proteins in parallel based on few

microgramms of protein samples without the use of specific antibodies. Therefore, MRM is a suitable approach for multi-marker assays and is extensively used in validation studies for large and precious clinical sample collections. Thus, in the verification phase, a MRM approach was employed to validate 17 target proteins, involved in several functional categories. Data were confirmed for 13 proteins when the same sample set used in the discovery phase (16 DCM patients) was analyzed. Because of the known variance within the DCM patient cohort e.g. age, disease status, or comorbidities, this number dropped down when more patients (n=33) were included. This finding underlines the hypothesis that idiopathic DCM patients are varying in their myocardial protein pattern. Therefore, it would be valuable to include as many samples as possible in the discovery phase experiments but, unfortunately, this is not always feasible in heart tissue studies. The present study with a relatively small sample number (n=16) used in the discovery phase provided meaningful results of proteins differing in level between responders and non-responders, and which are involved in lipid metabolism (perilipin-4, R/NR -1.69, p=0.006), cardioprotection (kininogen-1, R/NR 1.47, p=0.013), and immune regulation (protein S100-A8, R/NR 4.39, p=0.043). Nevertheless, when validation was performed in a larger number of patients (n=33), kininogen-1 (R/NR 1.30, p=0.013) and protein S100-A8 (R/NR 2.68, p=0.076) displayed the most robust candidates differentiating responders and non-responders at baseline.

In conclusion, the proteomic study of EMBs at baseline suggests that responders and non-responders differ in the abundance pattern of several proteins involved in energy and lipid metabolism, immune regulation and cardioprotection. However, these proteins cannot be directly implemented as a biomarker to discriminate both subgroups before therapy in the regular daily practices for clinicians as their extraction require complex surgical interventions. In this regard, blood plasma-based proteins must be screened to develop clinically applicable diagnostic tools and thus they were a further goal of the current study.

Proteome alterations induced by immunoadsorption therapy in responder and non-responder DCM patients

Benefit of IA/IgG in DCM patients have been well evaluated in various previous studies [48–51] but the molecular events induced by immunoadsorption therapy at protein levels have not been evaluated yet. Therefore, this study confined to elucidate the proteomic changes due to immunoadsorption therapy among responder and non-responder DCM patients employing label-free proteomic approach.

The effects of IA/IgG were observed on the levels of pro-b-type natriuretic peptide (NT-proBNP), which is a 32 amino acid polypeptide secreted by the ventricles of the heart in response to hypoxia, stress or excessive stretching of heart muscle cells (cardiomyocytes). The elevated levels of NT-proBNP in blood plasma/serum have been observed in several cardiac diseases including heart failure [134]. Higher concentrations of NT-pro-BNP in plasma or serum are a well-known indicator of heart diseases, and a gold standard for the diagnosis of heart failure patients [134]. In our data, six months after IA/IgG, improved heart function was accompanied by a decrease of NT-pro-BNP (1081 ± 1205 to 532 ± 1211, $p<0.007$) in responder DCM patients that was in line with the findings when reduced level of NT-proBNP was observed with favorable outcome after Cardiac Resynchronization Therapy (CRT) in heart failure patients [135]. NT-proBNP plays an important role in the regulation of intravascular blood volume and vascular tone, and its action has been considered to compensate for heart failure as it exerts its cardioprotective role via vasodilation and diuretic action mechanisms [136]. Its role has also been shown to be anti-fibrotic in the heart, as it inhibits the formation of collagen, an important component of extracellular matrix [137]. The protective effect of NT-proBNP occurs only to a certain extent, because, in heart failure, high BNP levels are found together with elevated levels of collagens. Apart from it, the beneficial effects of immunoadsorption therapy were also observed on the New York heart association (NYHA) class that categorizes patients according to their decreasing physical activity (class I-IV) thereby

displaying severity of heart failure. After immunoadsorption therapy, NYHA class of responder DCM patients decreased from higher to the lower class (NYHA I/II/III/IV, 0/5/7/0 to 5/4/3/0 after FU, p=0.02) indicating the benefits of therapy in this patient subgroup. A drop in NYHA class was also reported when heart failure patients treated with CRT [138] with improved cardiac functions. Also, immunoadsorption therapy reduced the morbidity and mortality in dilated cardiomyopathy patients at significant levels [58], as observed for CRT in heart failure patients [139].

Previous studies have disclosed the molecular changes in the myocardium at transcriptome, proteome, and metabolome levels after implantation of left ventricular assist device and CRT in dilated cardiomyopathy and heart failure patients [139–141]. In particular, the molecular changes induced by left ventricular assist device in failing heart were associated with alterations in many key pathways including energy metabolism, cytoskeletal and contractile proteins, cytokine signaling, calcium handling, cell survival, adrenergic receptor signaling, endothelial and microvascular functions [141]. In the current study, to obtain robust proteome results, data of a previous study carried out by Michelle Goritzka were included, and thus analyses of the IA/IgG effect could be performed on 23 DCM patients. Since at that time, data were acquired with a less sensitive instrument (FTICR) the common protein set quantified by both instrument settings were only 669, which were considered for further analysis. Among the total identified proteins, a small proportion of only approximately 2 % (16 proteins) in responders (R-FU/BL), and 5.7 % (43 proteins) in non-responders (NR-FU/BL) were differentially abundant after therapy, which is in line with the findings of the low number of differentially regulated genes (R 244 genes, NR 129 genes) obtained from gene expression analysis of 33 DCM (R 20, NR 13) patients (in press). A larger number of proteins were altered in non-responders than responders after IA/IgG. In contrast, gene expression analysis of these patient subgroups displayed a large number of altered genes in responders. The effect of therapy on the myocardial proteins seem to be different in responder and non-responder DCM patients, in particular responders displayed changes in ILK signaling, calcium

signaling, actin cytoskeletal signaling, and protein kinase A signaling, whereas non-responders displayed changes mainly to fibrosis, intrinsic prothrombin activated pathway, dendritic cell maturation, and calcium signaling. Similarly, myocardial changes were found different in responders and non-responder DCM patients treated with CRT [139]. Beneficial effects of CRT were mediated by the increased levels of mitochondrial proteins mainly including components of complex I, II, III, and VI of the respiratory chain [139]. In contrast, in the current study, benefits of IA/IgG were not involved with mitochondrial proteins, as only one mitochondrial protein (NADH dehydrogenase [ubiquinone] iron-sulfur protein 6) was found altered in responders, while, out of five, four altered proteins (Cytochrome c oxidase subunit 6B1, Glutaredoxin-related protein 5, Phosphate carrier protein, Cytochrome c oxidase assembly factor 6 homolog) of mitochondria were found more abundant in non-responders after IA/IgG.

Previous studies have also claimed that remodeling in heart due to the course of heart failure may be reversed for extracellular matrix volume by using left ventricular assist device [142]. In the current study, EMBs of healthy controls were not included. Therefore, reverse remodeling of proteins in myocardium due to the immunoadsorption therapy by directly comparing proteomes of responders and non-responders to healthy controls was restricted. However, to address this issue proteome alterations induced by immunoadsorption therapy in responders and non-responders were compared to the previously published myocardial proteome comparison of dilated cardiomyopathy patients with healthy controls [94]. Proteome differences of EMBs between dilated cardiomyopathy patients and healthy controls were confined to mitochondrial functions, extracellular matrix remodeling and cytoskeletal categories [94], and some proteins related to these pathways were found altered in responders and non-responders after 6 months of IA/IgG therapy. In-depth analysis revealed a fraction of proteins that was inversely regulated in responders (alpha actinin-1) and non-responders (galectin-1, F-actin capping protein, dermatopontin, destrin, and spectrin beta protein) after therapy, in comparison to the DCM associated proteome alterations (Fig. 40). Thus, functional

121

recovery of myocardium after therapy does not seem to be mainly associated with alterations in the protein composition. Probably, post-translational modifications that play a crucial role in signaling events might allow some more in-depth understanding of immunoadsorption therapy associated changes. In this aspects, a recently published study using a dog model of heart failure claimed that positive effects by CRT seem to be mediated by the phosphorylation of myocyte proteins by glycogen synthase kinase [143].

In addition, gene expression profiling of responders and non-responders at baseline in comparison to controls (normal LVEF) disclosed differentially expressed genes, which were assigned to oxidative phosphorylation, mitochondrial dysfunction, protein ubiquitination pathways, and cardiac hypertrophy. Except for mitochondrial dysfunction, none of these pathways were found to be altered in the proteome profiling of responder and non-responder DCM patients after immunoadsorption therapy. Likewise, gene expression data of these patient subgroups (responders and non-responders after therapy) also did not reverse DCM associated molecular alterations observed in comparison to controls (in press).

To define the differential effects of therapy on the proteome, comparisons of follow-up (after therapy-FU) over baseline (before therapy-BL) ratios of both subgroups (R-FU/BL versus NR-FU/BL) were analyzed. In total, 57 proteins differentially altered between both subgroups were discovered. Among the altered proteins, some play a vital role in heart failure pathophysiology [144]. Functional annotation of differentially abundant proteins of responders and non-responders indicated that both groups seem to be different in ILK signaling, actin cytoskeleton signaling, fibrosis, and calcium signaling, which was also supported by the findings of gene expression analysis of these subgroups (in press).

		DCM/Control		R-FU/BL	
ID	Description	Fold change	p-value	Fold change	p-value
P12814	Alpha actinin-1	2	5.70E-10	-1.32	7.13E-03
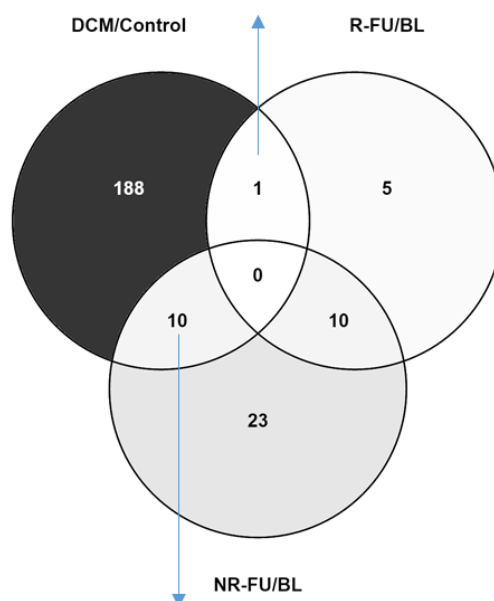
5 proteins with inverse abundance in "DCM/Control" and "NR-FU/BL":					
		DCM/Control		NR-FU/BL	
ID	Description	Fold change	p-value	Fold change	p-value
P11277	Spectrin beta chain, erythrocyte	1.4	4.30E-02	-1.56	1.89E-13
P60981	Destrin	-1.3	2.10E-02	1.36	1.25E-10
P47756	F-actin-capping protein subunit beta	-1.5	9.03E-04	1.34	4.08E-10
Q07507	Dermatopontin precursor	-1.7	1.50E-02	2.44	9.72E-18
P09382	Galectin-1	-2.2	2.38E-04	1.31	5.11E-09

Fig. 40. IA/IgG associated effects in responders and non-responders on myocardial proteins found to be altered in DCM patients in comparison with controls by Hammer et al. [94]

The Venn diagram shows the overlap of differentially abundant myocardial proteins upon IA/IgG in the patient subgroups and in DCM patients compared to controls. Proteins inversely regulated by IA/IgG are listed with fold change and p-value.

Integrin-linked kinase (ILK) signaling, which is required for proper cardiac development, growth, contractility, and repair [145] seemed to be influenced by immunoadsorption therapy in responder and non-responder DCM patients. Cardiac-specific deletion of ILK causes cardiomyopathy in mice, and it has been shown that ILK protein complexes are found in the sarcomeres that regulate the contractility of cardiomyocytes by interacting several structural proteins like actin, myosin, talin,

vinculin and alpha-actinin [145]. In addition, integrin-linked kinase has been shown to modulate cardiac contractility through interactions with the calcium regulatory protein sarcoplasmic/endoplasmic reticulum Ca(2+)ATPase isoform 2a (SERCA-2a) and phospholamban (PLN) in the human heart [146]. In the current study, some of the proteins of the ILK pathway were more abundant (myosin regulatory light chain 2, atrial isoform-MYL7, and cyclic AMP-responsive element-binding protein 3-like protein-4) whereas other's (vimentin, myosin regulatory light polypeptide 9, fibronectin, myosin-11, actin, cytoplasmic 2, and alpha-actinin-1) were found less abundant in responders after therapy. Therefore, the proteome data did not reveal clearly the overall direction of ILK pathway, but rather indicated disturbances among responder and non-responder DCM patients.

MYL7 is a calcium binding protein and participates in muscle contraction. Likewise, vimentin, actin, actinin-1, and myosin-11 are cytoskeletal proteins, and their levels have been increased when ILK was overexpressed in epithelial cells [147]. Upregulation of cytoskeletal proteins (desmin, tubulin, vinculin, and dystrophin) has been observed in heart failure patients with diastolic and contractile dysfunction [144]. In general, the level of those cytoskeletal proteins increases in the myocardium of failing human hearts, and these changes lead to cardiomyocytes remodeling [148]. Proteome profiling of endomyocardial biopsies revealed various deregulated cytoskeletal proteins (actin, F-actin capping proteins, catenin, talin 1 and 2, titin, alpha actinin-4, etc.) in dilated cardiomyopathy patients in comparison with those of control hearts (normal LVEF) [94]. Alpha actinin-1, an F-actin cross-linking protein, helps anchor the myofibrillar actin filaments, and its level increased in dilated cardiomyopathy patients [94], interestingly immunoadsorption therapy reversed (decreased) its abundance changes in responder DCM patients which displayed beneficial effect of therapy.

Apart from this observation, altered patterns of proteins involved in cardiac fibrosis were also seen in responders that benefit from IA/IgG. Fibrosis is a sequential molecular event characterized by

fibroblast accumulation and excessive deposition of extracellular matrix proteins that lead to distorted architecture with impaired cardiac function. Our proteome data suggested that therapy reduced the abundance of proteins that are involved in fibrotic events like fibronectin, collagen alpha-1(I) chain, and collagen alpha-2 (I) chain, in responders. Fibronectin is a protein that binds to the cell surface and extracellular matrix components such as collagen, fibrin, and heparin sulfate proteoglycans. Fibronectin protein is actively involved in fibrotic events, and its level in myocardial tissues has been shown higher (fold change 1.6, p=0.034) in dilated cardiomyopathy patients in comparison to healthy controls with normal LVEF [94]. Interestingly, the level of fibronectin decreased in responders after immunoadsorption therapy which suggests the reduction of fibrotic events. In general, the levels of collagen proteins increase in the myocardium of dilated cardiomyopathy and heart failure patients [149–151] which may deteriorate the functioning of the heart. Protein collagen alpha-1(I) chain (COL1A1) was found 5.1 fold higher (p=0.003) in dilated cardiomyopathy hearts when compared with healthy controls [94]. Also, the upregulation of COL1A1 transcripts (mRNA) was observed in the myocardium of rats with cardiac hypertrophy [152]. In the current study, the immunoadsorption therapy decreased the level of two collagen proteins (COL1A1, and COL1A2) in responders, indicating the benefits of therapy. In the same line, Felkin et al. showed the lower expression of transcripts for fibronectin and collagen (COLA1 and COL3A1) in heart failure patients, recovered after implantation of left ventricular assisted devices [153].

Furthermore, reduced fibrosis in responders after therapy was supported by a lower abundance of extracellular matrix proteins including lumican, biglycan, mimecan, periostin, prolargin, and dermatopontin. Lumican is an extracellular matrix proteoglycan that binds to the collagen fibrils and plays a crucial role in cardiac remodeling; its higher expression in mice and humans has been experimentally proven in heart failure [154]. Likewise, in patients with end stage of heart failure, higher levels of lumican at mRNA and protein level have been observed in cardiac biopsies,

indicating its role in heart failure development [154]. In addition, the critical role of biglycan and mimecan in ventricular remodeling also has been discussed extensively [155]. Biglycan is a proteoglycan that has been shown to be involved in several functions including cell adhesion, collagen fibril assembly, and growth factor interactions [156]. Elevation of myocardial biglycan in cardiac fibroblast has been seen in mice model of heart failure [156]. In addition, periostin plays a role in extracellular matrix mineralization, and the expression of its gene has been shown upregulated with the extent of myocardial fibrosis in human failing heart [157]. Also, the effect of immunoadsorption therapy on levels of lumican, biglycan and mimecan was supported by gene expression data of responder and non-responder DCM patients (in press). Thus, in conclusion, IA/IgG-therapy reduces the expression levels of several extracellular matrix proteins like lumican, biglycan, mimican, periostin, and prolargin further strengthening the assumptions of reduced fibrotic events in responders after immunoadsorption therapy. Surprisingly, in contrast to the molecular finding, analysis of endomyocardial biopsies employing Masson Trichrome stain and light microscopy did not reveal significant changes of fibrosis grades among responders and non-responders after IA/IgG.

Several studies have claimed the association of extracellular matrix proteins with transforming growth factor-β (TGF-β) which is a multifunctional cytokine and a key regulator of extracellular matrix assembly and remodeling [158]. In our proteome data, lower activity of TGF-β in responders after six months of IA/IgG was predicted based on the identified associated proteins that supported the lower level of fibrotic proteins in this patient subgroup. Additionally, lower TGF-β activity was further strengthened by the lower activity of SMAD3 in responders predicted by Ingenuity Pathway Analysis based on the change in protein abundance pattern upon therapy. Also, lower activity of TGF-β in responders were further independently supported by IPA analysis of gene expression data (in press). Furthermore, reduced TGF-β activity in gene expression data was supported by the down-regulation of the connective tissue growth factor gene (CTGF), which is

known as a key regulator of fibrosis and has been associated with cardiac remodeling and progression of heart failure [159]. In conclusion, higher activity TGF- β were seen in non-responders after immunoadsorption therapy in DCM patients by associated proteins and genes employing proteomic and gene expression data, but in both the study TGF- β molecule was not discovered directly.

Apart from it, therapy induced the abundance of cAMP-dependent protein kinase catalytic subunit beta (PRKACB) and cAMP responsive element binding protein 3-like 4 (CREB3L4) in responders. PRKACB mediates cAMP dependent signaling triggered by receptor binding to G-protein coupled receptors. Therefore, PRKACB may indirectly regulate the calcium ion signaling and myocardial contractility. Thus, therapy might also influence calcium ion signaling and contractility of cardiomyocytes through PRKACB but in-depth further studies are required to elaborate these findings.

In conclusion, in this proteome study we evaluated the proteome alterations associated with six months of immunoadsorption therapy in responder (R-FU/BL) and non-responder (NR-FU/BL) DCM patients but majorly reviewed the differences between responders and non-responders by looking at the ratios FU/BL between the subgroups. In summary, only mild alterations of the abundance pattern of proteins were found. The findings suggest a differential remodeling of proteins in responder and non-responders DCM patients particularly in cytoskeletal, fibrosis, and extracellular matrix categories. Furthermore, therapy-induced improvement of left ventricular function in responders was correlated with the lower abundance of fibrotic and extracellular matrix proteins along with the reduced activity of TGF-β signaling in comparison to non-responders after therapy. Compared to the data published earlier on DCM associated alteration in the heart, it can be assumed that the functional recovery of the LV is not accompanied with an extensive reverse regulation of proteins altered during disease.

Plasma proteomic profiling of responder and non-responder DCM patients at baseline

It is utmost important to find biomarkers of immunoadsorption therapy outcome in DCM patients that can be directly implemented to clinics for the selective and personalized treatment of therapy. Although proteome profiling of plasma, in general, is hampered by many challenges, advancement and implementation of mass spectrometric techniques along with the improvements of sample preparation protocols not only allowed the coverage of a higher number of plasma proteins, but also displayed the capabilities to identify and quantify low abundant plasma proteins with high accuracy [160, 161]. In the study presented here, robust mass spectrometric approaches were implemented to screen for plasma proteomic biomarkers differentiating responder and non-responder DCM patients before immunoadsorption therapy. The discovery phase workflow exploited the results of both label-free and label based (iTRAQ) approaches, whereas the validation phase included multiple reaction monitoring and ELISA methods. Label-free quantification allows acquisition of individual patient data, whereas the major advantage of using iTRAQ method is to dig deeper into the plasma proteome by reducing the complexity of peptides using strong cation exchange fractionation. Additionally, pooling of peptides of different patients/groups prior to mass spectrometric analysis in the iTRAQ workflow eliminates the impact of the run to run technical variation from quantitation and enhanced ionization of tagged peptides offers robust identification and quantification of proteins [162].

In total, by combining label-free and iTRAQ data, this study identified 467 non-redundant plasma proteins. In comparison to the recently published results by Hollander et al., where 138 plasma proteins were identified in recovered heart failure patients after transplantation using iTRAQ mass spectrometric method [87]. The number of identified proteins might be further increased by implementing extensive pre-fractionation method (anion exchange, cation exchange, and off-line fractionation) with multiple measurements before mass spectrometric analysis as described by

Farrah et al., where 1929 plasma proteins were identified with high confidence (1%FDR) from 91 experiments that included phase I and phase II human plasma proteome project [163]. The proteins obtained in our data were 50% classical plasma proteins synthesized and secreted by the liver, whereas another 50 % proteins were from various cellular categories including membrane, nucleus, endoplasmic reticulum, mitochondrial matrix, lysosome and peroxisomes that might have delivered into the plasma due to cell disruption, leakage or secretion. In general, blood plasma contains proteins span approximately 10^{12} orders of magnitude [92], whereas, in the current study, plasma proteins covered more than seven orders of magnitude in a concentration ranging from 6 pg/ml (CRISP3-cysteine-rich secretory protein-3) to 40mg/L (HPR-haptoglobin-related protein) (http://plasmaproteomedatabase.org/).

The discovery phase experiments (iTRAQ and label-free) delivered a large number (154, ≈32% of total identified) of differentially abundant plasma proteins between responders and non-responders at baseline, which was in line with the high number of differentially abundant plasma proteins (67, ≈50 % of total identified) discovered in the recovered heart failure patients after transplantation [87]. One reason for this finding is the lack of biological replicates, when pools are analyzed. Therefore, the protein candidates found need a further validation on individual patient level to minimize false positive results. Another approach would be the analyses not only of one pool, but more pools if sufficient patient samples are available. Along with this, the differentially abundant plasma proteins quantified with small fold changes (ranged from -2.95 to 3.88) were similarly observed in endomyocardial proteome (-3.03 to 3.08) and gene expression analyses of these patients subgroups [62]. Functional enrichment analysis of the differentially abundant proteins of endomyocardial biopsies revealed differences in the energy, lipid, and immune related pathways, whereas gene expression analysis of myocardial tissues revealed differences in oxidative phosphorylation, mitochondrial dysfunction, protein ubiquitination pathways, and cardiac hypertrophy [62] between responders and non-responders at baseline. Of course, plasma proteome

profiling at baseline did not reveal the differences between the subgroups as displayed by endomyocardial biopsies, because cellular differences cannot be expected to be seen globally in plasma. Here changes were observed mainly in LXR/RXR activation, acute phase signaling, immunodeficiency signaling, and the coagulation system. Liver X receptors (LXR) are the transcription factors that regulate glucose and lipid homeostasis by mediating the expression of proliferator-activated receptors gamma coactivator-1α (PGC-1), phosphoenol/pyruvate carboxykinase (PEPCK), and glucose -6-phosphatase [164]. Along with this, LXR receptors has been known to regulate the inflammation and immune responses in many metabolic diseases [165]. Deregulation of inflammation and immune system is very well known in dilated cardiomyopathy patients. Thus, speculation can be made that LXR receptors might also contribute to the progression and pathogenesis of dilated cardiomyopathy. In the current study, fifteen proteins related to LXR activation were found to be different in level between responder and non-responder DCM patients at baseline. Among them, based on the abundance pattern of 13 proteins (7 lower abundant in responders; transferrin, apolipoprotein C-II, albumin, prenylcysteine oxidase 1, serum paraoxonase 1, apolipoprotein L, phospholipid transfer protein, and 6 higher abundant in responders; inter-alpha-trypsin inhibitor heavy chain family member 4, serpin peptidase inhibitor clade F, orosomucoid-1, apolipoprotein C-IV, serum amyloid A1, and haptoglobin-related protein), IPA analysis predicted higher activity of LXR in responders, whereas levels of two proteins (lipopolysaccharide binding protein, and S100 calcium binding protein A8) predicted the lower activity of LXR in responders. Previous studies have shown that activation of LXR receptors might attenuate cardiac remodeling in hypertrophy [166]. Thus, deregulation of proteins related to LXR activation might be linked to the different cardiac remodeling among responders and non-responders at baseline.

It has been shown that viral infection may activate the coagulation system in order to limit the spread of the pathogens [167]. Coagulation is a dynamic process, and its imbalances may lead to critical conditions like excessive bleeding or obstructive blood clotting [168]. Previous studies have

suggested that left ventricle enlargement and dysfunction in dilated cardiomyopathy and atrial dilation in hypertrophic cardiomyopathy may also trigger the activation of coagulation cascades [169]. In general, the activated coagulation cascades in dilated cardiomyopathy and heart failure patients have been seen by measuring plasma specific markers for thrombosis and platelet activity [169]. In the current plasma proteomic profiling, four proteins (coagulation factor VII, IX, XI, and XII) of the coagulation cascades were found different between responders and non-responders. Coagulation factor VII initiates the extrinsic pathway of blood coagulation, whereas factor IX participate in the intrinsic pathway by converting factor X to its active form. Coagulation factor XII participates in the initiation of blood coagulation, fibrinolysis, and also helps to generate bradykinin and angiotensin that acts as a vasodilator. Lower concentrations of plasma coagulation factor VII and XI were associated with a higher risk of mortality in elderly heart failure patients [170]. Kaplan et al. reported the increased level of coagulation factor VII and XI after implantation of left ventricular assist device in heart failure patients [171]. In the current study, coagulation factor VII and XI was found higher in the responder DCM patients, and its higher abundance is associated with the better outcome of therapy.

Acute phase proteins are the blood proteins, whose concentration is regulated in blood as a part of the acute phase response like defense, innate immune regulation, stress, infection and inflammation, and their increased levels in plasma/serum have been reported to be associated with the severity of cardiovascular diseases including dilated cardiomyopathy and heart failure [172, 173]. In the current proteome study, the acute phase response proteins C-reactive protein and Serum amyloid A-1 displayed higher abundances in the plasma of responder DCM patients. C-reactive protein (CRP) is an inflammatory mediator in patients with heart failure, synthesized in the liver and released into circulation. The level of plasma C-reactive protein was found higher with the severity of heart failure. Also, an elevated level of CRP was directly correlated with the extent of mortality and morbidity in heart failure and dilated cardiomyopathy patients [173] [174]. The level

of CRP in blood has been shown as an independent predictor of disease outcome in idiopathic/ non-ischemic DCM patients. Along with this, the level of serum CRP was found decreased after statin treatment in DCM patients [175]. The pro-inflammatory effect of CRP on the heart via matrix metalloproteinase-1 (MMP-1) and IL-8 in endothelial cells, and also by CD11b and CC-chemokine receptor 2 (CRR2) has been discussed [176]. The previous study has reported that CRP shares many functional properties of IgG. Therefore, it may bind to the Fcγ-receptor [177] and competitive binding of CRP and IgG to the Fcγ-receptors might play a role in immunoadsorption therapy outcome. In this study, plasma level of CRP was found higher in responder DCM patients, and it might be speculated that binding of CRP to the Fcγ-receptors might further modulate the efficacy of immunoadsorption therapy, which must be further evaluated. Along with this, we did not found any association of plasma level of CRP with the left ventricular ejection fraction, the inflammation status in the heart (CD3+ T lymphocytes and CD68+ macrophages), and disease duration before IA/IgG. Serum amyloid A-1 is an acute phase protein and also considered as a member of apolipoprotein family because it is predominantly associated with the high-density lipoprotein (HDL) in plasma. Elevated levels of serum amyloid A-1 in plasma has been shown to predict myocardial infarction, stroke, congestive heart failure, and vascular events in women [178]. The specific function of serum amyloid A-1 protein in the heart is not very well known, but it has been hypothesized that serum amyloid A protein may modulate the metabolism of high-density lipoprotein [179]. In this study, responder DCM patients displayed higher levels of plasma amyloid A-1 protein, and its higher levels is associated with the better therapy response.

In addition, many studies on dilated cardiomyopathy and heart failure disclosed disturbances in immune response and inflammatory processes [18, 19, 22]. In the current study many plasma proteins like mannose binding lectin protein, lipopolysaccharide-binding-protein, galectin-3-binding protein, protein S100-A8, S100-A9, S100-A7 and haptoglobin related protein were found at higher level in responders. Mannose binding lectin protein is mainly involved in innate immune

defense and binds to various sugar moieties (mannose, fucose, and N-acetylglucosamine) on different microorganisms to activate the lectin complement pathways to kill microorganisms [180]. Therefore, deficiency of MBL increases the susceptibility of an individual to infectious diseases [180]. In addition, high level of MBL in plasma has been associated to predict decreased incidence of myocardial infarction particularly in diabetic patients [181]. On the other hand, mannose binding lectin protein binds to apoptotic and necrotic cells, and facilitates their removal by macrophages. Though the direct role of MBL in dilated cardiomyopathy has not been evaluated yet, but the higher level of MBL in responders seems to be associated with the better outcome of immunoadsorption therapy.

Lipopolysaccharide-binding protein binds to a bacterial glycoprotein (lipopolysaccharide-LPS) present on the outer membrane of gram-negative bacteria that may initiate immune response mediated via CD14 receptor or toll-like receptors to clear LPS from circulation [182]. It has been hypothesized that in patients with heart failure mesenteric venous congestion leads to an increased gut permeability for bacteria, and thereby bacteria and endotoxins translocate into the circulation. Consequently, with the activation of the immune system, the level of serum lipopolysaccharide-binding protein increases, enabling binding to LPS and result in a signaling cascade for the removal of lipopolysaccharides [182]. In chronic heart failure patients, human trials have indicated that removal of gut bacteria led to a decrease in lipopolysaccharide and might improve the outcome of these patients [183]. In addition, Galectin-3 binding protein promotes integrin mediated cell adhesion, and found at high levels in responder DCM patients. In summary, the proteins of immune response were found at higher levels in responders than in non-responders, but their higher abundance has been reported to be associated with the high mortality or severity of heart failure. Thus, responders seem to have a more impaired status of the immune system which can be cured by immunoadsorption therapy.

Many S100 family plasma proteins were deregulated between responders and non-responders at baseline. The S100 protein family are low molecular weight (10-14 kDa) calcium binding proteins that are involved in intracellular as well as extracellular functions, importantly regulation of proliferation, differentiation, apoptosis, Ca^{+2} homeostasis, energy metabolism, and inflammation by interactions with a variety of transcription factors and proteins [184]. The S100 protein family consists of 24 members, only expressed in vertebrates and display cell-specific expression patterns [184]. Protein S100-A8 and S100-A9 are members of this protein family. In general, increased levels of these proteins have been seen in a number of inflammatory and autoimmune diseases. Predominantly, protein S100-A8 exerts its function in combination with its binding partner S100-A9, known as calprotectin (S100A8/A9), but both proteins were also found independently in plasma and cellular extracts. Both S100-A8 and S100-A9 are calcium and zinc-binding proteins and are involved in pro-inflammatory, antimicrobial and pro-apoptotic activities. Also, they induce innate immunity via binding to pattern recognition receptors such as toll-like receptors (TLR-4) and receptors for advanced glycation end product (AGER) [185]. The expression of S100-A8 and S100-A9 is very low in normal cardiomyocytes, but an induced expression has been observed in HL1 cardiomyocytes, isolated primary cardiomyocytes, and whole heart of mice upon LPS treatment [185]. In addition, overexpression of S100-A8 and S100-A9 led to decreased cardiac ejection fraction as well as RAGE-dependent calcium flux, whereas knockdown of S100-A9 reduces LPS induced cardiac dysfunction. Along with this, it was claimed that protein S100A8 and S100-A9 interacts with the calcium gating protein SERCA2 and may regulate the cardiomyocytes contractility by a RAGE-dependent mechanism [185]. Higher levels of plasma S100-A8/A9 heterodimer have been observed in acute myocardial infarction patients [186], and it has also been described as an independent risk factor for cardiovascular events [186, 187]. Also, S100A8/A9 complex has been shown as a biomarker to predict the mortality in elderly patients with severe heart failure [188]. In a recent study, blood plasma and platelet level of protein S100-A8 were found to be higher in heart failure patients with preserved ejection fraction in comparison to healthy

controls, as well as Ca+2 concentration and action potential was adversely affected when recombinant S100-A8 was incubated on iPSC-derived cardiomyocytes [189]. In total, higher levels of protein S100-A8 and S100-A9 have been shown associated with the severity of many diseases. In contrast, in this current study higher level of protein S100-A8 and S100-A9 in responders was associated with the beneficial outcome of immunoadsorption therapy. Higher abundance of S100-A8 protein in responders was further supported by the myocardial proteome profiling (R/NR, FC 3.02, p=0.003, n=16) and gene expression profiling results (R/NR, FC 2.82, p=0.019) [62]. In general, high levels of immune proteins such as S100-A8, S100-A9, and CRP were found in inflammatory diseases, and their high values also have been shown as an indicator of cardiac dysfunctions. In contrast to the literature where high S100-A8 levels are reported in more severe disease states, we found high values of this protein in responders associated with cardiac improvement. Such higher values might be associated with a higher susceptibility to infection or persistence of infectious agents. Thus, a very recent study showed, that higher S100A8/S100A9 levels are linked to increased CVB3 copy numbers in a myocarditis mouse model [190].

In addition, plasma level of apolipoprotein C-IV was found higher abundant in responder DCM patients than those of non-responders. Apolipoprotein C-IV participates in lipoprotein metabolism and regulates triglyceride homeostasis, but its role in heart failure and dilated cardiomyopathy has not been well evaluated yet. Along with this, pigment epithelium-derived factor, caprin-1, myelin transcription factor 1, actin-binding LIM protein 1, and desmocollin-1 were found higher abundant in responders, whereas insulin-like growth factor II, neuropilin-1 and microfibril-associated glycoprotein 4 were found lower abundant in the plasma of responders in comparison to non-responders. Pigment epithelium-derived factor is a multifunctional and pleiotropic protein with antioxidant, antiproliferative, antithrombotic and anti-inflammatory properties, and considered as a potential therapeutic target in cardiovascular diseases [191]. Elevated serum level of pigment epithelium-derived factor in metabolic syndrome and coronary artery disease patients has been

shown in the Chinese population, which may counter represent a protective response against vascular damage [192]. Also, its protective function is further strengthened when pigment epithelium-derived factor was injected in rats with acute myocardial infarction, and improved cardiac function was shown by inhibiting left ventricular remodeling [193]. In addition, its higher levels might affect the progression of cardiomyopathy and heart failure by inducing apoptosis of cardiac myocytes and fibroblasts via the activation of caspase-3 [194]. In this plasma proteomic study, the higher abundance of pigment epithelium-derived factor in responders showing a cardioprotective action after immunoadsorption therapy, but the direct link of therapy and its level in plasma has to be further elaborated. Some of the plasma proteins like caprin-1, myelin transcription factor 1, and neural cell adhesion molecule L1-like proteins in the plasma of responders and non-responders were different, but surprisingly their functions are more oriented towards nervous system development and in synaptic plasticity. In addition, Neuropilin-1 -a multidomain membrane receptor and a co-factor of cardiac VEGF receptors, was found lower abundant in the plasma of responder DCM patients. It is majorly involved in angiogenesis and development of neuronal circuits, but in a recently published study, its cardioprotective role has been experimentally proven in a cardiomyopathy and ischemic heart failure mouse model [195]. Therefore, neuropilin-1 might also play a role in the differential response of responders and non-responders upon IA/IgG.

To confirm the results obtained in the discovery phase, multiple reaction monitoring (MRM) was implemented. Validation was performed in a large number of samples. MRM result displayed the strongest differences in protein abundance for protein S100-A8, S100-A9, C-reactive protein (CRP), lipopolysaccharide-binding protein (LBP) and cysteine-rich secretory protein 3 (CRISP3). These candidates might be the potential biomarkers to distinguish responders and non-responders at baseline. In addition, among the five most robust candidates, protein S100-A8, S100-A9, and CRP displayed relatively strongest differences, whereas fold changes were rather smaller for

lipopolysaccharide-binding protein and cysteine-rich secretory protein 3. The potential of all five proteins to classify DCM patients as responders was assessed individually using Receiver Operative Characteristic (ROC) curve, in which S100-A8 displayed the most robust candidate (AUC 0.70, p=0.003) differentiating responders and non-responders. Many previous studies have explained the utility of multiple biomarkers instead of using only one marker in risk stratification or prediction of cardiovascular events and heart failure [196, 197]. Recently Hollander et al., discovered a seventeen-protein biomarker panel to predict recovered heart failure patients after heart transplantation with 93% sensitivity and 89% specificity employing iTRAQ and MRM mass spectrometric method [87]. Recently, a six plasma protein biosignatures (cardiotropin1, cardiac troponin T, clusterin, dickopff1, C-reactive protein and growth differentiating factor 15) were identified, that may predict the response to medical treatment or mechanical circulatory support, in patients with inotrope-dependent acute heart failure (AHF) and may help to identify patients who would benefit from the intervention before it starts [198]. In contrast, in the current study, when biomarker potential was evaluated by combing five proteins together, the area under the receiver operating characteristic curve (AUC=0.64) did not improve. In addition, a previous study of myocardial gene expression analysis, Ameling et al., [62] included the negative ionotropic activity to the mRNA levels of four genes (ras-related nuclear binding protein 1, regulator of G-protein signaling 10, ubiquitin protein ligase E3B, and ubiquitin specific peptidase 22) allowed robust discrimination of responders and non-responders, but this approach cannot be implemented directly in the clinics as it is limited by obtaining human heart biopsies as well as primary cardiomyocytes of rats.

In conclusion, the discovery phase plasma proteome analysis employing iTRAQ and label-free quantification provided a number of differentially abundant plasma proteins mainly involved in immune response, inflammation, and blood coagulation categories. Furthermore, twenty proteins were selected, and validation was performed using multiple reaction monitoring in a larger number

of DCM patients. The top five proteins (S100-A8, S100-A9, CRP, CRISP3, and LBP) were evaluated for their potential to discriminate responders and non-responders using Receiver Operating Characteristic (ROC) curve. Among them, protein S100-A8 displayed the highest potential in discriminating responders and non-responders before immunoadsorption therapy.

Establishment a workflow for the relative quantitation of phosphopeptides and elucidation of the effects of TGF-β on the phosphopeptide pattern in HL-1 cardiomyocytes

The major goal of this part of the study was to establish a workflow for the global phosphoproteome analysis that can be implemented for samples that are generally accessible only in small amounts like myocardial biopsies. Instead of using precious heart tissues, HL-1 cardiomyocytes were used in the protocol establishment and the TGF- β1 induced effects on the phosphoproteome were analyzed as a proof-of-principle experiment in HL-1 cardiomyocytes. Phosphopeptides were enriched using commercially available polyMAC-Ti which has been applied in some previously published phosphoproteomic studies [199, 200]. Global phosphoproteome studies, in general, require a large amount (1-100mg protein) of starting material due to the low proportions of phosphopeptides [201–203]. PolyMAC-Ti allows enrichment of phosphopeptides from 100-200 µg of protein digest. Mass spectrometric analysis revealed approximately 2000 phosphopeptides in each sample (controls and TGF-β1 treated) which was almost twice the number of phosphopeptides enriched from whole cell extracts of the human Burkitt lymphoma B cell line using polyMAC [199]. In addition, the total number of identified phosphopeptides in this study was almost equivalent (≈1800 phosphopeptides) when phosphopeptides were enriched from human neutrophils using polyMAC [200]. The number of identified phosphopeptides might be increased further by integrating various fractionation techniques as applied in many studies [203, 204] but these strategies would be limited to samples available at large scale. In the present study, the enrichment efficiency of phosphopeptides for every sample was quite high (≈97-99%) and reproducible,

thereby being in-line with the phosphoproteomic analysis of human neutrophils [200]. Serine and threonine amino acids undergo phosphorylation more often than tyrosine residues and in vertebrate cells ratio of pS: pT: and pY was described as 1800:200:1 [205]. The present study covered ≈ 3000 phosphosites per sample with the ratios of pS: pT: and pY being 300:15:1. Furthermore, to assess the impact of TGF-ß1 on the phosphorylation status, a label-free approach was performed that has been extensively used in various phosphoproteomic studies [206, 207].

In various cardiac diseases leading to heart failure, the TGF-β cytokine has been observed at higher levels [208, 209], and experiments have proven that the suppression of TGF-β in cardiomyocytes protects against cardiac remodeling by reducing the expression of fibrotic proteins [210]. It is known from the previous studies that TGF-β1 exerts its action through SMAD dependent and SMAD independent pathways via phosphorylation of SMAD proteins [211]. In the current phosphoproteome study, phosphorylation of the peptide sQsPHYPMVK of the SMAD nuclear interacting protein- 1 (SNIP1) at serine amino acid position 89 and 91 was found significantly decreased after 6 hour upon TGF-β1 treatment (Fig.39 A). Phosphorylation at serine 91 at SNIP1 is known, but at position 89 is a new site for further investigation. The importance of SNIP, for the regulation of TGF-β dependent SMAD4/p300 complex has been shown [212]. SNIP1 is a 396 amino acid nuclear protein of 50 KD that is abundantly expressed in heart and skeletal muscle. Thus, alteration of SNIP1 phosphorylation may directly affect TGF-β signaling pathways, as it interacts with several SMAD proteins (SMAD1, SMAD2 and SMAD4 [212], but the impact of phosphorylation events on protein-protein interaction in those complexes have not been investigated yet. Surprisingly, the present study did not reveal any phosphopeptides of SMAD proteins, whose phosphorylation is generally activated by the induction of TGF-β and initiates translocation to the nucleus and transcriptional regulation. It might be due to very low abundance of these phosphopeptides which might not be enriched in the employed workflow. Along with this, elevated level of TGF-β has been shown associated with higher levels of contractile proteins

including tropomyosin, calponin, smooth muscle protein-22 alpha, cofilin and heat shock 27 KD protein in myofibroblasts [213]. In the current study, TGF-β1 altered the level of phosphopeptides of the cytoskeletal proteins myosin regulatory light chain 2, atrial isoform (Fig.39 B) and myosin-10 (Fig.39 C). Some of the phosphopeptides might be further validated using either immunoassay methods like western blotting or multiple reaction monitoring.

Thus, in the present study, a phosphoproteome workflow for relative quantitation of phosphopeptides was well established, and may be applied to the small amount of protein accessible from myocardial biopsy samples. Additionally, incubation of TGF-β1 in cardiomyocytes induced the alteration of many phosphopeptides. The differentially abundant proteins associated with altered phosphopeptides were assigned to various pathways including ubiquitin-proteasome pathway, cytoskeletal regulation by Rho GTPase, calcium signaling, and TGF-β signaling. Most interestingly, phosphopeptide sQsPHYPMVK of Smad nuclear interacting protein-1 was reduced after TGF- β1 incubation which may be further evaluated in understanding the TGF-β1 induced changes in heart diseases.

In summary, this study delivered a proteome map of endomyocardial biopsies (baseline and after therapy) and plasma (before therapy) of responder and non-responder DCM patients. At baseline, many differentially abundant proteins were identified. Among those, proteins S100-A8 displayed the highest potential in discriminating responders and non-responders before IA/IgG. Along with this, therapy altered the abundance of several myocardial proteins in responders and non-responders that were mainly involved in fibrotic and extracellular matrix remodeling. Apart from it, a phosphoproteome workflow was established for the relative quantitation of phosphopeptides. Simultaneously, TGF- β1 induced phosphoproteome analysis in HL-1 cardiomyocytes delivered many differentially altered phosphoproteins that were involved in many signaling pathways including ubiquitin-proteasome pathway, cytoskeletal regulation by Rho GTPase, calcium signaling, and TGF-β signaling.

5. References

1. Elliott P, Andersson B, Arbustini E, Bilinska Z, Cecchi F, Charron P, Dubourg O, Kühl U, Maisch B, McKenna WJ, Monserrat L, Pankuweit S, Rapezzi C, Seferovic P, Tavazzi L, Keren A (2008) Classification of the cardiomyopathies: a position statement from the European Society Of Cardiology Working Group on Myocardial and Pericardial Diseases. European heart journal 29(2), 270–276. 10.1093/eurheartj/ehm342.

2. (1980) Report of the WHO/ISFC task force on the definition and classification of cardiomyopathies. Heart (British Cardiac Society) 44(6), 672–673. 10.1136/hrt.44.6.672.

3. Maron BJ, Towbin JA, Thiene G, Antzelevitch C, Corrado D, Arnett D, Moss AJ, Seidman CE, Young JB (2006) Contemporary definitions and classification of the cardiomyopathies: an American Heart Association Scientific Statement from the Council on Clinical Cardiology, Heart Failure and Transplantation Committee; Quality of Care and Outcomes Research and Functional Genomics and Translational Biology Interdisciplinary Working Groups; and Council on Epidemiology and Prevention. Circulation 113(14), 1807–1816. 10.1161/CIRCULATIONAHA.106.174287.

4. Towbin JA, Bowles NE (2002) The failing heart. Nature 415(6868), 227–233. 10.1038/415227a.

5. O'Connell JB (2000) The economic burden of heart failure. Clinical cardiology 23(3 Suppl), III6-10.

6. Mozaffarian D, Benjamin EJ, Go AS, Arnett DK, Blaha MJ, Cushman M, Ferranti Sd, Després J, Fullerton HJ, Howard VJ, Huffman MD, Judd SE, Kissela BM, Lackland DT, Lichtman JH, Lisabeth LD, Liu S, Mackey RH, Matchar DB, McGuire DK, Mohler ER, Moy CS, Muntner P, Mussolino ME, Nasir K, Neumar RW, Nichol G, Palaniappan L, Pandey DK, Reeves MJ, Rodriguez CJ, Sorlie PD, Stein J, Towfighi A, Turan TN, Virani SS, Willey JZ, Woo D, Yeh RW, Turner MB (2015) Heart disease and stroke statistics-2015 update: a report from the American Heart Association. Circulation 131(4), e29-322. 10.1161/CIR.0000000000000152.

7. Luk A, Ahn E, Soor GS, Butany J (2009) Dilated cardiomyopathy: a review. Journal of clinical pathology 62(3), 219–225. 10.1136/jcp.2008.060731.

8. Olson TM, Michels VV, Thibodeau SN, Tai YS, Keating MT (1998) Actin mutations in dilated cardiomyopathy, a heritable form of heart failure. Science (New York, N.Y.) 280(5364), 750–752.

9. Li D, Tapscoft T, Gonzalez O, Burch PE, Quiñones MA, Zoghbi WA, Hill R, Bachinski LL, Mann DL, Roberts R (1999) Desmin mutation responsible for idiopathic dilated cardiomyopathy. Circulation 100(5), 461–464.

10. Tsubata S, Bowles KR, Vatta M, Zintz C, Titus J, Muhonen L, Bowles NE, Towbin JA (2000) Mutations in the human delta-sarcoglycan gene in familial and sporadic dilated cardiomyopathy. The Journal of clinical investigation 106(5), 655–662. 10.1172/JCI9224.

11. Kamisago M, Sharma SD, DePalma SR, Solomon S, Sharma P, McDonough B, Smoot L, Mullen MP, Woolf PK, Wigle ED, Seidman JG, Seidman CE (2000) Mutations in sarcomere protein genes as a cause of dilated cardiomyopathy. The New England journal of medicine 343(23), 1688–1696. 10.1056/NEJM200012073432304.

12. Barresi R, Di Blasi C, Negri T, Brugnoni R, Vitali A, Felisari G, Salandi A, Daniel S, Cornelio F, Morandi L, Mora M (2000) Disruption of heart sarcoglycan complex and severe

cardiomyopathy caused by beta sarcoglycan mutations. Journal of medical genetics 37(2), 102–107.

13. Fatkin D, MacRae C, Sasaki T, Wolff MR, Porcu M, Frenneaux M, Atherton J, Vidaillet HJ, Spudich S, Girolami Ud, Seidman JG, Seidman C, Muntoni F, Müehle G, Johnson W, McDonough B (1999) Missense mutations in the rod domain of the lamin A/C gene as causes of dilated cardiomyopathy and conduction-system disease. The New England journal of medicine 341(23), 1715–1724. 10.1056/NEJM199912023412302.

14. Towbin JA (1998) The role of cytoskeletal proteins in cardiomyopathies. Current opinion in cell biology 10(1), 131–139.

15. Ahmad F, Seidman JG, Seidman CE (2005) The genetic basis for cardiac remodeling. Annual review of genomics and human genetics 6, 185–216. 10.1146/annurev.genom.6.080604.162132.

16. Murphy RT, Starling RC (2005) Genetics and cardiomyopathy: where are we now? Cleveland Clinic journal of medicine 72(6), 465-6, 469-70, 472-3 passim.

17. Bowles NE, Rose ML, Taylor P, Banner NR, Morgan-Capner P, Cunningham L, Archard LC, Yacoub MH (1989) End-stage dilated cardiomyopathy. Persistence of enterovirus RNA in myocardium at cardiac transplantation and lack of immune response. Circulation 80(5), 1128–1136.

18. Martino TA, Liu P, Sole MJ (1994) Viral infection and the pathogenesis of dilated cardiomyopathy. Circulation research 74(2), 182–188.

19. Kandolf R, Sauter M, Aepinus C, Schnorr JJ, Selinka HC, Klingel K (1999) Mechanisms and consequences of enterovirus persistence in cardiac myocytes and cells of the immune system. Virus research 62(2), 149–158.

20. Schultz JC, Hilliard AA, Cooper LT, Rihal CS (2009) Diagnosis and treatment of viral myocarditis. Mayo Clinic proceedings 84(11), 1001–1009. 10.1016/S0025-6196(11)60670-8.

21. Yajima T, Knowlton KU (2009) Viral myocarditis: from the perspective of the virus. Circulation 119(19), 2615–2624. 10.1161/CIRCULATIONAHA.108.766022.

22. Staudt A, Staudt Y, Dörr M, Böhm M, Knebel F, Hummel A, Wunderle L, Tiburcy M, Wernecke KD, Baumann G, Felix SB (2004) Potential role of humoral immunity in cardiac dysfunction of patients suffering from dilated cardiomyopathy. Journal of the American College of Cardiology 44(4), 829–836. 10.1016/j.jacc.2004.04.055.

23. Badorff C, Noutsias M, Kühl U, Schultheiss HP (1997) Cell-mediated cytotoxicity in hearts with dilated cardiomyopathy: correlation with interstitial fibrosis and foci of activated T lymphocytes. Journal of the American College of Cardiology 29(2), 429–434.

24. Barry WH (1994) Mechanisms of immune-mediated myocyte injury. Circulation 89(5), 2421–2432.

25. Sanderson JE, Koech D, Iha D, Ojiambo HP (1985) T-lymphocyte subsets in idiopathic dilated cardiomyopathy. The American journal of cardiology 55(6), 755–758.

26. Kühl U, Noutsias M, Seeberg B, Schultheiss HP (1996) Immunohistological evidence for a chronic intramyocardial inflammatory process in dilated cardiomyopathy. Heart (British Cardiac Society) 75(3), 295–300.

27. Efthimiadis I, Skendros P, Sarantopoulos A, Boura P (2011) CD4+/CD25+ T-Lymphocytes and Th1/Th2 regulation in dilated cardiomyopathy. Hippokratia 15(4), 335–342.

28. Eriksson U, Ricci R, Hunziker L, Kurrer MO, Oudit GY, Watts TH, Sonderegger I, Bachmaier K, Kopf M, Penninger JM (2003) Dendritic cell-induced autoimmune heart failure requires cooperation between adaptive and innate immunity. Nature medicine 9(12), 1484–1490. 10.1038/nm960.

29. Kaya Z, Leib C, Katus HA (2012) Autoantibodies in heart failure and cardiac dysfunction. Circulation research 110(1), 145–158. 10.1161/CIRCRESAHA.111.243360.

30. Caforio, Alida L. P., Mahon NJ, Tona F, McKenna WJ (2002) Circulating cardiac autoantibodies in dilated cardiomyopathy and myocarditis: pathogenetic and clinical significance. European journal of heart failure 4(4), 411–417.

31. Mobini R, Maschke H, Waagstein F (2004) New insights into the pathogenesis of dilated cardiomyopathy: possible underlying autoimmune mechanisms and therapy. Autoimmunity reviews 3(4), 277–284. 10.1016/j.autrev.2003.10.005.

32. Jahns R, Boivin V, Schwarzbach V, Ertl G, Lohse MJ (2008) Pathological autoantibodies in cardiomyopathy. Autoimmunity 41(6), 454–461. 10.1080/08916930802031603.

33. Schulze K, Becker BF, Schauer R, Schultheiss HP (1990) Antibodies to ADP-ATP carrier-an autoantigen in myocarditis and dilated cardiomyopathy-impair cardiac function. Circulation 81(3), 959–969.

34. Caforio AL, Grazzini M, Mann JM, Keeling PJ, Bottazzo GF, McKenna WJ, Schiaffino S (1992) Identification of alpha- and beta-cardiac myosin heavy chain isoforms as major autoantigens in dilated cardiomyopathy. Circulation 85(5), 1734–1742.

35. Limas CJ, Goldenberg IF, Limas C (1989) Autoantibodies against beta-adrenoceptors in human idiopathic dilated cardiomyopathy. Circulation research 64(1), 97–103.

36. Baba A, Yoshikawa T, Ogawa S (2002) Autoantibodies produced against sarcolemmal Na-K-ATPase: possible upstream targets of arrhythmias and sudden death in patients with dilated cardiomyopathy. Journal of the American College of Cardiology 40(6), 1153–1159.

37. Stavrakis S, Kem DC, Patterson E, Lozano P, Huang S, Szabo B, Cunningham MW, Lazzara R, Yu X (2011) Opposing cardiac effects of autoantibody activation of β-adrenergic and M2 muscarinic receptors in cardiac-related diseases. International journal of cardiology 148(3), 331–336. 10.1016/j.ijcard.2009.11.025.

38. Jahns R, Boivin V, Hein L, Triebel S, Angermann CE, Ertl G, Lohse MJ (2004) Direct evidence for a beta 1-adrenergic receptor-directed autoimmune attack as a cause of idiopathic dilated cardiomyopathy. The Journal of clinical investigation 113(10), 1419–1429. 10.1172/JCI20149.

39. Magnusson Y, Wallukat G, Waagstein F, Hjalmarson A, Hoebeke J (1994) Autoimmunity in idiopathic dilated cardiomyopathy. Characterization of antibodies against the beta 1-adrenoceptor with positive chronotropic effect. Circulation 89(6), 2760–2767.

40. Klein R, Maisch B, Kochsiek K, Berg PA (1984) Demonstration of organ specific antibodies against heart mitochondria (anti-M7) in sera from patients with some forms of heart diseases. Clinical and experimental immunology 58(2), 283–292.

41. Schultheiss HP, Bolte HD (1985) Immunological analysis of auto-antibodies against the adenine nucleotide translocator in dilated cardiomyopathy. Journal of molecular and cellular cardiology 17(6), 603–617.

42. Warraich RS, Griffiths E, Falconar A, Pabbathi V, Bell C, Angelini G, Suleiman M, Yacoub MH (2006) Human cardiac myosin autoantibodies impair myocyte contractility: a cause-and-

effect relationship. FASEB journal official publication of the Federation of American Societies for Experimental Biology 20(6), 651–660. 10.1096/fj.04-3001com.

43. Li Y, Heuser JS, Cunningham LC, Kosanke SD, Cunningham MW (2006) Mimicry and antibody-mediated cell signaling in autoimmune myocarditis. Journal of immunology (Baltimore, Md. 1950) 177(11), 8234–8240.

44. Kuan AP, Zuckier L, Liao L, Factor SM, Diamond B (2000) Immunoglobulin isotype determines pathogenicity in antibody-mediated myocarditis in naïve mice. Circulation research 86(3), 281–285.

45. Morita H, Seidman J, Seidman CE (2005) Genetic causes of human heart failure. The Journal of clinical investigation 115(3), 518–526. 10.1172/JCI24351.

46. Okazaki T, Tanaka Y, Nishio R, Mitsuiye T, Mizoguchi A, Wang J, Ishida M, Hiai H, Matsumori A, Minato N, Honjo T (2003) Autoantibodies against cardiac troponin I are responsible for dilated cardiomyopathy in PD-1-deficient mice. Nature medicine 9(12), 1477–1483. 10.1038/nm955.

47. Portig I, Pankuweit S, Maisch B (1997) Antibodies against stress proteins in sera of patients with dilated cardiomyopathy. Journal of molecular and cellular cardiology 29(8), 2245–2251. 10.1006/jmcc.1997.0463.

48. Felix SB, Staudt A, Dörffel WV, Stangl V, Merkel K, Pohl M, Döcke WD, Morgera S, Neumayer HH, Wernecke KD, Wallukat G, Stangl K, Baumann G (2000) Hemodynamic effects of immunoadsorption and subsequent immunoglobulin substitution in dilated cardiomyopathy: three-month results from a randomized study. Journal of the American College of Cardiology 35(6), 1590–1598.

49. Felix SB, Staudt A, Landsberger M, Grosse Y, Stangl V, Spielhagen T, Wallukat G, Wernecke KD, Baumann G, Stangl K (2002) Removal of cardiodepressant antibodies in dilated cardiomyopathy by immunoadsorption. Journal of the American College of Cardiology 39(4), 646–652.

50. Bulut D, Scheeler M, Niedballa LM, Miebach T, Mügge A (2011) Effects of immunoadsorption on endothelial function, circulating endothelial progenitor cells and circulating microparticles in patients with inflammatory dilated cardiomyopathy. Clinical research in cardiology official journal of the German Cardiac Society 100(7), 603–610. 10.1007/s00392-011-0287-2.

51. Staudt A, Schäper F, Stangl V, Plagemann A, Böhm M, Merkel K, Wallukat G, Wernecke KD, Stangl K, Baumann G, Felix SB (2001) Immunohistological changes in dilated cardiomyopathy induced by immunoadsorption therapy and subsequent immunoglobulin substitution. Circulation 103(22), 2681–2686.

52. Koll R, Müller-Derlich J, Felix S, Reinke P, Brehme S, Baumann G, Spaethe R (2006) treatment of cardiomyopathy by removal of autoantibodies: Google Patents. https://www.google.com.ar/patents/US7022322.

53. Wallukat G, Reinke P, Dörffel WV, Luther HP, Bestvater K, Felix SB, Baumann G (1996) Removal of autoantibodies in dilated cardiomyopathy by immunoadsorption. International journal of cardiology 54(2), 191–195.

54. Schimke I, Müller J, Priem F, Kruse I, Schön B, Stein J, Kunze R, Wallukat G, Hetzer R (2001) Decreased oxidative stress in patients with idiopathic dilated cardiomyopathy one year after immunoglobulin adsorption. Journal of the American College of Cardiology 38(1), 178–183.

55. Staudt A, Staudt Y, Hummel A, Empen K, Dörr M, Trimpert C, Birkenmeier K, Kühl U, Noutsias M, Russ D, Felix SB (2006) Effects of immunoadsorption on the nt-BNP and nt-ANP plasma levels of patients suffering from dilated cardiomyopathy. Therapeutic apheresis and dialysis official peer-reviewed journal of the International Society for Apheresis, the Japanese Society for Apheresis, the Japanese Society for Dialysis Therapy 10(1), 42–48. 10.1111/j.1744-9987.2006.00343.x.

56. Bulut D, Scheeler M, Wichmann T, Börgel J, Miebach T, Mügge A (2010) Effect of protein A immunoadsorption on T cell activation in patients with inflammatory dilated cardiomyopathy. Clinical research in cardiology official journal of the German Cardiac Society 99(10), 633–638. 10.1007/s00392-010-0162-6.

57. Kallwellis-Opara A, Staudt A, Trimpert C, Noutsias M, Kühl U, Pauschinger M, Schultheiss H, Grube M, Böhm M, Baumann G, Völker U, Kroemer HK, Felix SB (2007) Immunoadsorption and subsequent immunoglobulin substitution decreases myocardial gene expression of desmin in dilated cardiomyopathy. Journal of molecular medicine (Berlin, Germany) 85(12), 1429–1435. 10.1007/s00109-007-0263-5.

58. Knebel F, Böhm M, Staudt A, Borges AC, Tepper M, Jochmann N, Wernicke KD, Felix S, Baumann G (2004) Reduction of morbidity by immunoadsorption therapy in patients with dilated cardiomyopathy. International journal of cardiology 97(3), 517–520. 10.1016/j.ijcard.2003.12.003.

59. Staudt A, Herda LR, Trimpert C, Lubenow L, Landsberger M, Dörr M, Hummel A, Eckerle LG, Beug D, Müller C, Hoffmann W, Weitmann K, Klingel K, Kandolf R, Kroemer HK, Greinacher A, Felix SB (2010) Fcgamma-receptor IIa polymorphism and the role of immunoadsorption in cardiac dysfunction in patients with dilated cardiomyopathy. Clinical pharmacology and therapeutics 87(4), 452–458. 10.1038/clpt.2009.246.

60. Hessel FP, Wegner C, Müller J, Glaveris C, Wasem J (2004) Economic evaluation and survival analysis of immunoglobulin adsorption in patients with idiopathic dilated cardiomyopathy. The European journal of health economics HEPAC health economics in prevention and care 5(1), 58–63. 10.1007/s10198-003-0202-5.

61. Trimpert C, Herda LR, Eckerle LG, Pohle S, Müller C, Landsberger M, Felix SB, Staudt A (2010) Immunoadsorption in dilated cardiomyopathy: long-term reduction of cardiodepressant antibodies. European journal of clinical investigation 40(8), 685–691. 10.1111/j.1365-2362.2010.02314.x.

62. Ameling S, Herda LR, Hammer E, Steil L, Teumer A, Trimpert C, Dörr M, Kroemer HK, Klingel K, Kandolf R, Völker U, Felix SB (2013) Myocardial gene expression profiles and cardiodepressant autoantibodies predict response of patients with dilated cardiomyopathy to immunoadsorption therapy. European heart journal 34(9), 666–675. 10.1093/eurheartj/ehs330.

63. James P (1997) Protein identification in the post-genome era: the rapid rise of proteomics. Quarterly reviews of biophysics 30(4), 279–331.

64. O'Farrell PH (1975) High resolution two-dimensional electrophoresis of proteins. The Journal of biological chemistry 250(10), 4007–4021.

65. Lilley KS, Friedman DB (2004) All about DIGE: quantification technology for differential-display 2D-gel proteomics. Expert review of proteomics 1(4), 401–409. 10.1586/14789450.1.4.401.

66. Hammer E, Phong TQ, Steil L, Klingel K, Salazar MG, Bernhardt J, Kandolf R, Kroemer HK, Felix SB, Völker U (2010) Viral myocarditis induced by Coxsackievirus B3 in A.BY/SnJ mice: analysis of changes in the myocardial proteome. Proteomics 10(9), 1802–1818. 10.1002/pmic.200900734.

67. Patel VB, Corbett JM, Dunn MJ, Winrow VR, Portmann B, Richardson PJ, Preedy VR (1997) Protein profiling in cardiac tissue in response to the chronic effects of alcohol. Electrophoresis 18(15), 2788–2794. 10.1002/elps.1150181513.

68. Wei Y, Huang Y, Shen Y, Cui C, Zhang X, Zhang H, Hu S (2009) Proteomic analysis reveals significant elevation of heat shock protein 70 in patients with chronic heart failure due to arrhythmogenic right ventricular cardiomyopathy. Molecular and cellular biochemistry 332(1-2), 103–111. 10.1007/s11010-009-0179-1.

69. McGregor E, Dunn MJ (2006) Proteomics of the heart: unraveling disease. Circulation research 98(3), 309–321. 10.1161/01.RES.0000201280.20709.26.

70. Evans G, Wheeler CH, Corbett JM, Dunn MJ (1997) Construction of HSC-2DPAGE: a two-dimensional gel electrophoresis database of heart proteins. Electrophoresis 18(3-4), 471–479. 10.1002/elps.1150180322.

71. Müller EC, Thiede B, Zimny-Arndt U, Scheler C, Prehm J, Müller-Werdan U, Wittmann-Liebold B, Otto A, Jungblut P (1996) High-performance human myocardial two-dimensional electrophoresis database: edition 1996. Electrophoresis 17(11), 1700–1712. 10.1002/elps.1150171107.

72. Pleissner KP, Sander S, Oswald H, Regitz-Zagrosek V, Fleck E (1996) The construction of the World Wide Web-accessible myocardial two-dimensional gel electrophoresis protein database "HEART-2DPAGE": a practical approach. Electrophoresis 17(8), 1386–1392. 10.1002/elps.1150170818.

73. Li XP, Pleissner KP, Scheler C, Regitz-Zagrosek V, Salnikow J, Jungblut PR (1999) A two-dimensional electrophoresis database of rat heart proteins. Electrophoresis 20(4-5), 891–897. 10.1002/(SICI)1522-2683(19990101)20:4/5<891:AID-ELPS891>3.0.CO;2-2.

74. Arrell DK, Neverova I, Fraser H, Marbán E, van Eyk, J. E. (2001) Proteomic analysis of pharmacologically preconditioned cardiomyocytes reveals novel phosphorylation of myosin light chain 1. Circulation research 89(6), 480–487.

75. Yuan C, Guo Y, Ravi R, Przyklenk K, Shilkofski N, Diez R, Cole RN, Murphy AM (2006) Myosin binding protein C is differentially phosphorylated upon myocardial stunning in canine and rat hearts- evidence for novel phosphorylation sites. Proteomics 6(14), 4176–4186. 10.1002/pmic.200500894.

76. Opiteck GJ, Jorgenson JW (1997) Two-dimensional SEC/RPLC coupled to mass spectrometry for the analysis of peptides. Analytical chemistry 69(13), 2283–2291.

77. Yates JR (2004) Mass spectral analysis in proteomics. Annual review of biophysics and biomolecular structure 33, 297–316. 10.1146/annurev.biophys.33.111502.082538.

78. Gregorich ZR, Chang Y, Ge Y (2014) Proteomics in heart failure: top-down or bottom-up? Pflügers Archiv European journal of physiology 466(6), 1199–1209. 10.1007/s00424-014-1471-9.

79. McDonald WH, Yates JR (2003) Shotgun proteomics: integrating technologies to answer biological questions. Current opinion in molecular therapeutics 5(3), 302–309.

80. Ong S, Mann M (2006) A practical recipe for stable isotope labeling by amino acids in cell culture (SILAC). Nature protocols 1(6), 2650–2660. 10.1038/nprot.2006.427.

81. Gygi SP, Rist B, Gerber SA, Turecek F, Gelb MH, Aebersold R (1999) Quantitative analysis of complex protein mixtures using isotope-coded affinity tags. Nature biotechnology 17(10), 994–999. 10.1038/13690.

82. Yao X, Freas A, Ramirez J, Demirev PA, Fenselau C (2001) Proteolytic 18O labeling for comparative proteomics: model studies with two serotypes of adenovirus. Analytical chemistry 73(13), 2836–2842.

83. Lottspeich F, Kellermann J (2011) ICPL labeling strategies for proteome research. Methods in molecular biology (Clifton, N.J.) 753, 55–64. 10.1007/978-1-61779-148-2\textunderscore.

84. Evans C, Noirel J, Ow SY, Salim M, Pereira-Medrano AG, Couto N, Pandhal J, Smith D, Pham TK, Karunakaran E, Zou X, Biggs CA, Wright PC (2012) An insight into iTRAQ: where do we stand now? Analytical and bioanalytical chemistry 404(4), 1011–1027. 10.1007/s00216-012-5918-6.

85. Thompson A, Schäfer J, Kuhn K, Kienle S, Schwarz J, Schmidt G, Neumann T, Johnstone R, Mohammed, A. Karim A., Hamon C (2003) Tandem mass tags: a novel quantification strategy for comparative analysis of complex protein mixtures by MS/MS. Analytical chemistry 75(8), 1895–1904.

86. Abdallah C, Dumas-Gaudot E, Renaut J, Sergeant K (2012) Gel-based and gel-free quantitative proteomics approaches at a glance. International journal of plant genomics 2012, 494572. 10.1155/2012/494572.

87. Hollander Z, Lazárová M, Lam, Karen K. Y., Ignaszewski A, Oudit GY, Dyck, Jason R. B., Schreiner G, Pauwels J, Chen V, Cohen Freue, Gabriela V., Ng RT, Wilson-McManus JE, Balshaw R, Tebbutt SJ, McMaster RW, Keown PA, McManus BM (2014) Proteomic biomarkers of recovered heart function. European journal of heart failure 16(5), 551–559. 10.1002/ejhf.65.

88. Li X, Ren Y, Sorokin V, Poh KK, Ho HH, Lee CN, Kleijn Dd, Lim SK, Tam JP, Sze SK (2014) Quantitative profiling of the rat heart myoblast secretome reveals differential responses to hypoxia and re-oxygenation stress. Journal of proteomics 98, 138–149. 10.1016/j.jprot.2013.12.025.

89. Tan HT, Ling LH, Dolor-Torres MC, Yip JW, Richards AM, Chung, Maxey C. M. (2013) Proteomics discovery of biomarkers for mitral regurgitation caused by mitral valve prolapse. Journal of proteomics 94, 337–345. 10.1016/j.jprot.2013.10.009.

90. Yan L, Wang D, Liu H, Zhang X, Zhao H, Hua L, Xu P, Li Y (2014) A pro-atherogenic HDL profile in coronary heart disease patients: an iTRAQ labelling-based proteomic approach. PloS one 9(5), e98368. 10.1371/journal.pone.0098368.

91. Jüllig M, Hickey AJ, Middleditch MJ, Crossman DJ, Lee SC, Cooper, Garth J. S. (2007) Characterization of proteomic changes in cardiac mitochondria in streptozotocin-diabetic rats using iTRAQ™ isobaric tags. Proteomics. Clinical applications 1(6), 565–576. 10.1002/prca.200600831.

92. Anderson NL, Anderson NG (2002) The human plasma proteome: history, character, and diagnostic prospects. Molecular & cellular proteomics MCP 1(11), 845–867.

93. Bantscheff M, Schirle M, Sweetman G, Rick J, Kuster B (2007) Quantitative mass spectrometry in proteomics: a critical review. Analytical and bioanalytical chemistry 389(4), 1017–1031. 10.1007/s00216-007-1486-6.

94. Hammer E, Goritzka M, Ameling S, Darm K, Steil L, Klingel K, Trimpert C, Herda LR, Dörr M, Kroemer HK, Kandolf R, Staudt A, Felix SB, Völker U (2011) Characterization of the human myocardial proteome in inflammatory dilated cardiomyopathy by label-free quantitative shotgun proteomics of heart biopsies. Journal of proteome research 10(5), 2161–2171. 10.1021/pr1008042.

95. Iliuk AB, Martin VA, Alicie BM, Geahlen RL, Tao WA (2010) In-depth analyses of kinase-dependent tyrosine phosphoproteomes based on metal ion-functionalized soluble nanopolymers. Molecular & cellular proteomics MCP 9(10), 2162–2172. 10.1074/mcp.M110.000091.

96. Reinartz M, Raupach A, Kaisers W, Gödecke A (2014) AKT1 and AKT2 induce distinct phosphorylation patterns in HL-1 cardiac myocytes. Journal of proteome research 13(10), 4232–4245. 10.1021/pr500131g.

97. Haas S, Jahnke H, Moerbt N, Bergen Mv, Aharinejad S, Andrukhova O, Robitzki AA (2012) DIGE proteome analysis reveals suitability of ischemic cardiac in vitro model for studying cellular response to acute ischemia and regeneration. PloS one 7(2), e31669. 10.1371/journal.pone.0031669.

98. White SM, Constantin PE, Claycomb WC (2004) Cardiac physiology at the cellular level: use of cultured HL-1 cardiomyocytes for studies of cardiac muscle cell structure and function. American journal of physiology. Heart and circulatory physiology 286(3), H823-9. 10.1152/ajpheart.00986.2003.

99. Kitteringham NR, Jenkins RE, Lane CS, Elliott VL, Park BK (2009) Multiple reaction monitoring for quantitative biomarker analysis in proteomics and metabolomics. Journal of chromatography. B, Analytical technologies in the biomedical and life sciences 877(13), 1229–1239. 10.1016/j.jchromb.2008.11.013.

100. Picotti P, Aebersold R (2012) Selected reaction monitoring-based proteomics: workflows, potential, pitfalls and future directions. Nature methods 9(6), 555–566. 10.1038/nmeth.2015.

101. Aebersold R, Burlingame AL, Bradshaw RA (2013) Western blots versus selected reaction monitoring assays: time to turn the tables? Molecular & cellular proteomics MCP 12(9), 2381–2382. 10.1074/mcp.E113.031658.

102. Cohen Freue, Gabriela V., Borchers CH (2012) Multiple reaction monitoring (MRM): principles and application to coronary artery disease. Circulation. Cardiovascular genetics 5(3), 378. 10.1161/CIRCGENETICS.111.959528.

103. Lam, Maggie P. Y., Scruggs SB, Kim T, Zong C, Lau E, Wang D, Ryan CM, Faull KF, Ping P (2012) An MRM-based workflow for quantifying cardiac mitochondrial protein phosphorylation in murine and human tissue. Journal of proteomics 75(15), 4602–4609. 10.1016/j.jprot.2012.02.014.

104. Mahrholdt H, Wagner A, Deluigi CC, Kispert E, Hager S, Meinhardt G, Vogelsberg H, Fritz P, Dippon J, Bock C, Klingel K, Kandolf R, Sechtem U (2006) Presentation, patterns of myocardial damage, and clinical course of viral myocarditis. Circulation 114(15), 1581–1590. 10.1161/CIRCULATIONAHA.105.606509.

105. Kindermann I, Kindermann M, Kandolf R, Klingel K, Bültmann B, Müller T, Lindinger A, Böhm M (2008) Predictors of outcome in patients with suspected myocarditis. Circulation 118(6), 639–648. 10.1161/CIRCULATIONAHA.108.769489.

106. Kapelko VI (2001) Extracellular matrix alterations in cardiomyopathy: The possible crucial role in the dilative form. Experimental and clinical cardiology 6(1), 41–49.

107. Proteomic analysis of human biopsy samples by single two-dimensional electrophoresis: Coomassie, silver, mass spectrometry, and Western blotting.

108. McGregor E, Dunn MJ (2006) Proteomics of the heart: unraveling disease. Circulation research 98(3), 309–321. 10.1161/01.RES.0000201280.20709.26.

109. Knecht M, Regitz-Zagrosek V, Pleissner KP, Jungblut P, Steffen C, Hildebrandt A, Fleck E (1994) Characterization of myocardial protein composition in dilated cardiomyopathy by two-dimensional gel electrophoresis. European heart journal 15 Suppl D, 37–44.

110. Roselló-Lletí E, Alonso J, Cortés R, Almenar L, Martínez-Dolz L, Sánchez-Lázaro I, Lago F, Azorín I, Juanatey, Jose R González, Portolés M, Rivera M (2012) Cardiac protein changes in ischaemic and dilated cardiomyopathy: a proteomic study of human left ventricular tissue. Journal of cellular and molecular medicine 16(10), 2471–2486. 10.1111/j.1582-4934.2012.01565.x.

111. Gygi SP, Corthals GL, Zhang Y, Rochon Y, Aebersold R (2000) Evaluation of two-dimensional gel electrophoresis-based proteome analysis technology. Proceedings of the National Academy of Sciences of the United States of America 97(17), 9390–9395. 10.1073/pnas.160270797.

112. Garbis S, Lubec G, Fountoulakis M (2005) Limitations of current proteomics technologies. Journal of Chromatography A 1077(1), 1–18. 10.1016/j.chroma.2005.04.059.

113. Sharma P, Cosme J, Gramolini AO (2013) Recent advances in cardiovascular proteomics. Journal of proteomics 81, 3–14. 10.1016/j.jprot.2012.10.026.

114. Zhu W, Smith JW, Huang C (2010) Mass spectrometry-based label-free quantitative proteomics. Journal of biomedicine & biotechnology 2010, 840518. 10.1155/2010/840518.

115. Dávila-Román VG, Vedala G, Herrero P, de las Fuentes, Lisa, Rogers JG, Kelly DP, Gropler RJ (2002) Altered myocardial fatty acid and glucose metabolism in idiopathic dilated cardiomyopathy. Journal of the American College of Cardiology 40(2), 271–277. 10.1016/S0735-1097(02)01967-8.

116. Ventura-Clapier R, Garnier A, Veksler V (2004) Energy metabolism in heart failure. The Journal of physiology 555(Pt 1), 1–13. 10.1113/jphysiol.2003.055095.

117. Auffermann W, Wu ST, Parmley WW, Wikman-Coffelt J (1990) Glycolysis in heart failure: a 31P-NMR and surface fluorometry study. Basic research in cardiology 85(4), 342–357.

118. Jahns R, Boivin V, Schwarzbach V, Ertl G, Lohse MJ (2008) Pathological autoantibodies in cardiomyopathy. Autoimmunity 41(6), 454–461. 10.1080/08916930802031603.

119. Trimpert C, Herda LR, Eckerle LG, Pohle S, Müller C, Landsberger M, Felix SB, Staudt A (2010) Immunoadsorption in dilated cardiomyopathy: long-term reduction of cardiodepressant antibodies. European journal of clinical investigation 40(8), 685–691. 10.1111/j.1365-2362.2010.02314.x.

120. Schulze K, Becker BF, Schauer R, Schultheiss HP (1990) Antibodies to ADP-ATP carrier--an autoantigen in myocarditis and dilated cardiomyopathy--impair cardiac function. Circulation 81(3), 959–969.

121. Chen W, Chang B, Wu X, Li L, Sleeman M, Chan L (2013) Inactivation of Plin4 downregulates Plin5 and reduces cardiac lipid accumulation in mice. American journal of physiology. Endocrinology and metabolism 304(7), E770-9. 10.1152/ajpendo.00523.2012.

122. Kienesberger PC, Pulinilkunnil T, Nagendran J, Dyck, Jason R B (2013) Myocardial triacylglycerol metabolism. Journal of molecular and cellular cardiology 55, 101–110. 10.1016/j.yjmcc.2012.06.018.

123. Crabos M, Yamakado T, Heizmann CW, Cerletti N, Bühler FR, Erne P (1991) The calcium binding protein tropomyosin in human platelets and cardiac tissue: elevation in hypertensive cardiac hypertrophy. European journal of clinical investigation 21(5), 472–478.

124. Tardiff JC (2010) Tropomyosin and dilated cardiomyopathy: revenge of the actinomyosin "gatekeeper". Journal of the American College of Cardiology 55(4), 330–332. 10.1016/j.jacc.2009.11.018.

125. Moriyama K, Nishida E, Yonezawa N, Sakai H, Matsumoto S, Iida K, Yahara I (1990) Destrin, a mammalian actin-depolymerizing protein, is closely related to cofilin. Cloning and expression of porcine brain destrin cDNA. The Journal of biological chemistry 265(10), 5768–5773.

126. Sahoo SK, Kim T, Kang GB, Lee J, Eom SH, Kim DH (2009) Characterization of calumenin-SERCA2 interaction in mouse cardiac sarcoplasmic reticulum. The Journal of biological chemistry 284(45), 31109–31121. 10.1074/jbc.M109.031989.

127. Campbell DJ (2001) The kallikrein-kinin system in humans. Clinical and experimental pharmacology & physiology 28(12), 1060–1065.

128. Averill MM, Kerkhoff C, Bornfeldt KE (2012) S100A8 and S100A9 in cardiovascular biology and disease. Arteriosclerosis, thrombosis, and vascular biology 32(2), 223–229. 10.1161/ATVBAHA.111.236927.

129. Katashima T, Naruko T, Terasaki F, Fujita M, Otsuka K, Murakami S, Sato A, Hiroe M, Ikura Y, Ueda M, Ikemoto M, Kitaura Y (2010) Enhanced Expression of the S100A8/A9 Complex in Acute Myocardial Infarction Patients. Circ J 74(4), 741–748. 10.1253/circj.CJ-09-0564.

130. Kim H, Kang HJ, Lee H, Lee S, Yu M, Kim H, Lee C (2009) Identification of S100A8 and S100A9 as serological markers for colorectal cancer. Journal of proteome research 8(3), 1368–1379. 10.1021/pr8007573.

131. Raphael R, Purushotham D, Gastonguay C, Chesnik MA, Kwok W, Wu H, Shah SJ, Mirza SP, Strande JL (2016) Combining patient proteomics and in vitro cardiomyocyte phenotype testing to identify potential mediators of heart failure with preserved ejection fraction. Journal of translational medicine 14(1), 18. 10.1186/s12967-016-0774-3.

132. Aebersold R, Burlingame AL, Bradshaw RA (2013) Western blots versus selected reaction monitoring assays: time to turn the tables? Molecular & cellular proteomics MCP 12(9), 2381–2382. 10.1074/mcp.E113.031658.

133. Bluemlein K, Ralser M (2011) Monitoring protein expression in whole-cell extracts by targeted label- and standard-free LC-MS/MS. Nature protocols 6(6), 859–869. 10.1038/nprot.2011.333.

134. Panagopoulou V, Deftereos S, Kossyvakis C, Raisakis K, Giannopoulos G, Bouras G, Pyrgakis V, Cleman MW (2013) NTproBNP: an important biomarker in cardiac diseases. Current topics in medicinal chemistry 13(2), 82–94.

135. Yu C, Fung JW, Zhang Q, Chan C, Chan I, Chan Y, Kong S, Sanderson JE, Lam CW (2005) Improvement of serum NT-ProBNP predicts improvement in cardiac function and favorable prognosis after cardiac resynchronization therapy for heart failure. Journal of cardiac failure 11(5 Suppl), S42-6.

136. Nishikimi T, Maeda N, Matsuoka H (2006) The role of natriuretic peptides in cardioprotection. Cardiovascular research 69(2), 318–328. 10.1016/j.cardiores.2005.10.001.

137. Ogawa Y, Tamura N, Chusho H, Nakao K (2001) Brain natriuretic peptide appears to act locally as an antifibrotic factor in the heart. Canadian journal of physiology and pharmacology 79(8), 723–729.

138. Abraham WT, Hayes DL (2003) Cardiac resynchronization therapy for heart failure. Circulation 108(21), 2596–2603. 10.1161/01.CIR.0000096580.26969.9A.

139. Barth AS, Chakir K, Kass DA, Tomaselli GF (2012) Transcriptome, proteome, and metabolome in dyssynchronous heart failure and CRT. Journal of cardiovascular translational research 5(2), 180–187. 10.1007/s12265-011-9339-2.

140. de Weger, Roel A, Schipper, Marguerite E I, Siera-de Koning E, van der Weide, Petra, van Oosterhout, Matthijs F M, Quadir R, Steenbergen-Nakken H, Lahpor JR, Jonge N de, Bovenschen N (2011) Proteomic profiling of the human failing heart after left ventricular assist device support. The Journal of heart and lung transplantation the official publication of the International Society for Heart Transplantation 30(5), 497–506. 10.1016/j.healun.2010.11.011.

141. Soppa, Gopal K R, Barton, Paul J R, Terracciano, Cesare M N, Yacoub MH (2008) Left ventricular assist device-induced molecular changes in the failing myocardium. Current opinion in cardiology 23(3), 206–218. 10.1097/HCO.0b013e3282fc7010.

142. Bruggink AH, van Oosterhout, Matthijs F M, Jonge N de, Ivangh B, van Kuik J, Voorbij, Ron H A M, Cleutjens, Jack P M, Gmelig-Meyling, Frits H J, de Weger, Roel A (2006) Reverse remodeling of the myocardial extracellular matrix after prolonged left ventricular assist device support follows a biphasic pattern. The Journal of heart and lung transplantation the official publication of the International Society for Heart Transplantation 25(9), 1091–1098. 10.1016/j.healun.2006.05.011.

143. Neubauer S, Redwood C (2014) New mechanisms and concepts for cardiac-resynchronization therapy. The New England journal of medicine 370(12), 1164–1166. 10.1056/NEJMcibr1315508.

144. Kostin S, Hein S, Arnon E, Scholz D, Schaper J (2000) The cytoskeleton and related proteins in the human failing heart. Heart failure reviews 5(3), 271–280. 10.1023/A:1009813621103.

145. Hannigan GE, Coles JG, Dedhar S (2007) Integrin-linked kinase at the heart of cardiac contractility, repair, and disease. Circulation research 100(10), 1408–1414. 10.1161/01.RES.0000265233.40455.62.

146. Traister A, Li M, Aafaqi S, Lu M, Arab S, Radisic M, Gross G, Guido F, Sherret J, Verma S, Slorach C, Mertens L, Hui W, Roy A, Delgado-Olguín P, Hannigan G, Maynes JT, Coles JG (2014) Integrin-linked kinase mediates force transduction in cardiomyocytes by modulating SERCA2a/PLN function. Nature communications 5, 4533. 10.1038/ncomms5533.

147. Dedhar S (2000) Cell-substrate interactions and signaling through ILK. Current opinion in cell biology 12(2), 250–256.

148. Heling A, Zimmermann R, Kostin S, Maeno Y, Hein S, Devaux B, Bauer E, Klövekorn WP, Schlepper M, Schaper W, Schaper J (2000) Increased expression of cytoskeletal, linkage, and extracellular proteins in failing human myocardium. Circulation research 86(8), 846–853.

149. Marijianowski MM, Teeling P, Mann J, Becker AE (1995) Dilated cardiomyopathy is associated with an increase in the type I/type III collagen ratio: a quantitative assessment. Journal of the American College of Cardiology 25(6), 1263–1272. 10.1016/0735-1097(94)00557-7.

150. López B, González A, Querejeta R, Larman M, Díez J (2006) Alterations in the pattern of collagen deposition may contribute to the deterioration of systolic function in hypertensive patients with heart failure. Journal of the American College of Cardiology 48(1), 89–96. 10.1016/j.jacc.2006.01.077.

151. Martos R, Baugh J, Ledwidge M, O'Loughlin C, Conlon C, Patle A, Donnelly SC, McDonald K (2007) Diastolic heart failure: evidence of increased myocardial collagen turnover linked to diastolic dysfunction. Circulation 115(7), 888–895. 10.1161/CIRCULATIONAHA.106.638569.

152. Namba T, Tsutsui H, Tagawa H, Takahashi M, Saito K, Kozai T, Usui M, Imanaka-Yoshida K, Imaizumi T, Takeshita A (1997) Regulation of fibrillar collagen gene expression and protein accumulation in volume-overloaded cardiac hypertrophy. Circulation 95(10), 2448–2454.

153. Felkin LE, Lara-Pezzi E, George R, Yacoub MH, Birks EJ, Barton, Paul J R (2009) Expression of extracellular matrix genes during myocardial recovery from heart failure after left ventricular assist device support. The Journal of heart and lung transplantation the official publication of the International Society for Heart Transplantation 28(2), 117–122. 10.1016/j.healun.2008.11.910.

154. Engebretsen, Kristin V T, Lunde IG, Strand ME, Waehre A, Sjaastad I, Marstein HS, Skrbic B, Dahl CP, Askevold ET, Christensen G, Bjørnstad JL, Tønnessen T (2013) Lumican is increased in experimental and clinical heart failure, and its production by cardiac fibroblasts is induced by mechanical and proinflammatory stimuli. The FEBS journal 280(10), 2382–2398. 10.1111/febs.12235.

155. Bereczki E, Sántha M (2008) The role of biglycan in the heart. Connective tissue research 49(3), 129–132. 10.1080/03008200802148504.

156. Ahmed MS, Øie E, Vinge LE, Yndestad A, Andersen G, Geir Øystein, Andersson Y, Attramadal T, Attramadal H (2003) Induction of myocardial biglycan in heart failure in rats--an extracellular matrix component targeted by AT(1) receptor antagonism. Cardiovascular research 60(3), 557–568.

157. Zhao S, Wu H, Xia W, Chen X, Zhu S, Zhang S, Shao Y, Ma W, Di Yang, Zhang J (2014) Periostin expression is upregulated and associated with myocardial fibrosis in human failing hearts. Journal of cardiology 63(5), 373–378. 10.1016/j.jjcc.2013.09.013.

158. Lim H, Zhu YZ (2006) Role of transforming growth factor-beta in the progression of heart failure. Cellular and molecular life sciences CMLS 63(22), 2584–2596. 10.1007/s00018-006-6085-8.

159. Koshman YE, Patel N, Chu M, Iyengar R, Kim T, Ersahin C, Lewis W, Heroux A, Samarel AM (2013) Regulation of connective tissue growth factor gene expression and fibrosis in human heart failure. Journal of cardiac failure 19(4), 283–294. 10.1016/j.cardfail.2013.01.013.

160. Luque-Garcia JL, Neubert TA (2007) Sample preparation for serum/plasma profiling and biomarker identification by mass spectrometry. Journal of chromatography. A 1153(1-2), 259–276. 10.1016/j.chroma.2006.11.054.

161. Zolotarjova N, Mrozinski P, Chen H, Martosella J (2008) Combination of affinity depletion of abundant proteins and reversed-phase fractionation in proteomic analysis of human plasma/serum. Journal of chromatography. A 1189(1-2), 332–338. 10.1016/j.chroma.2007.11.082.

162. Wiese S, Reidegeld KA, Meyer HE, Warscheid B (2007) Protein labeling by iTRAQ: a new tool for quantitative mass spectrometry in proteome research. Proteomics 7(3), 340–350. 10.1002/pmic.200600422.

163. Farrah T, Deutsch EW, Omenn GS, Campbell DS, Sun Z, Bletz JA, Mallick P, Katz JE, Malmström J, Ossola R, Watts JD, Lin B, Zhang H, Moritz RL, Aebersold R (2011) A high-confidence human plasma proteome reference set with estimated concentrations in PeptideAtlas. Molecular & cellular proteomics MCP 10(9), M110.006353. 10.1074/mcp.M110.006353.

164. Laffitte BA, Chao LC, Li J, Walczak R, Hummasti S, Joseph SB, Castrillo A, Wilpitz DC, Mangelsdorf DJ, Collins JL, Saez E, Tontonoz P (2003) Activation of liver X receptor improves glucose tolerance through coordinate regulation of glucose metabolism in liver and adipose tissue. Proceedings of the National Academy of Sciences of the United States of America 100(9), 5419–5424. 10.1073/pnas.0830671100.

165. Bensinger SJ, Tontonoz P (2008) Integration of metabolism and inflammation by lipid-activated nuclear receptors. Nature 454(7203), 470–477. 10.1038/nature07202.

166. Kuipers I, Li J, Vreeswijk-Baudoin I, Koster J, van der Harst, Pim, Silljé, Herman H W, Kuipers F, van Veldhuisen, Dirk J, van Gilst, Wiek H, de Boer, Rudolf A (2010) Activation of liver X receptors with T0901317 attenuates cardiac hypertrophy in vivo. European journal of heart failure 12(10), 1042–1050. 10.1093/eurjhf/hfq109.

167. Antoniak S, Mackman N (2014) Multiple roles of the coagulation protease cascade during virus infection. Blood 123(17), 2605–2613. 10.1182/blood-2013-09-526277.

168. Palta S, Saroa R, Palta A (2014) Overview of the coagulation system. Indian journal of anaesthesia 58(5), 515–523. 10.4103/0019-5049.144643.

169. Yamamoto K, Ikeda U, Furuhashi K, Irokawa M, Nakayama T, Shimada K (1995) The coagulation system is activated in idiopathic cardiomyopathy. Journal of the American College of Cardiology 25(7), 1634–1640.

170. Alehagen U, Dahlström U, Lindahl TL (2010) Low plasma concentrations of coagulation factors II, VII and XI indicate increased risk among elderly with symptoms of heart failure. Blood coagulation & fibrinolysis an international journal in haemostasis and thrombosis 21(1), 62–69. 10.1097/MBC.0b013e328332aa2b.

171. Kaplon RJ, Gillinov AM, Smedira NG, Kottke-Marchant K, Wang IW, Goormastic M, McCarthy PM (1999) Vitamin K reduces bleeding in left ventricular assist device recipients. The Journal of heart and lung transplantation the official publication of the International Society for Heart Transplantation 18(4), 346–350.

172. Danesh J, Muir J, Wong YK, Ward M, Gallimore JR, Pepys MB (1999) Risk factors for coronary heart disease and acute-phase proteins. A population-based study. European heart journal 20(13), 954–959. 10.1053/euhj.1998.1309.

173. Anand IS, Latini R, Florea VG, Kuskowski MA, Rector T, Masson S, Signorini S, Mocarelli P, Hester A, Glazer R, Cohn JN (2005) C-reactive protein in heart failure: prognostic value and the effect of valsartan. Circulation 112(10), 1428–1434. 10.1161/CIRCULATIONAHA.104.508465.

174. Chitose Ishikawa, Takayoshi Tsutamoto, Masanori Fujii, Hiroshi Sakai, Toshinari Tanaka, Minoru Horie, Prediction of Mortality by High-Sensitivity C-Reactive Protein and Brain Natriuretic Peptide in Patients With Dilated Cardiomyopathy, Circ J. 2006 Jul;70(7):857-63.

175. Kaneko K, Kanda T, Yamauchi Y, Hasegawa A, Iwasaki T, Arai M, Suzuki T, Kobayashi I, Nagai R (1999) C-Reactive protein in dilated cardiomyopathy. Cardiology 91(4), 215–219.

176. Fairweather D, D. E, J. M (2011) Biomarkers of Heart Failure in Myocarditis and Dilated Cardiomyopathy, in: Cihakova D (ed.) Myocarditis: InTech.

177. Bharadwaj D, Stein MP, Volzer M, Mold C, Du Clos, T W (1999) The major receptor for C-reactive protein on leukocytes is fcgamma receptor II. The Journal of experimental medicine 190(4), 585–590.

178. Johnson BD, Kip KE, Marroquin OC, Ridker PM, Kelsey SF, Shaw LJ, Pepine CJ, Sharaf B, Bairey Merz, C Noel, Sopko G, Olson MB, Reis SE (2004) Serum amyloid A as a predictor of coronary artery disease and cardiovascular outcome in women: the National Heart, Lung, and Blood Institute-Sponsored Women's Ischemia Syndrome Evaluation (WISE). Circulation 109(6), 726–732. 10.1161/01.CIR.0000115516.54550.B1.

179. Malle E, Steinmetz A, Raynes JG (1993) Serum amyloid A (SAA): an acute phase protein and apolipoprotein. Atherosclerosis 102(2), 131–146. 10.1016/0021-9150(93)90155-N.

180. Turner M (2003) The role of mannose-binding lectin in health and disease. Molecular Immunology 40(7), 423–429. 10.1016/S0161-5890(03)00155-X.

181. Saevarsdottir S, Oskarsson OO, Aspelund T, Eiriksdottir G, Vikingsdottir T, Gudnason V, Valdimarsson H (2005) Mannan binding lectin as an adjunct to risk assessment for myocardial infarction in individuals with enhanced risk. The Journal of experimental medicine 201(1), 117–125. 10.1084/jem.20041431.

182. Niebauer J, Volk H, Kemp M, Dominguez M, Schumann RR, Rauchhaus M, Poole-Wilson PA, Coats AJS, Anker SD (1999) Endotoxin and immune activation in chronic heart failure: a prospective cohort study. The Lancet 353(9167), 1838–1842. 10.1016/S0140-6736(98)09286-1.

183. Charalambous BM, Stephens, Robert C M, Feavers IM, Montgomery HE (2007) Role of bacterial endotoxin in chronic heart failure: the gut of the matter. Shock (Augusta, Ga.) 28(1), 15–23. 10.1097/shk.0b013e318033ebc5.

184. Donato R, Cannon BR, Sorci G, Riuzzi F, Hsu K, Weber DJ, Geczy CL (2013) Functions of S100 proteins. Current molecular medicine 13(1), 24–57.

185. Boyd JH, Kan B, Roberts H, Wang Y, Walley KR (2008) S100A8 and S100A9 mediate endotoxin-induced cardiomyocyte dysfunction via the receptor for advanced glycation end products. Circulation research 102(10), 1239–1246. 10.1161/CIRCRESAHA.107.167544.

186. Healy AM, Pickard MD, Pradhan AD, Wang Y, Chen Z, Croce K, Sakuma M, Shi C, Zago AC, Garasic J, Damokosh AI, Dowie TL, Poisson L, Lillie J, Libby P, Ridker PM, Simon DI (2006) Platelet expression profiling and clinical validation of myeloid-related protein-14 as a novel determinant of cardiovascular events. Circulation 113(19), 2278–2284. 10.1161/CIRCULATIONAHA.105.607333.

187. Katashima T, Naruko T, Terasaki F, Fujita M, Otsuka K, Murakami S, Sato A, Hiroe M, Ikura Y, Ueda M, Ikemoto M, Kitaura Y (2010) Enhanced Expression of the S100A8/A9 Complex in Acute Myocardial Infarction Patients. Circ J 74(4), 741–748. 10.1253/circj.CJ-09-0564.

188. Ma L, Haugen E, Ikemoto M, Fujita M, Terasaki F, Fu M (2012) S100A8/A9 complex as a new biomarker in prediction of mortality in elderly patients with severe heart failure. International journal of cardiology 155(1), 26–32. 10.1016/j.ijcard.2011.01.082.

189. Raphael R, Purushotham D, Gastonguay C, Chesnik MA, Kwok W, Wu H, Shah SJ, Mirza SP, Strande JL (2016) Combining patient proteomics and in vitro cardiomyocyte phenotype testing to identify potential mediators of heart failure with preserved ejection fraction. Journal of translational medicine 14(1), 18. 10.1186/s12967-016-0774-3.

190. Tschoepe C, Müller I, Vogl T, Pieske B, van Linthout S (2016) ROLE OF S100A8 AND S100A9 ALARMINS IN COXSACKIEVIRUS B3-INDUCED MYOCARDITIS. Journal of the American College of Cardiology 67(13), 1398. 10.1016/S0735-1097(16)31399-7.

191. Rychli K, Huber K, Wojta J (2009) Pigment epithelium-derived factor (PEDF) as a therapeutic target in cardiovascular disease. Expert opinion on therapeutic targets 13(11), 1295–1302. 10.1517/14728220903241641.

192. Wang F, Ma X, Zhou M, Pan X, Ni J, Gao M, Lu Z, Hang J, Bao Y, Jia W (2013) Serum pigment epithelium-derived factor levels are independently correlated with the presence of coronary artery disease. Cardiovascular diabetology 12, 56. 10.1186/1475-2840-12-56.

193. Ueda S, Yamagishi S, Matsui T, Jinnouchi Y, Imaizumi T (2011) Administration of pigment epithelium-derived factor inhibits left ventricular remodeling and improves cardiac function in rats with acute myocardial infarction. The American journal of pathology 178(2), 591–598. 10.1016/j.ajpath.2010.10.018.

194. Rychli K, Niessner A, Hohensinner PJ, Mahdy Ali K, Kaun C, Neuhold S, Zorn G, Richter B, Hülsmann M, Berger R, Mörtl D, Huber K, Maurer G, Pacher R, Wojta J (2010) Prognostic value of pigment epithelium-derived factor in patients with advanced heart failure. Chest 138(3), 656–664. 10.1378/chest.09-2739.

195. Wang Y, Cao Y, Yamada S, Thirunavukkarasu M, Nin V, Joshi M, Rishi MT, Bhattacharya S, Camacho-Pereira J, Sharma AK, Shameer K, Kocher JA, Sanchez JA, Wang E, Hoeppner LH, Dutta SK, Leof EB, Shah V, Claffey KP, Chini EN, Simons M, Terzic A, Maulik N, Mukhopadhyay D (2015) Cardiomyopathy and Worsened Ischemic Heart Failure in SM22-α Cre-Mediated Neuropilin-1 Null Mice: Dysregulation of PGC1α and Mitochondrial Homeostasis. Arteriosclerosis, thrombosis, and vascular biology 35(6), 1401–1412. 10.1161/ATVBAHA.115.305566.

196. Allen LA, Felker GM (2010) Multi-marker strategies in heart failure: clinical and statistical approaches. Heart failure reviews 15(4), 343–349. 10.1007/s10741-009-9144-z.

197. Wang TJ, Gona P, Larson MG, Tofler GH, Levy D, Newton-Cheh C, Jacques PF, Rifai N, Selhub J, Robins SJ, Benjamin EJ, D'Agostino RB, Vasan RS (2006) Multiple biomarkers for the prediction of first major cardiovascular events and death. The New England journal of medicine 355(25), 2631–2639. 10.1056/NEJMoa055373.

198. Meredith AJ, Dai, Darlene L. Y., Chen V, Hollander Z, Ng R, Kaan A, Tebbutt S, Ramanathan K, Cheung A, McManus BM (2016) Circulating biomarker responses to medical management vs. mechanical circulatory support in severe inotrope-dependent acute heart failure. ESC Heart Failure 3(2), 86–96. 10.1002/ehf2.12076.

199. Iliuk AB, Martin VA, Alicie BM, Geahlen RL, Tao WA (2010) In-depth analyses of kinase-dependent tyrosine phosphoproteomes based on metal ion-functionalized soluble nanopolymers. Molecular & cellular proteomics MCP 9(10), 2162–2172. 10.1074/mcp.M110.000091.

200. Muschter S, Berthold T, Bhardwaj G, Hammer E, Dhople VM, Wesche J, Reil A, Bux J, Bakchoul T, Steil L, Greinacher A, Völker U (2015) Mass spectrometric phosphoproteome analysis of small-sized samples of human neutrophils. Clinica chimica acta; international journal of clinical chemistry 451(Pt B), 199–207. 10.1016/j.cca.2015.09.030.

201. Chang Y, Chang Y, Wang Q, Lin JJ, Chen Y, Chen C (2013) Quantitative phosphoproteomic study of pressure-overloaded mouse heart reveals dynamin-related protein 1 as a modulator of cardiac hypertrophy. Molecular & cellular proteomics MCP 12(11), 3094–3107. 10.1074/mcp.M113.027649.

202. Thingholm TE, Jensen ON, Larsen MR (2009) Analytical strategies for phosphoproteomics. Proteomics 9(6), 1451–1468. 10.1002/pmic.200800454.

203. Villén J, Beausoleil SA, Gerber SA, Gygi SP (2007) Large-scale phosphorylation analysis of mouse liver. Proceedings of the National Academy of Sciences of the United States of America 104(5), 1488–1493. 10.1073/pnas.0609836104.

204. Albuquerque CP, Smolka MB, Payne SH, Bafna V, Eng J, Zhou H (2008) A multidimensional chromatography technology for in-depth phosphoproteome analysis. Molecular & cellular proteomics MCP 7(7), 1389–1396. 10.1074/mcp.M700468-MCP200.

205. Mann M, Ong SE, Grønborg M, Steen H, Jensen ON, Pandey A (2002) Analysis of protein phosphorylation using mass spectrometry: deciphering the phosphoproteome. Trends in biotechnology 20(6), 261–268.

206. Resjö S, Ali A, Meijer, Harold J G, Seidl MF, Snel B, Sandin M, Levander F, Govers F, Andreasson E (2014) Quantitative label-free phosphoproteomics of six different life stages of the late blight pathogen Phytophthora infestans reveals abundant phosphorylation of members of the CRN effector family. Journal of proteome research 13(4), 1848–1859. 10.1021/pr4009095.

207. Manes NP, Dong L, Zhou W, Du X, Reghu N, Kool AC, Choi D, Bailey CL, Petricoin EF, Liotta LA, Popov SG (2011) Discovery of mouse spleen signaling responses to anthrax using label-free quantitative phosphoproteomics via mass spectrometry. Molecular & cellular proteomics MCP 10(3), M110.000927. 10.1074/mcp.M110.000927.

208. Dobaczewski M, Chen W, Frangogiannis NG (2011) Transforming growth factor (TGF)-β signaling in cardiac remodeling. Journal of molecular and cellular cardiology 51(4), 600–606. 10.1016/j.yjmcc.2010.10.033.

209. Heling A, Zimmermann R, Kostin S, Maeno Y, Hein S, Devaux B, Bauer E, Klövekorn WP, Schlepper M, Schaper W, Schaper J (2000) Increased expression of cytoskeletal, linkage, and extracellular proteins in failing human myocardium. Circulation research 86(8), 846–853.

210. Koitabashi N, Danner T, Zaiman AL, Pinto YM, Rowell J, Mankowski J, Zhang D, Nakamura T, Takimoto E, Kass DA (2011) Pivotal role of cardiomyocyte TGF-β signaling in the murine pathological response to sustained pressure overload. The Journal of clinical investigation 121(6), 2301–2312. 10.1172/JCI44824.

211. Derynck R, Zhang YE (2003) Smad-dependent and Smad-independent pathways in TGF-beta family signalling. Nature 425(6958), 577–584. 10.1038/nature02006.

212. Kim RH, Wang D, Tsang M, Martin J, Huff C, de Caestecker, M P, Parks WT, Meng X, Lechleider RJ, Wang T, Roberts AB (2000) A novel smad nuclear interacting protein, SNIP1, suppresses p300-dependent TGF-beta signal transduction. Genes & development 14(13), 1605–1616.

213. Malmström J, Lindberg H, Lindberg C, Bratt C, Wieslander E, Delander E, Särnstrand B, Burns JS, Mose-Larsen P, Fey S, Marko-Varga G (2004) Transforming growth factor-beta 1 specifically induce proteins involved in the myofibroblast contractile apparatus. Molecular & cellular proteomics MCP 3(5), 466–477. 10.1074/mcp.M300108-MCP200.

6. Supplementary Tables

Supplementary Table 1. List of 10 common plasma proteins displaying opposite abundance pattern between R++/NR++ and R- -/NR++

Swiss prot ID	Description	Gene ID	R++/ NR++ Ratio	R--/ NR++ Ratio
P01871	Ig mu chain C region	IGHM	0.18	-0.12
Q14997	Proteasome activator complex subunit 4	PSME4	0.16	-0.09
P07737	Profilin-1 OS=Homo sapiens	PROF1	0.16	-0.08
P63267	Actin, gamma-enteric smooth muscle	ACTH	0.16	-0.14
P01814	Ig heavy chain V-II region OU	HV201	0.15	-0.20
P18206	Vinculin	VINC	0.09	-0.08
P00915	Carbonic anhydrase 1	CA1	-0.16	0.09
Q3T8J9	GON-4-like protein	GON4L	-0.16	0.30
Q5MNZ6	WD repeat domain phosphoinositide-interacting protein 3	WIPI3	-0.17	0.26
P04745	Alpha-amylase 1	AMY1	-0.44	0.11

Supplementary Table 2. List of 45 plasma proteins exclusively differentially abundant in R++/NR++

Swiss prot ID	Description	Gene ID	R++/NR++ Ratio
P00738	Haptoglobin	HP	3.88
P69905	Hemoglobin subunit alpha	HBA1	3.41
P00739	Haptoglobin-related protein	HPR	3.27
P68871	Hemoglobin subunit beta	HBB	3.05
P05109	Protein S100-A8	S10A8	2.29
P06702	Protein S100-A9	S10A9	2.07
P60709	Actin, cytoplasmic 1	ACTB	1.62
P31151	Protein S100-A7	S10A7	1.50
P63104	14-3-3 protein zeta/delta	1433Z	1.47
Q9BS26	Endoplasmic reticulum resident protein 44	ERP44	1.46
P28330	Long-chain specific acyl-CoA dehydrogenase, mitochondrial	ACADL	1.45
P24592	Insulin-like growth factor-binding protein 6	IBP6	1.38
P14151	L-selectin	SELL	1.36
P53804	E3 ubiquitin-protein ligase TTC3	TTC3	1.36
Q9Y6R7	IgGFc-binding protein	FCGBP	1.34

Swiss prot ID	Description	Gene ID	R++/NR++ Ratio
Q8NDH2	Coiled-coil domain-containing protein 168	CC168	1.33
P37802	Transgelin-2	TAGL2	1.32
P0CG05	Ig lambda-2 chain C regions	LAC2	1.32
Q13228	Selenium-binding protein 1	SBP1	1.31
P11021	78 kDa glucose-regulated protein	GRP78	1.30
P02750	Leucine-rich alpha-2-glycoprotein	LRG1	1.28
P27797	Calreticulin	CALR	1.27
P13727	Bone marrow proteoglycan	PRG2	1.21
O00592	Podocalyxin	PODXL	1.21
Q06033	Inter-alpha-trypsin inhibitor heavy chain H3	ITIH3	1.21
P12081	Histidine--tRNA ligase, cytoplasmic	SYHC	1.20
O60832	H/ACA ribonucleoprotein complex subunit 4	DKC1	0.83
Q8TAQ9	SUN domain-containing protein 3	SUN3	0.82
P41271	Neuroblastoma suppressor of tumorigenicity 1	NBL1	0.82
P19021	Peptidyl-glycine alpha-amidating monooxygenase	AMD	0.79
Q86V97	Kelch repeat and BTB domain-containing protein 6	KBTB6	0.78
P23141	Liver carboxylesterase 1	EST1	0.75
P02768	Serum albumin	ALB	0.74
P05362	Intercellular adhesion molecule 1	ICAM1	0.73
Q9UBR2	Cathepsin Z	CATZ	0.72
Q16853	Membrane primary amine oxidase	AOC3	0.70
O95497	Pantetheinase	VNN1	0.70
P19022	Cadherin-2	CADH2	0.68
P49747	Cartilage oligomeric matrix protein	COMP	0.66
Q92621	Nuclear pore complex protein Nup205	NU205	0.65
P11717	Cation-independent mannose-6-phosphate receptor	MPRI	0.64
P01860	Ig gamma-3 chain C region	IGHG3	0.63
P02787	Serotransferrin	TRFE	0.53
Q03591	Complement factor H-related protein 1	CFHR1	0.51
P11226	Mannose-binding protein C	MBL2	0.34

Supplementary Table 3. List of 43 plasma proteins exclusively differentially abundant in R--/NR++

Swiss prot ID	Description	Gene ID	R- -/ NR++ Ratio
P49913	Cathelicidin antimicrobial peptide	CAMP	2.02
Q08554	Desmocollin-1	DSC1	1.80
P01009	Alpha-1-antitrypsin	SERPINA1	1.71
Q9Y217	Myotubularin-related protein 6	MTMR6	1.70
P04275	von Willebrand factor	VWF	1.67
Q9H4G4	Golgi-associated plant pathogenesis-related protein 1	GAPR1	1.63
Q02985	Complement factor H-related protein 3	FHR3	1.54
Q16613	Serotonin N-acetyltransferase	SNAT	1.43
P02656	Apolipoprotein C-III	APOC3	1.40
Q96QR1	Secretoglobin family 3A member 1	SG3A1	1.34
P02751	Fibronectin	FN1	1.34
P46531	Neurogenic locus notch homolog protein 1	NOTC1	1.31
P04040	Catalase	CATA	1.29
Q6UWP8	Suprabasin	SBSN	1.28
P0C0L4	Complement C4-A	C4A	1.26
P40121	Macrophage-capping protein	CAPG	1.26
A1L4H1	Soluble scavenger receptor cysteine-rich domain-containing protein SSC5D	SRCRL	1.24
O75015	Low affinity immunoglobulin gamma Fc region receptor III-B	FCG3B	1.23
P61626	Lysozyme C	LYZ	0.83
Q9BY67	Cell adhesion molecule 1	CADM1	0.83
B9A064	Immunoglobulin lambda-like polypeptide 5	IGLL5	0.82
P10643	Complement component C7	C7	0.82
P08195	4F2 cell-surface antigen heavy chain	4F2	0.79
Q5T7N7	Putative protein FAM27E1	F27E1	0.77
Q9NQ79	Cartilage acidic protein 1	CRAC1	0.76
P08185	Corticosteroid-binding globulin	SERPINA6	0.76
Q13093	Platelet-activating factor acetylhydrolase	PAFA	0.76
P19320	Vascular cell adhesion protein 1	VCAM1	0.75
Q9Y5C1	Angiopoietin-related protein 3	ANGL3	0.75
Q9HDC9	Adipocyte plasma membrane-associated protein	APMAP	0.75
P03950	Angiogenin	ANGI	0.74
P10586	Receptor-type tyrosine-protein phosphatase F	PTPRF	0.69
Q12913	Receptor-type tyrosine-protein phosphatase eta	PTPRJ	0.68
P61769	Beta-2-microglobulin	B2M	0.63
P08294	Extracellular superoxide dismutase [Cu-Zn]	SODE	0.60

Swiss prot ID	Description	Gene ID	R- -/ NR++ Ratio
P01617	Ig kappa chain V-II region TEW	KV204	0.53
P01861	Ig gamma-4 chain C region	IGHG4	0.52
P01593	Ig kappa chain V-I region AG	KV101	0.52
P02775	Platelet basic protein	PPBP	0.48
P01625	Ig kappa chain V-IV region Len	KV402	0.46
P02776	Platelet factor 4	PLF4	0.43
P07996	Thrombospondin-1	TSP1	0.42
P01857	Ig gamma-1 chain C region	IGHG1	0.40

Eigenständigkeitserklärung

Hiermit erkläre ich, dass diese Arbeit bisher von mir weder an der Mathematisch-Naturwissenschaftlichen Fakultät der Ernst-Moritz-Arndt-Universität Greifswald noch einer anderen wissenschaftlichen Einrichtung zum Zwecke der Promotion eingereicht wurde.
Ferner erkläre ich, daß ich diese Arbeit selbständig verfasst und keine anderen als die darin angegebenen Hilfsmittel benutzt und keine Textabschnitte eines Dritten ohne Kennzeichnung übernommen habe.

Gourav Bhardwaj, 23th June, 2016

Gourav Bhardwaj

Curriculum Vitae

Personal Details

Name :   Gourav Bhardwaj

Date of Birth: January 1, 1983

Place of Birth: Moradabad, India

Nationality: Indian

Educational Qualification

1. High School (1995-1997): Uttar Pradesh Board, U.P., India.

2. Intermediate School (1997-1999): Uttar Pradesh Board, U.P., India.

3. Bachelor of Science (2000-2003): Hindu Collage, Rohilkhand University, Bareilly, U.P., India.

4. Master of Science (2005-2007): Guru Nanak Dev University, Amritsar, Punjab, India.

5. Diploma in Bioinformatics (2007-2008): Jamia Hamdard University, New Delhi, India.

Work Experience

1. Research Fellow (January 2009-March 2012) at Institute of Genomics and Integrative Biology (IGIB-CSIR), New Delhi, India.

Doctoral Study (since 04/2012): Doctoral student at the Interfaculty Institute for Genetics and Functional Genomics, Department of Functional Genomics, University Medicine Greifswald, Germany.

Publications

1. Stefan Muschter, Tom Berthold, **Gourav Bhardwaj**, Elke Hammer, Vishnu Mukund Dhople, Jan Wesche, Angelika Reil, Jürgen Bux, Tamam Bakchoul, Leif Steil, Andreas Greinacher and Uwe Völker. Mass spectrometric phosphoproteome analysis of small-sized samples of human neutrophils, Clinica Chimica Acta 451 (2015) 199–207.

2. Sabine Ameling, **Gourav Bhardwaj**, Elke Hammer, Daniel Beug, Leif Steil, Yvonne Reinke, Kerstin Weitmann, Markus Grube , Christiane Trimpert, Karin Klingel, Reinhard Kandolf , Wolfgang Hoffmann, Matthias Nauck, Marcus Dörr, Klaus Empen , Stephan B. Felix, and Uwe Völker. Changes of myocardial gene expression and protein composition in patients with dilated cardiomyopathy after immunoadsorption with subsequent immunoglobulin substitution, in press

3. **Bhardwaj Gourav**, Marcus Dörr, Praveen Kumar Sappa, Sabine Ameling, Vishnu Dhople, Leif Steil, Karin Klingel, Klaus Empen, Daniel Beug, Uwe Völker, Stephan B. Felix, Elke Hammer. Endomyocardial proteomic signature corresponding to the response of patients with dilated cardiomyopathy to immunoadsorption therapy, submitted

Abstracts/Poster presented

1. Poster presentation titled "Elucidation of alteration of the phosphoproteome induced by transforming growth factor β1 in cardiomyocytes using a label-free quantitative approach" at EMBO-PTM workshop- April 2015, University of Southern Denmark, Odense, Denmark.

2. Poster presentation titled "Endomyocardial protein profiling of DCM patients with different response to immunoadsorption therapy" at HUPO-2014, Madrid, Spain.

3. Poster presentation titled "Proteomic analysis of myocardial tissue from wild-type and NOD2 knockout mice after chronic pressure overload" at Proteomic Forum- 2013, Berlin, Germany.

Workshop/Symposia Participated

1. EMBO practical course and workshop titled "The characterization of post-translational modifications" at Department of Molecular Biology and Biochemistry, University of Southern Denmark, Odense, Denmark (9th – 15th April 2015).

2. EMBO practical course and workshop titled "Targeted Proteomics: Experimental design and data analysis" at CRG, Barcelona, Spain (28th Sep. – 3rd Oct. 2014).

3. OMICs meet cardiology, German Centre for Cardiovascular Research (DZHK) Munich, Germany (18th–19th December, 2014).

Fellowship

Travel Grant of the European Molecular Biology Organization (EMBO) to participate in "Targeted Proteomics: Experimental Design and data analysis" at CRG, Barcelona, Spain (2014).

Gourav Bhardwaj

Acknowledgements

It is my pleasure to express my sincere gratitude to Prof. Dr. Uwe Völker, Director, Department of Functional Genomics, Interfacultary Institute for Genetics and Functional Genomics for providing me an excellent opportunity to pursue my doctoral thesis work in his group. My scientific discussions with him and his constructive criticisms and guidance have always paved me to think logically and scientifically. I appreciate many of his qualities that have encouraged me to look far forward towards my career. I thank him for his kind and endless support that made my thesis work successfully leading to Ph.D. and my stay here at Greifswald peaceful and joyful.

It is very difficult to express in words my gratitude to Dr. Elke Hammer, she supervised my thesis work and also supported me personally. My special thanks to her for guiding me scientifically throughout the entire duration of my stay. I improved my technological, theoretical and analytical knowledge by fruitful discussions with her. She provided me a fearless and friendly environment in the lab that gave me the freedom to plan and execute new and innovative experiments. It is due to her encouragement; I could present my scientific achievements at national and international workshops, and conferences. I thank her for providing critical and valuable suggestions in my research articles and in thesis corrections.

I thank Dr. Vishnu Dhople for his support and scientific discussions. He helped and encouraged me to establish new technologies. I would like to thank Dr. Leif Steil for his help to understand several technological and data analysis aspects. I also express my thankfulness to Dr. Praveen Sappa for his significant contribution in multiple reaction monitoring experiments and friendly support. I am thankful to Dr. Sabine Ameling for scientific discussions and critical inputs to my research projects.

I express my gratitude to Prof. Dr. Stephan Felix and his team, Department of Cardiology, University Medicine, Greifswald, for providing the crucial samples for my study and also for their

167